Electron Donating 2,7-Carbazole Derivatives: Synthesis and Characterization

Rizgar Maher Zubair

Submitted to the
Institute of Graduate Studies and Research
in partial fulfillment of the requirements for the Degree of

Master of Science
in
Chemistry

Eastern Mediterranean University
June 2013
Gazimağusa, North Cyprus

Approval of the Institute of Graduate Studies and Research

Prof. Dr. Elvan Yılmaz
Director

I certify that this thesis satisfies the requirements as a thesis for the degree of Master of Science in Chemistry.

Prof. Dr. Mustafa Halilsoy
Chair, Department of Chemistry

We certify that we have read this thesis and that in our opinion it is fully adequate in scope and quality as a thesis for the degree of Master of Science in Chemistry.

Prof. Dr. Huriye İcil
Supervisor

Examining Committee

1. Prof. Dr. Huriye İcil

2.Asst. Prof. Dr. Hamit Caner

3. Prof. Dr. Nur P. Aydinic

ABSTRACT

Carbazoles (Cbz)s are well known electron-donating materials because of the conjugated π-electrons present in their structures, they are one of the most suitable candidates for construction of electronic devices.

In the present work, we synthesized a 2,7-dibromo-N-dodecyl carbazole (dodecylcbz) via a two step procedure. In the first step, 2,7-dibromocarbazole (cbz) was synthesized (via another two step procedure–nitration of dibromobiphenyl and consequent cadogan ring closing steps). In the second step, the targeted dodecylcbz was synthesized via nucleophilic substitution. The synthesized compounds were characterized by mp, FTIR, UV-vis, NMR, and emission techniques. The FTIR spectra confirm the structures. The solubility is very high for both the cbz and dodecylcbz in all common organic solvents.

The absorption spectra of both cbz and dodecylcbz show high energy forbidden $S_0 \rightarrow S_2$ transition absorptions with high intensity at around 240 nm comparing to $\pi \rightarrow \pi^*$ electronic transition absorptions at around 303 nm, respectively in all of the common organic solvents studied. Most importantly, $\pi \rightarrow \pi^*$ electronic transition absorptions of both carbazole and dodecylcarbazole were unchanged with respect to the polarity and type of the solvent. Whereas, $S_0 \rightarrow S_2$ transition absorptions have undergone solvent-dependent shifts.

Both the cbz and dodecylcarbazole exhibited intense excimer emissions in all of the solvents. These interesting optical properties are very useful for present-day organic-based optoelectronic applications.

Keywords: Carbazole, 2,7-Dibromocarbazole, Excimer Emission, Forbidden Transitions

ÖZ

Karbazoller yapılarında mevcut olan konjuge π-elektronları nedeniyle elektron-verici maddeler olarak bilinmektedirler. Bu yüzden, karbazoller elektronik cihazların yapımı için en uygun adaylardan biridir.

Bu çalışmada, 2,7-dibromo-N-dodesil karbazol (dodesilcbz) iki basamakta sentezlenmiştir. İlk basamakta 2,7-dibromokarbazol (cbz) sentezlenmiştir (başka bir iki basamaklı prosedür ile – dibromofenil nitrasyonu ve Cadogan halka kapanma işlemi). İkinci basamakta hedeflenen dodesilkarbazol nükleofil yer değiştirme tepkimesi ile sentezlenmiştir. Sentezlenen bileşikler, erime noktası, FTIR, UV-vis, NMR ve emisyon teknikleri kullanılarak karakterize edilmiştir. FTIR spektrumları yapıları teyit etmektedir. Çözünürlük yaygın olarak kullanılan tüm organik çözücülerde cbz ve dodesilcbz için çok yüksektir.

Karbazol ve dodesilkarbazolun yaygın olarak kullanılan tüm organik çözücülerdeki absorpsiyon spektrumlarında, 240 nm civarındaki $S_0 \rightarrow S_2$ yasaklanmış geçiş absorpsiyonu 303 nm civarındaki $\pi \rightarrow \pi^*$ elektronik geçiş absorpsiyonu ile karşılaştırıldığında daha şiddetlidir. En önemlisi, karbazol ve dodesilkarbazolun $\pi \rightarrow \pi^*$ elektronik geçiş absorpsiyonu çözücünün türü ve polaritesinden bağımsızken $S_0 \rightarrow S_2$ geçiş absorpsiyonu çözücüye bağlı olarak kaymaktadır. Karbazol ve dodesilkarbazol tüm çözücülerde yoğun ekzimer emisyonu sergilemiştir. Bu ilginç optic özellikler, günümüz organik-bazlı optoelektronik uygulamalar için çok kullanışlıdır.

Anahtar Kelimeler: Karbazol, 2,7-Dibromokarbazol, Ekzimer Emisyonu, Yasaklanmış Geçişler.

To My Family

ACKNOWLEDGMENTS

First and foremost, I am actually grateful and thankful to my supervisor Prof. Dr. Huriye İcil for all her guidance, support and encouragement throughout my MS thesis work at Eastern Mediterranean University; for her valuable teaching of organic chemistry; and for advices in general life.

I am also very thankful to the family of organic group at Eastern Mediterranean University.

I am indebted to my family for their complete encouragement.

TABLE OF CONTENTS

LIST OF TABLES

LIST OF FIGURES

LIST OF SCHEMES

LIST OF SYMBOLS/ABBREVIATIONS

$\mathring{A}$	:	Armstrong
A	:	Absorption
AU	:	Arbitrary unit
BHJ	:	Bulk-heterojunction
BHJ-PSCs	:	Bulk-heterojunction polymer solar cells
Cbz	:	Carbazole
$CDCl_3$	:	Deuterated chloroform
C	:	Concentration
CT	:	Charge transfer
DBBP	:	4,4′-dibromobiphenyl
DBNBP	:	4,4′-Dibromo-2-nitro-biphenyl
DMF	:	Dimethylformamide
DMSO	:	Dimethyl sulfoxide
DSC	:	Differential scanning calorimetry
ε	:	Extinction coefficient
ε_{max}	:	Maximum Extinction coefficient/Molar absorptivity
E_g	:	Band gap energy
E_s	:	Singlet energy (Excited state energy of 0-0 electronic)
FETs	:	Field-effect transistors
FT-IR	:	Fourier transform infrared spectroscopy
FWHM	:	Full width half maximum
f	:	Oscillator strength
h	:	Hour

HOMO	:	Highest occupied molecular orbital
IDRF	:	Identification radio-frequency
k_f	:	Fluorescence rate constant
l	:	Path length
M	:	Molar concentration
MeOH	:	Methanol
mp	:	Melting point
NMP	:	*N*-methylpyrrolidinone
NMR	:	Nuclear magnetic resonance spectroscopy
OLED	:	Organic light emitting diode
OFET	:	Organic field-effect transistor
Φ_f	:	Fluorescence quantum yield
R-Br	:	1-bromododecane
R-Cbz	:	2,7-dibromo-N-dodecylcarbazole
τ_0	:	Theoretical radiative lifetime
τ_f	:	Fluorescence lifetime
TCE	:	1,1,2,2-tetrachloroethane
TGA	:	Thermogravimetric analysis
THF	:	Tetrahydrofuran
TMS	:	Tetramethyl silane
UV-vis	:	Ultraviolet visible light absorption
$\bar{\nu}$	:	Wavenumber
$\Delta\bar{\nu}_{1/2}$	:	Half-width (of the selected absorption)
$\bar{\nu}_{max}$	:	Maximum wavenumber/Mean frequency
λ	:	Wavelength

λ_{exc}	:	Excitation wavelength
λ_{em}	:	Emission wavelength
λ_{max}	:	Maximum wavelength

Chapter 1

INTRODUCTION

1.1 Introduction to Carbazole Compounds

Carbazole and its derivatives are one of the most important types of organic heterocyclic aromatic compounds. Carbazole has tricyclic structure with dibenzopyrrole unit and also known as 9-azofluorine due to the structural similarity to fluorine (Al- Sultani K. T. 2010). The chemical structure of carbazole and numbering system on its structure is shown in Figure 1.1. At the first time, carbazole was isolated from coal tar by Graebe and Glazer in 1872 and simple carbazole alkaloids were isolated from plants as natural products in 1960 (Hussain et al 2011).

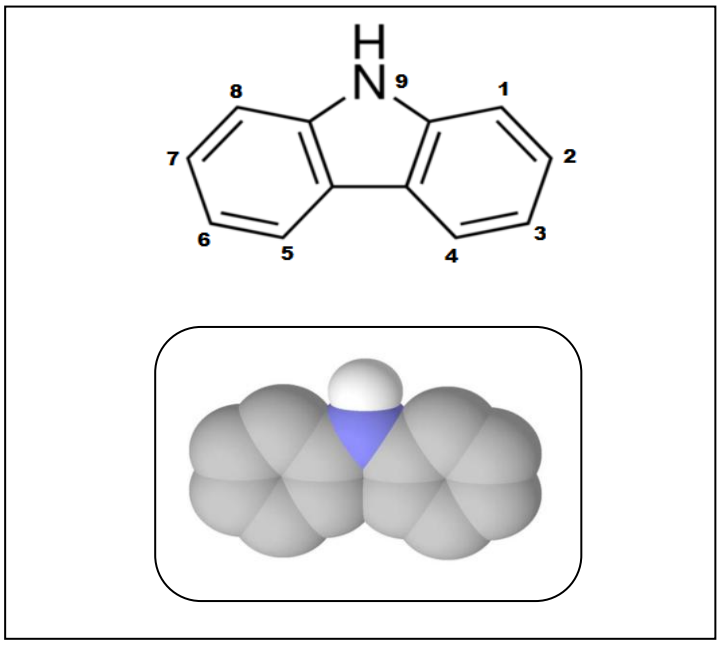

Figure 1.1: Chemical Structure of Carbazole and Numbering System on its Structure

Carbazoles are a great and attractive group of organic compounds. The pyrrole ring fused between two phenyl groups makes the tricyclic carbazole completely aromatic and rich in electrons including its electron donating nitrogen atom (Bian et al. 2012). From the organic structural viewpoint (Figure1.1), diphenylamine has a kink structure, but the nitrogen atom on carbazole unit increase the planarity for its structure. In fact, because of their planarity and rigidity, carbazole unit has a big band gap, and this leads to exhibit relatively intense electroluminescence (Liaw et al. 2012).

Carbazoles are promising electron donating materials with electron unsaturation and a nitrogen atom. The conjugated double bonds offer substitution at different places and therefore different substituted carbazoles can be prepared. Another advantage is the possible substitution at nitrogen atom. The hydrogen at 9-carbon (9H) can be replaced with some other substituents. Tailoring of materials according to the purpose is a very attractive property as shown in Figure 1.2. Utilizing these advantages, different carbazole materials can be prepared and their applicability in various fields can be characterized.

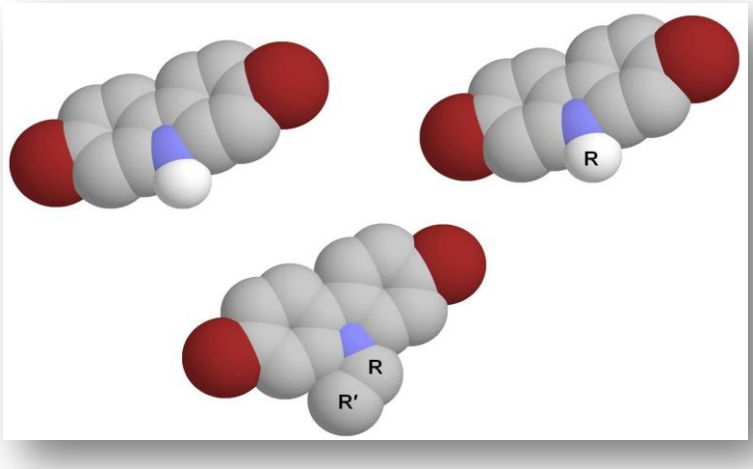

Figure 1.2: Different 2,7-Substituted and Nitrogen-Substituted Carbazole Materials

1.2 Importance of Carbazoles

Carbazole is a cheap raw material (Vehoff et al. 2008). Yet, carbazoles are while-known as good electron-donating (*p*-type) chromophores, emits light in the short wavelength, and also is a basic substance of having fluorescent properties. Moreover, the high thermal stability or the glass transition temperatures of the organic molecules can be significantly improved by incorporation of a carbazole or its derivatives into the core structure (Gupta et al. 2011 and Koyuncu et al. 2009). Furthermore, different molecular organic groups can be straightforwardly functionalized to specific positions on the carbazole units as shown in Figure 1.1. For example, the thermal stability and good electro-optical properties can be significantly improved by substituting phenyl group at the N-position of the carbazole structures (Fujita et al. 2012 and Liu et al. 2006). Moreover, as a result of its unique photo-electronic property, and great π −conjugated organization, carbazole unit was widely used in both side chain and main chain of carbazole containing compounds, in the side chain used as a functional substituent or in the main chain as functional building blocks for organic electronic devices (Ruiren et al. 2009).

Currently, due to their extensive appearance in both natural and synthetic materials, carbazole and its derivatives have much attention in the literature (Vyprachticky et al. 2012). In synthetic materials, carbazole unit plays a significant role as a functional building block for carbazole containing materials such as polymer materials and low-molecular-weight materials (Vyprachticky et al. 2012). In addition, carbazole containing materials are well-known to easily form radical cations which are relatively stable (called as holes), display high charge carrier mobilities, high thermal and chemical stabilities. In the field of organic electronic devices, carbazole

derivatives are extensively used such as hole-conducting resources with an extensive energy gaps. For example, carbazole containing materials were used to fabricate dye-sensitized solar cells and blue organic light emitting diodes (OLED) (Vehoff et al. 2008). Many carbazole derivatives can be able to host red, green, and even blue triplet emitters because of their high triplet energy level (Liu et al. 2006).

It is the objective of this work to prepare different monomeric 2,7-substituted carbazole materials (Figures 1.3 – 1.5). Firstly, 2,7-substitution was carried out and then substitution at the nitrogen atom was made to the carbazole structure. All the synthesized substances were characterized in detail to explore their potential applications using FTIR, elemental, NMR, UV-vis, Fluorescence, DSC, and TGA measurements.

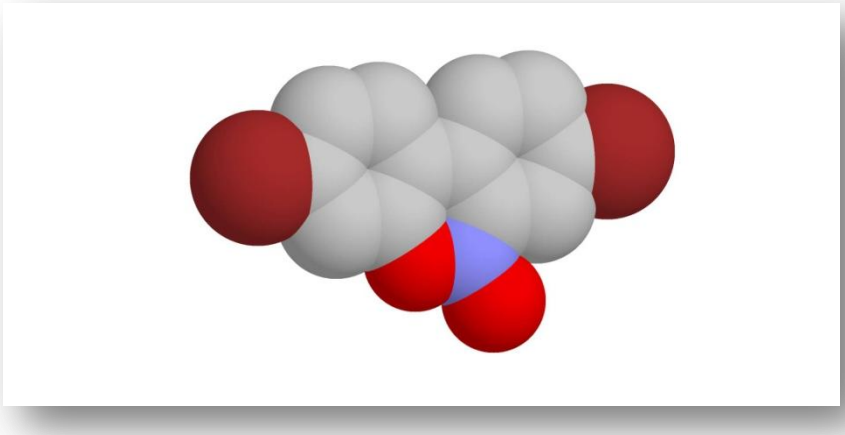

Figure 1.3: 4,4′-Dibromo-2-nitro-biphenyl (DBNBP)

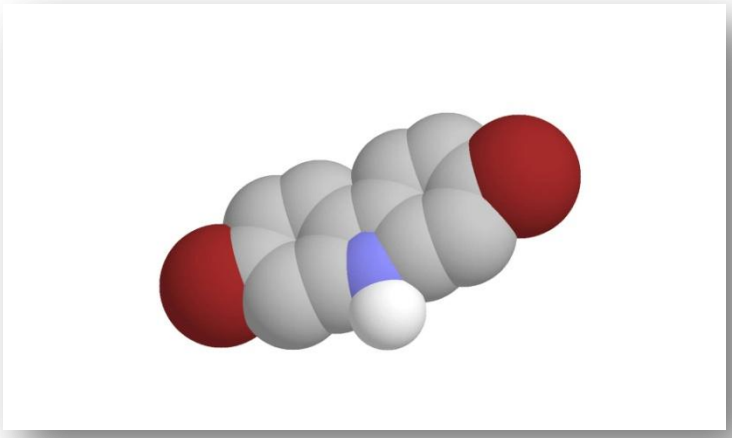

Figure 1.4: 2,7-Dibromo-9H-carbazole (cbz)

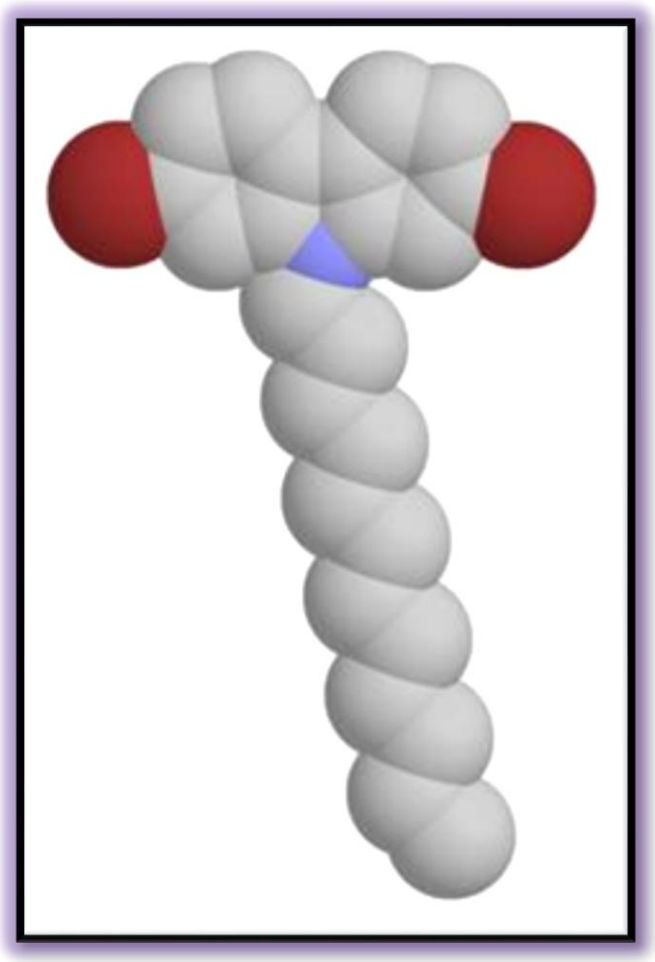

Figure 1.5: *N*-Dodecyl-2,7-dibromocarbazole (dodecylcbz)

Chapter 2

THEORETICAL

2.1 Types of Carbazole Compounds

Based on the substitution of different groups to the phenyl rings present in the carbazole, they are three mainly divided important types of carbazoles. As shown in the Figure 2.1, 1,8–carbazoles, 3,6–carbazoles and 2,7–carbazoles are the most familiar types and among these carbazoles, 3,6–carbazoles and 2,7–carbazoles are mostly studied due to their extended conjugated aromatic structure. Consequently, 3,6–carbazoles and 2,7–carbazoles have potential to be applicable in many organic-based devices.

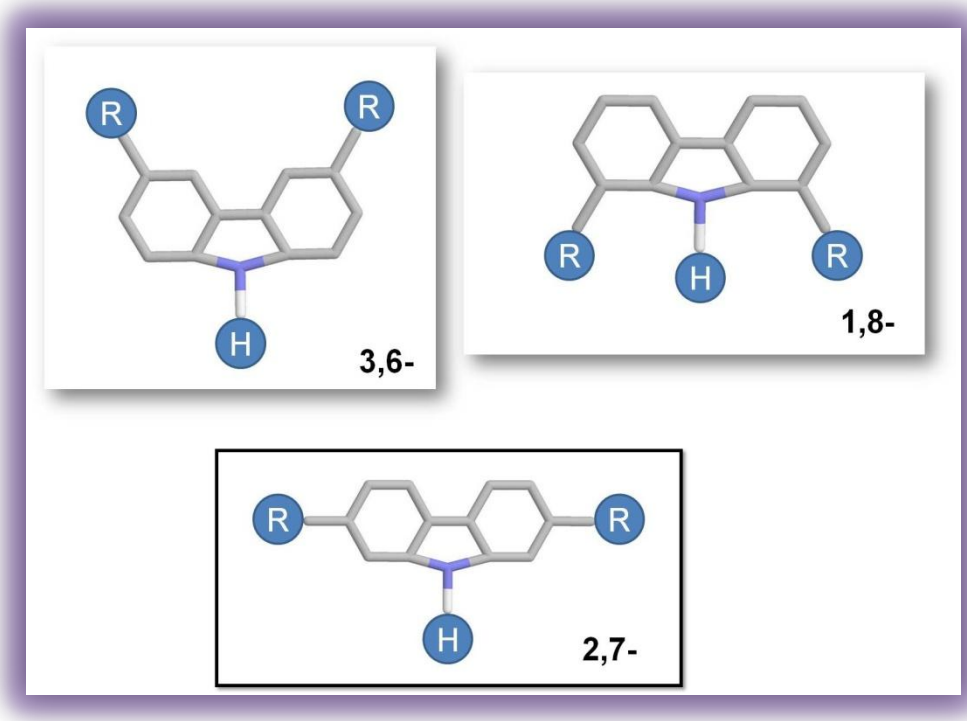

Figure 2.1: The Most Familiar 3,6–, 1,8–, and 2,7–Carbazole Compounds

The electron density on the carbon atoms affects the reactivity on their positions towards electrophilic aromatic substitution. The substitutions at para-, meta-, ortho-positions and corresponding electron density determine the ease of carbazole modifications. In other words, the positions of 3,6- , 1,8- , and 2,7- with respect to amino group of carbazole is key factor for relevant substitution. As an example, the presence of both 2- and 7- in meta positions with respect to *N*–H group of carbazole unit, electrophilic substitution cannot be made easily by standard functionalization procedures.

2.1.1 2,7-Carbazoles

From the mechanistic organic chemistry point of view, the synthesis of 2,7–dihalocarbazoles is not as easy as the preparation of 3,6–dihalocarbazole derivatives (Vyprachticky et al. 2012). This is due to the presence of both 2- and 7- substitutions in meta positions with respect to *N*–H group of carbazole unit, electrophilic substitution cannot be made easily by standard functionalization procedures. Contrary to the difficulties in functionalization, 2,7–dihalocarbazoles are the most conjugated structures among carbazoles and therefore are very efficient with high charge carrier mobility (Bouchard et al. 2004). Moreover, the extended conjugation of 2,7–dihalocarbazoles provides excellent optoelectronic properties. Notably, there are two important procedures reported for the synthesis of 2,7–dihalocarbazoles. The first method is based on Diels – Alder sequential reaction where the pyrrole-based materials are pre-functionalized. In the second method, 4,4′–disubstituted biphenyls are modified by ring closing mechanism to yield 2,7-disubstituted carbazole derivatives (Bouchard et al. 2004).

Theoretically found that the energy gaps of 2,7-diheteroaromatic carbazoles are smaller than the band gap energies of 3,6-diheteroaromatic carbazoles (Kawabata et al.2010). Compared to 3,6-carbazole derivative analogues and with several electron donating conjugated polymers, the poly(2,7-carbazole)s exhibit higher hole-transporting and slightly lower HOMO energy levels (Xie et al. 2012 and Zhao et al. 2010). Moreover, 2,7-carbazole derivatives were also widely used to make conjugated polymers for different optoelectronic devices, mainly used as a donor materials for very efficient bulk heterojunction polymer solar cells (Xie et al. 2012).

2.1.2 3,6-Carbazoles

The non-bonding electrons of nitrogen atom increases the electron density on the 3- and 6-positions of carbazole unit and can be reactive for electrophilic aromatic substitution. Utilizing the ease in synthesis, functionalized 3,6- carbazole units are produced in higher number comparing to other carbazole derivatives. Certainly, polymer with 3,6- carbazole derivatives are widely studied for a variety of optoelectronic devices, for example, bulk-heterojunction polymer solar cells (BHJ-PSCs), electrochromic devices, light emitting diodes (OLEDs) and etc. (Xie et al. 2012).

2.1.3 1,8-Carbazoles

Comparing to the 3,6-carbazoles, approximately the 1,8-carbazole derivatives and 2,7-carbazole derivative compounds have a similar effective conjugation connectivity. Moreover, due to their high electron density can be easily functionalized 1,8-positions of carbazole units.

Related to the nitrogen atom in carbazoles, conjugation connectivity of 1,8-carbazole based polymers are essentially almost similar to 3,6-carbazole based polymers. Yet,

by substituting alkyl groups to the *N*-positions of poly(1,8-carbazole) the maximum absorption appear at the visible region (Michinobu et al. 2008).

Conclusively, one can easily understand that the reactivity trend of carbon atoms for electrophilic aromatic substitution decreases gradually on 3,6–; 1,8–; 4,5–; and 2,7–carbazole units, respectively. The efficiency order of the carbazole derivatives for high thermal stability, optimized optical and electronic properties, and being π-spacer is: 2,7-carbazoles > 1,8-carbazoles > 3,6-carbazoles (Fujita et al. 2012).

2.2 General Properties of Carbazoles

Carbazoles are well known strong electron donating materials and also efficient short wavelength emitters. Due to their large conjugated π-electrons, they are one of the most suitable materials for construction of electronic devices. They have several advantages such as chemical stability, possibility for versatile substitutions at N-position for tuning the thermal, optical and electrical properties, high solubility, low band gaps, and substitution at (3,6),(2,7) and (1,8) positions of carbazole units (Koyuncu et al. 2009 and Kanaparthi et al. 2012). Therefore, carbazole rings can be easily functionalized to various carbazole derivatives and they can be covalently combined to other chemical materials. However, the incorporation of the N-position of carbazole units into aromatic systems is difficult by the classical methods, thus the intense reaction conditions are required for this kind of incorporation due to the pair of nonbonding electrons on the nitrogen atoms making it a weak nucleophile (Velasco et al. 2007).

In general, the hole-carrier properties and photoconductivities of many polymers can be greatly developed by incorporation the carbazole units in the side or main chains of the polymers as pendant groups or building molecules. Also the high thermal stability and photochemical stabilities of carbazole derivatives are significant properties for its technological applications (Velasco et al. 2007). In addition, many of carbazole derivatives are capable to host blue triplet emitters rather than red and green emitters, due to their sufficient high triplet energy (Liu et al. 2006).

2.2.1 Electron Donating and Charge Carrier Properties

Charge transporting (CT) materials are divided into two different classes: The first one, hole-transporting (*p*-type) and the second, electron-transporting (*n*-type) dipolar

materials based on the charge-transporting kinds. Actually, the hole or electron transfer takes place through the charge migrations between both of the electron donor- and acceptor- materials (Figure 2.2). In other words it can be explained that this process occur as one electron oxidation-reduction operations. Commonly in denser phase of organic systems, the charge transfer depends on the molecules entity and the routes in which the molecules are aggregated in the condensed phase (Tomkeviciene et al. 2011).

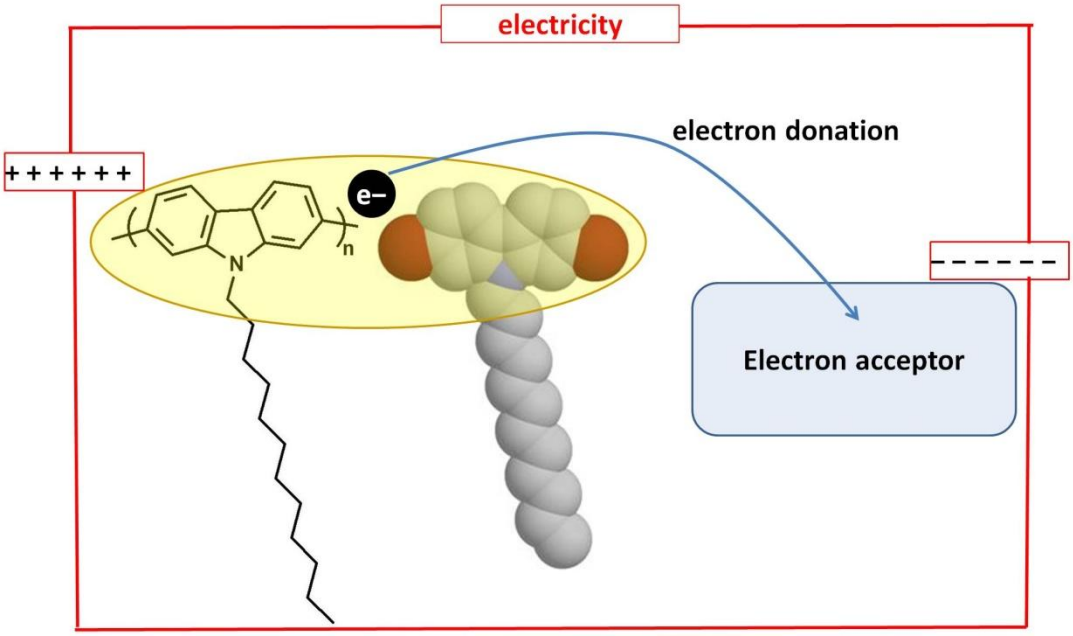

Figure 2.2: The Schematic Diagram Explaining the Electron Donation and Possible Acceptance Leading to Produce Electricity

Charge transporting factors can be designed based on two properties: large π-electron conjugation and strong electron donating ability. The two properties are possessed by carbazole derivatives (Kim et al. 1999). For example, inducing intramolecular CT complex and carrying charge generate in the visible area via functionalizing the 3,6-position of carbazole derivatives by electron withdrawing groups, therefore the charge can be transfered over the carbazole rings (Kim et al. 1999). The charge

transfer property of carbazoles have attracted great comprehensive study (Lao et al. 2000).

Carbazole compounds are well known having good electron donating behaviors (Gutierrez et al. 2011). But, some times the coplanarity of the main chain is destroyed partially because of the steric effects that results from the bulk structures.

Due to the high electron-donating nature of carbazole groups, it emits light in the long wave length region (red light). This occurs when the compounds absorbed light and subsequently losses its excess energy by dissipation of the energy in all of the internal conversion mechanisms (vibronic states) or by interaction with the solvent molecules about the excited dipole, or via charge complex formation and hydrogen bonding (Gupta et al. 2011).

2.2.2 Optical Properties

Carbazoles are heterocyclic compounds that emit light at λ_{max}~340 nm in dilute solutions. This is due to the n $\rightarrow \pi^*$ transitions which belong to the non- sharing electrons on nitrogen atom and the electronic spectrum have properties comparable to those of $\pi \rightarrow \pi^*$ transitions belong to the aromatic conjugated double bonds (C□C) (Velasco et al. 2007). Therefore by functionalization, *N*-position of carbazole pendant group can be tuned both of the energy levels and photophysical properties of polymers (Wang et al. 2011).

Compared to the low-molecular weight carbazoles, the absorption locations of corresponding carbazole pendant groups in a side chain of polymers are red-shifted. For example, carbazole unit absorption in ethanol exhibits at the wavelength 300–

345 nm with λ_{max}~323 nm. This refers to the presence of small electronic interaction between the carbazole unit (pendant groups) and the main chain (Kim et al. 2001).

Generally, the excitation spectra are not punctually similar to the absorption spectra and are unrelated to the emission wavelength. In addition, carbazole unit as a pendant group absorbs light around the wave length of 320–350 nm and this leads to the emission by contribution of dominant backbone. This can be ascribed to the transfer of energy from the side chains (pendant) to the main chain (backbone) (Kim et al. 2001).

Generally, the absorption spectra of copolymer both in solutions or solid states consist of two peaks. In the solid states, absorption peaks appear at around λ=370 nm due to carbazole group. This absorption peak is ascribed to electron transition from $\pi \rightarrow \pi^*$ of carbazole part in the copolymer (Liu et al. 2008).

Compared to the fluorescence spectra of poly(2,7-carbazole)s and their analogous polymers and monomers, the 3,6-carbazole-based monomer and polymers absorb light at the short wavelength causing hypsochromic shift (blue-shift) rather than absorbing lights at the longer wavelengths giving bathochromic shift (red-shift). On the other hand, the 2,7-carbazole-based polymers generally exhibit higher hole transportation and the HOMO energy levels are slightly lower than their 3,6-carbazole derivative analogues (Xie et al. 2012).

2.3. Applications of Carbazole Materials

Carbazole is a rich π-conjugated unit that has special attractive electronic and optical properties like photoconductivity and photorefracttivity (Liawa et al. 2012). Carbazole and its derivatives have a great potential for both electronic and photonic applications, in general, for fluorescent markers, charge-transfer materials, solar energy collectors, nonlinear optical and two-photon absorbing materials (Gupta et al. 2011).

Due to their unique advantageous properties like good hole transporting (transporting the positive charge) ability, thermal and oxidation stabilities, carbazole-based polymers are widely utilized in BHJ-PSCs as donor materials. The electron-donating capability of carbazole units results from moving the lone pair of electrons that exist on nitrogen atom around the carbazole moiety. In fact, polymer with 3,6- carbazole derivatives are widely studied and utilized in different optoelectronic devices, such as OLEDs, BHJ-PSCs, electrochromic devices and etc. Furthermore, polymer with 2,7- carbazole derivatives are widely utilized to create conjugated polymers for a variety of optoelectronic devices, in particular for BHJ-PSCs with highly efficiency (Xie et al. 2012).

In pharmaceutical industries, the synthetic carbazole derivatives for many different cell lines are used as good inhibitors as well as for the treatment of obesity. On the other hand, due to their good optical and electrical features it is not surprising to find carbazole derivatives in various organic devices like organic materials-based field effect transistors, sensors, photodiodes, *etc*. (Bouchard et al. 2004). Therefore, carbazole containing materials that are highly fluoresces and chemically stable are

used as probes and tags in diverse microenvironments to sense different temperatures, pH, polarity and microviscosity (Lao et al. 2012). In addition, due to their peculiar properties like hole transporting and electroluminescence, carbazole and its derivatives are extensively utilized as building blocks or pendant groups both in the main chain or side chains to construct the organic photoconductors, photorefractive materials, electroluminescence, and also nonlinear optical materials (Hu et al. 2010 and Cabaj et al. 2006).

2.3.1 Organic Electronic Devices

Organic electronic devices, for example, organic materials-based light emitting diodes (OLED)s and organic materials-based field-effect transistors (OFET)s have an important role in terms of potential applications in technology and fundamental science. Therefore, in general, organic electronic devices have several commercial benefits such as cheap, flexible and rugged, light-weight, and also available to use for wide area of applications (Tomkeviciene et al. 2011).

Organic Light-Emitting Diodes (OLEDs)

These types of devices are named sometimes as electroluminescent devices (Tomkeviciene et al. 2011). At the first time, Tang et al. doped emission layer with a fluorescent dye in OLED devices. Although OLEDs' photo-electronic properties are systematically achieved, enormous developments in tailoring of materials provided new light-emitting organic materials for OLEDs. Generally, charge-carrying blue emissive materials that have large band gaps could not be injected easily into the active layer (light-emitting layer) of the devices. Furthermore, achieving full-color displays is quite difficult and requires high color purity besides good current efficiency and intense luminosity. This needs involvement of good amorphous organic materials with high thermal stability that can also exhibit good operational

stability (Chen et al. 2012). Thus, due to their structural stability and the intense luminosity, the carbazole and its derivatives becoming an important subject of research. They are extensively utilized as a suitable hole-transporting materials that results from reversible oxidation processes along with the good emitters in organic light emitting diodes (OLEDs) (Liu et al. 2010). Carbazole-based oligomers, polymers, and dimers are applied in OLEDs as red, blue, white, and green emitters. The simple scheme of OLEDs mechanism is shown in Figure 2.3 (Gutierrez et al. 2011).

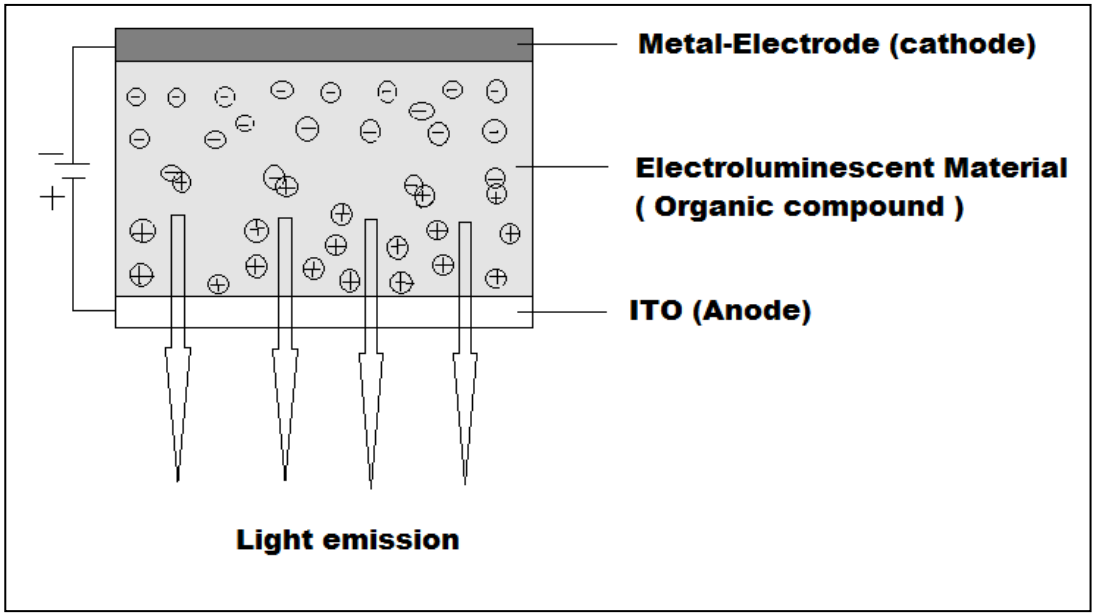

Figure 2.3: The Simple Scheme of OLED Mechanism

Organic Field-Effect Transistors

At the first time, Tsumura and coworkers in 1986 demonstrate the Organic field-effect transistors (OFETs) by utilizing organic semiconductors (polythiophene) in active layers. Afterwards, the efficiency of OFETs improved significantly and nowadays, some of the OFETs are parallel with the amorphous silicon FETs in the speed. In general, these types of OFETs are used in active-matrix flat-panel displays like a pixel-switch. Organic semiconductors compared to their inorganic analogues

offer numerous advantages, such as capability to fabricate with low melt processing and low-cost, flexibility, natural compatibility on plastic layers, etc. Indeed, OFETs applications are appeared in the sensors, electronic paper, and also identification radio-frequency (IDRF) cards. An OFET consists of three main parts: presence of electrodes (gate, drain, and source), organic semiconducting layer, and dielectric layer (Figure 2.4). Semiconducting layer and its deposition are the main steps of OFETs construction (Liu et al. 2009). There are several (*p*- and *n*-) types of organic materials that are prepared for OFET devices, for example carbazoles are one of the most familiar hole-transporting materials in semiconducting layers (Gutierrez et al. 2011).

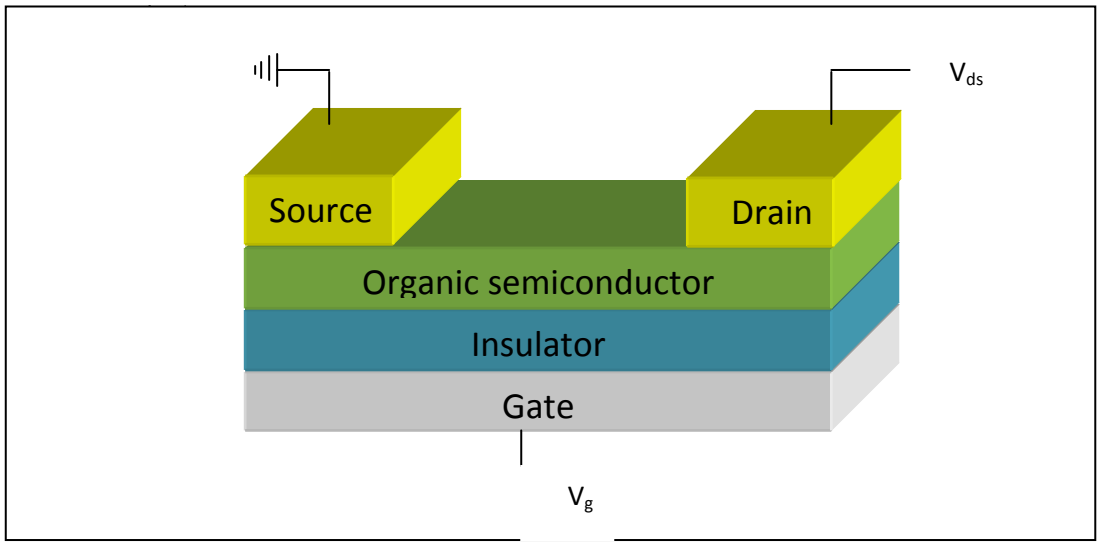

Figure 2.4: Construction of an Organic Field-Effect Transistor

2.3.2 Renewable Energy Systems

As the demand for energy is growing steadily, leading to the rapid growth in the need to traditional fossil fuels is also increasing proportionally. On the other hand, the traditional sources are limited and rapidly decreasing, consequently this threatens the balance of the power required/generation in the future. Furthermore, the greenhouse gases that cause global warming increases during power producing by classical

energy sources. Thus, the renewable energy system is one of the effective solutions to supply sustainable energy systems.

Currently, photovoltaic cells are the best practical attention that can address increasing requirement for renewable and environment friendly energy sources. Due to several advantages, polymer BHJ solar cells are the best devices among many types of photovoltaic cells. In these devices the major ways to get high photoconversion activity are based on developing the electron donating (*p*-type) semiconducting polymers that have high charge carrier mobilities and low band gaps (Promarak et al. 2007).

Carbazole-based materials are one of the best *p*-type choices for the construction of efficient oranic-based bulk heterounction and dye sensitized solar cells.

Chapter 3

EXPERIMENTAL

3.1 Materials/Chemicals

The syntheses were carried out straightway by using commercial chemicals unless otherwise specified. 4,4′-dibromobiphenyl is a commercial compound that was employed as starting material for the synthesis of 2,7-dibromocarbazole. Some of the needed solvents were freshly purified by common distillation procedures prior to use. Pure commercial solvents were directly employed for spectroscopic analyses.

4,4′-dibromobiphenyl, nitric acid, acetic acid, ethyl acetate, triethylphosphite, acetic anhydride, 1-bromododecane, sodium hydride, sodium sulfate, and potassium hydroxide were purchased from sigma Aldrich.

3.2 Instruments

The synthesized products were purified by using gravity column chromatography on silica gel 4 Å using a mixture of ethyl acetate and n-hexane (1:4) as the eluent. FT-IR spectra of the compounds were recorded in the solid states by using KBr pellets on a JASCO FT-IR spectrophotometer. Solution absorptions were recorded on Varian-cary-100 spectrophotometer. The Fluorescence/ emission spectra measurements for the synthesized carbazole compounds were carried out by VarianCaryEclipse spectrophotometer. ^{1}H- and ^{13}C- NMR spectra of the targeted dodecylcarbazole was acquired using Bruker/XWIN spectrometer in deuterated chloroform ($CDCl_3$) with tetramethyl silane as an internal reference on 400 MHz and 100 MHz analyzers, respectively.

3.3 Syntheses Methods

The focus of this work is to design and synthesize a new electron donating 2,7-dibromo-substituted carbazole derivative for BHJ solar cells. According to the theory, it was demonstrated that the synthesis of 2,7-dibromo- substituted carbazole derivatives was not straightforward. Although, the substitution is difficult at 2,7-positions (reference), we have successfully synthesized the 2,7-dibromcarbazole derivative.

The general scheme for the synthesis of 2,7-dibromo-substituted carbazole derivative is shown in scheme 3.1.

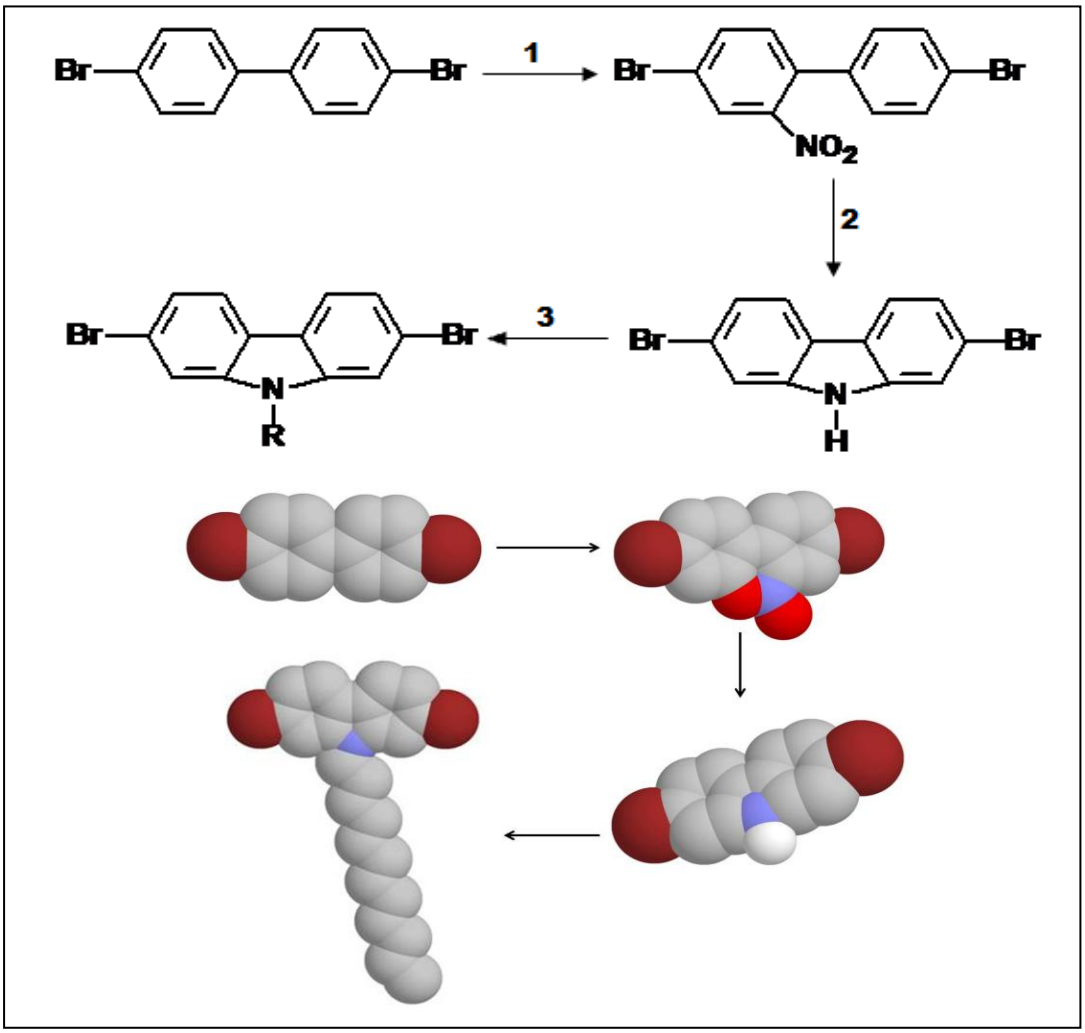

Scheme 3.1: Synthetic Route of 2,7-Dibromo-Substituted-N-alkyl Carbazole Derivative

According to the general scheme (Scheme 3.1), the starting material 4,4′-dibromobiphenyl (DBBP) was converted to a 4,4′-dibromo-2-nitrobiphenyl (DBNBP) in the first step. In the second step, DBNBP synthesized in the first step was converted to 2,7-dibromocarbazole and finally converted it to 2,7-dibromo-N-dodecylcarbazole in the third step.

In the first step, the starting material DBBP was converted to DBNBP in presence of nitric acid and acetic acid, and purified by the method given in literature (Dierschke et al. 2003) as shown in Scheme 3.2.

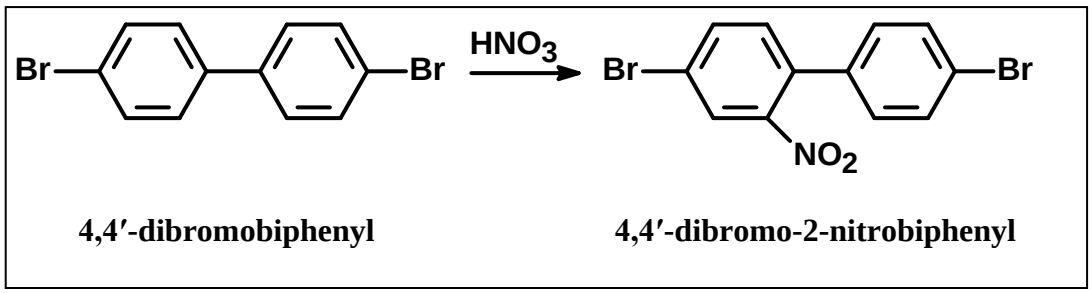

Scheme 3.2: Synthesis of Dibromonitrobiphenyl, DBNBP (Dierschke et al. 2003)

In the second step, the synthesized nitrobiphenyl was converted to 2,7-dibromocarbazole (Cbz) in presence of triethylphosphite and purified by extraction with water as explained in the literature (Dierschke et al. 2003).

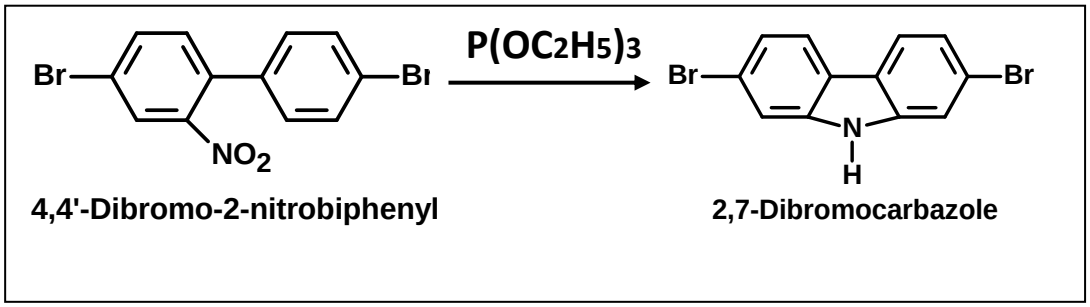

Scheme 3.3: Synthesis of 2,7-Dibromo-NH-carbazole, Cbz (Dierschke et al. 2003)

Finally in the third step, the synthesized Cbz was converted successfully to 2,7-dibromo-N-dodecylcarbazole (Dodecylcbz) in presence of 1-bromododecane and sodium hydride (NaH) as shown in Scheme 3.4.

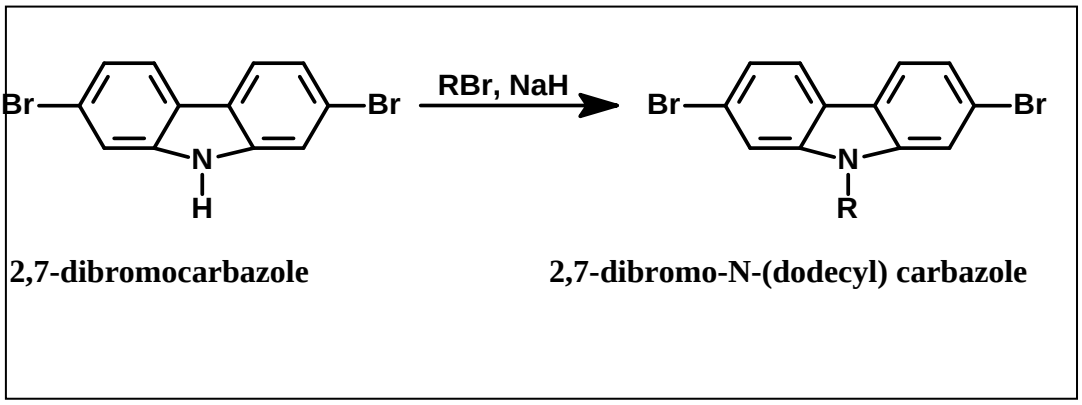

Scheme 3.4: Synthesis of 2,7-Dibromo-N-dodecylcarbazole (Dodecylcbz)

3.4 Synthesis of 4,4′-Dibromo-2-nitrobiphenyl

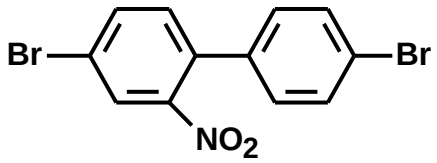

The DBNBP was synthesized and purified by following a literature method (Dierschke et al. 2003). Briefly, the starting material, dibromobiphenyl was dissolved in acetic acid and added nitric acid drop wise to yield a yellow colored precipitate. Later, the precipitate was recrystallized using ethanol.

The synthesis of intermediate product was confirmed by FTIR and melting point results.

3.5 Synthesis of 2,7-Dibromo-9H-carbazole

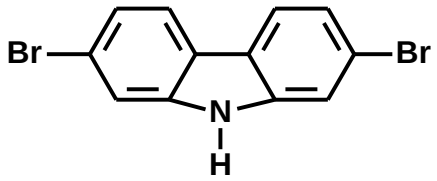

In the second step, Cbz was synthesized and purified by following a literature method described by Dierschke and et al.

Triethylphosphite was used as the reagent to synthesize the targeted compound and the product was separated by gravity column.

The synthesis of intermediate product was confirmed by FTIR and melting point results.

3.6 Synthesis of 2,7-Dibromo-N-dodecylcarbazole

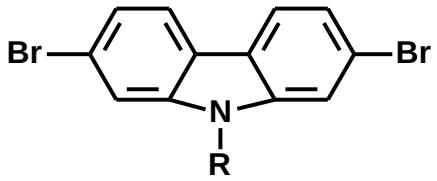

A three-necked balloon was equipped with a magnetic stirrer, a condenser and a thermometer was kept under argon atmosphere for 10 min. The balloon was added first N,N-dimethylformamide (DMF) (30 mL) and degassed for 10 min. Sodium hydride (NaH) (0.09 g, 3.75 mmol) was slowly added and after obtaining a homogeneous mixture, added 2,7-dibromocarbazole (0.5 g, 1.53 mmol) and were stirred for 1 h at room temperature. 1-Bromododecane (0.5 ml, 20.8 mmol) was added finally to the reaction mixture under argon and stirred for 20 h at 70 ºC by increasing the temperature gradually.

Afterwards the reaction was quenched by adding distilled water (40 mL) and extracted with (200 mL) of dichloromethane (CH_2Cl_2) for 3 times. The organic layer was dried using sodium sulfate and the solvent was removed under vacuum to obtain white solid.

Yield: 83%**, Color:** White solid**.**

FT-IR (KBr, cm^{-1}): ν = 2926, 2853, 1656, 1415, 1390.

UV-Vis ($CHCl_3$) (λ_{max}/nm; (ε_{max}/ L mol^{-1} cm^{-1})): 308 (2080).

3.7. Reaction Mechanism for the Synthesis of 2,7-Dibromo-N-dodecylcarbazole

Part-I:

Step 1:

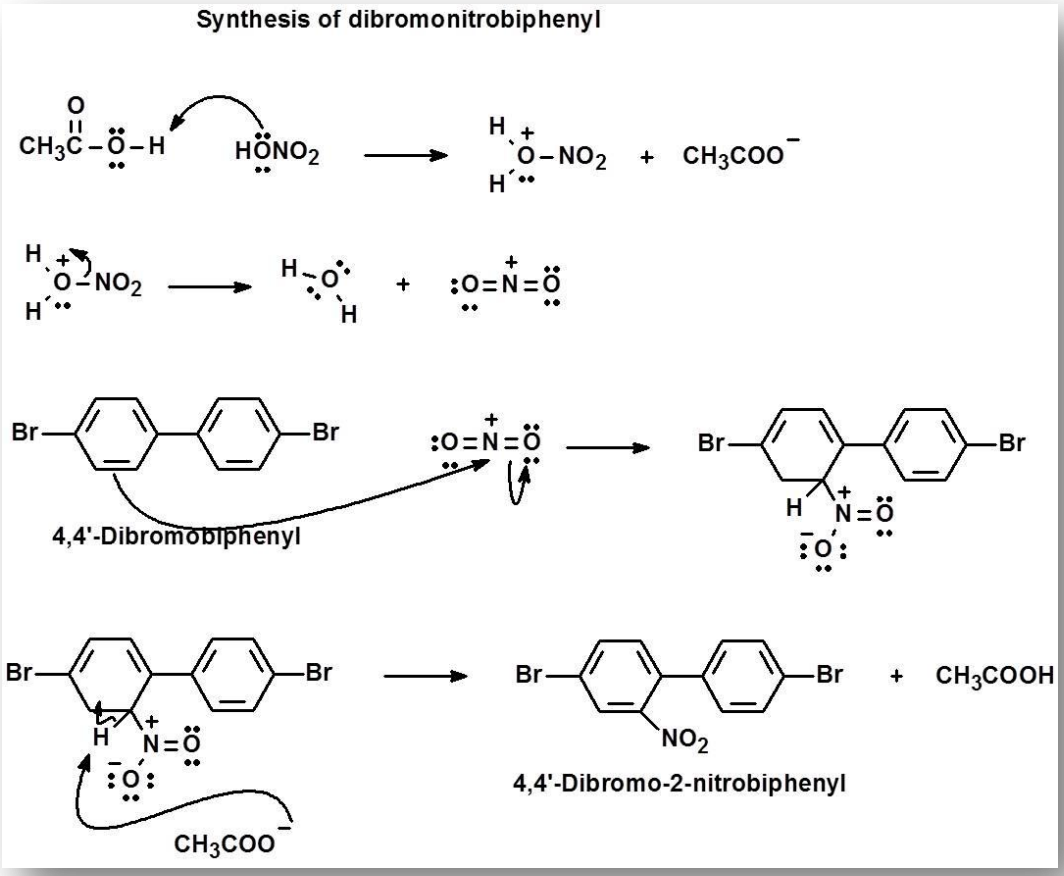

Scheme 3.5: Mechanism for 4,4′-Dibromo-2-nitrobiphenyl Synthesis

Step II:

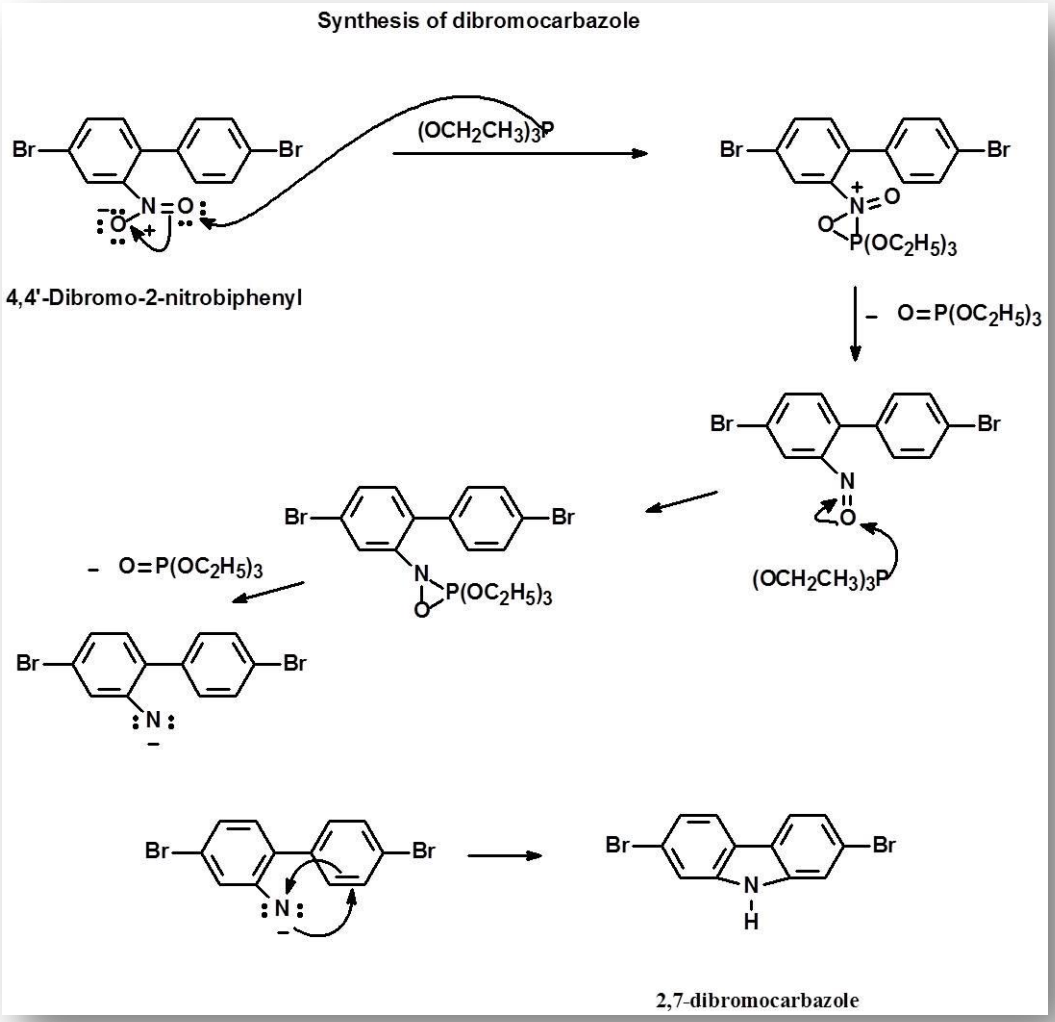

Scheme 3.6: Mechanism for 2,7-Dibromo-NH-carbazole Synthesis

Part-II:

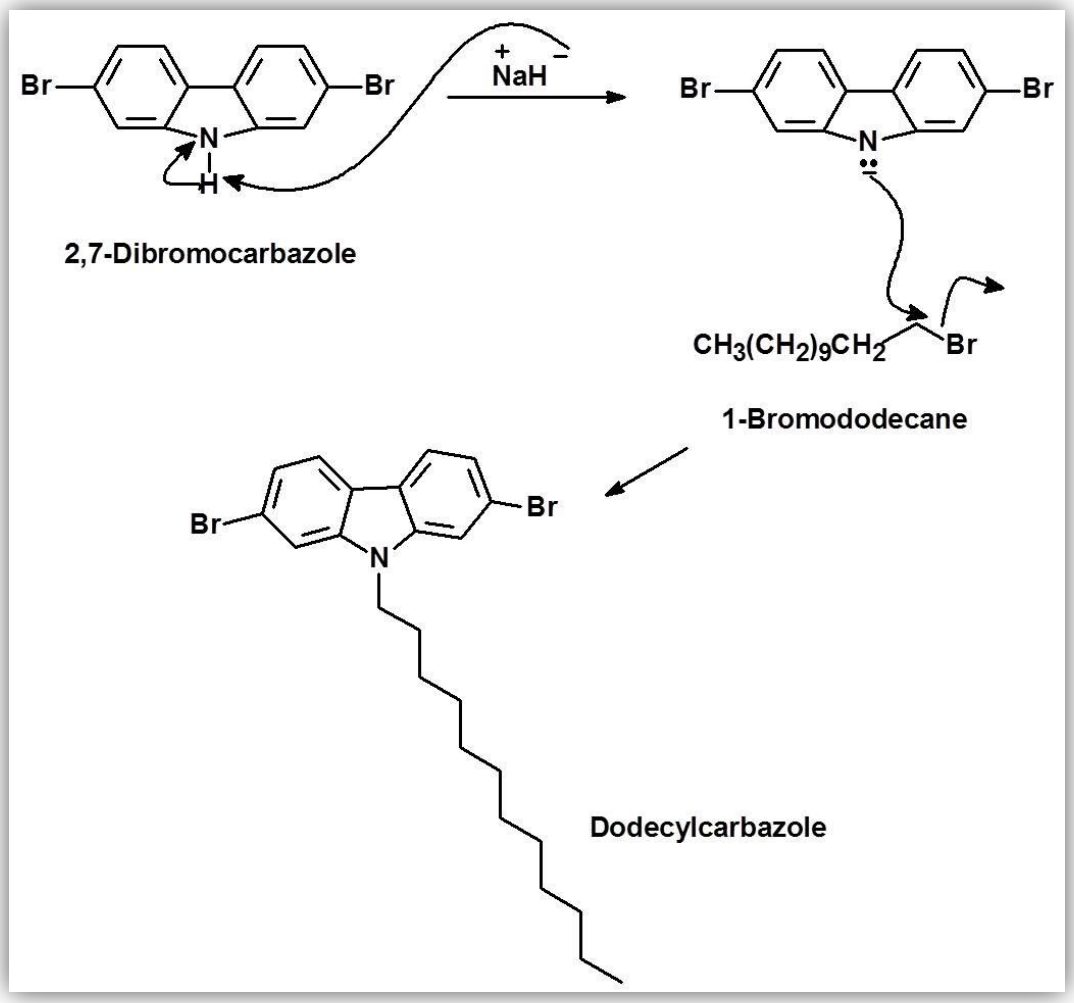

Scheme 3.7: Mechanism for 2,7-Dibromo-N-dodecylcarbazole Synthesis

Chapter 4

DATA AND CALCULATIONS

4.1 Calculation of Maximum Molar Absorptivity (ε_{max})

The maximum molar absorptivity of the compounds is calculated by the following equation (Beer-lamberts low).

$$\varepsilon_{max} = \frac{A}{Cl}$$

Where, ε_{max}: maximum molar absorptivity in $L \cdot mol^{-1} \cdot cm^{-1}$ at λ_{max}

A: Absorbance

C: concentration in $mol \cdot L^{-1}$

l : cell length in cm

ε_{max} Calculation of Cbz:

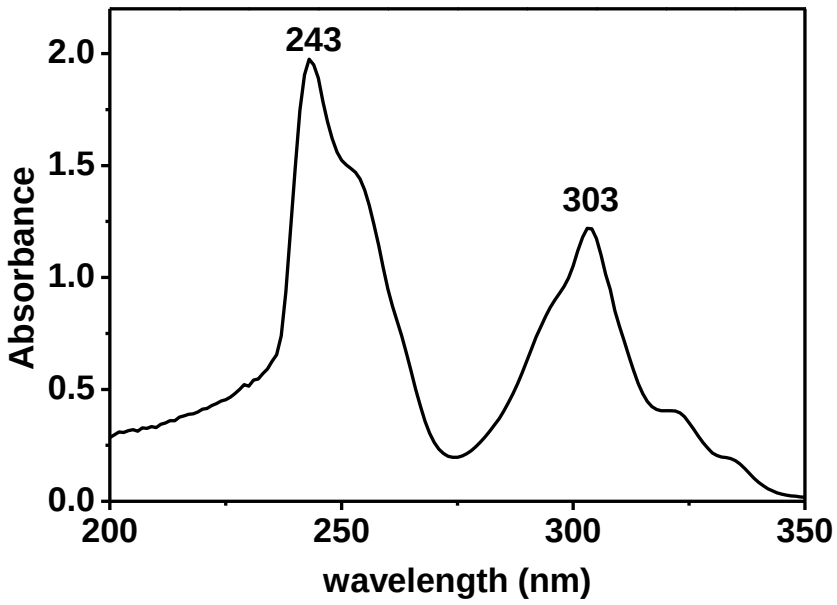

Figure 4.1: Absorption Spectrum of Cbz at 5×10^{-5} M in Chloroform

According to Figure 4.1, the light absorption is 1.218 at $\lambda_{max} = 303$ nm.

⇨ $\varepsilon_{max} = \frac{1.218}{5 \times 10^{-5} M \times 1\text{cm}} = 24360$ L • mol^{-1} • cm^{-1}

⇨ ε_{max} of Cbz $= 24360$ L • mol^{-1} • cm^{-1}

The same procedure and equation is used to calculate the molar absorptivity of both Cbz and Dodecylcbz in different solvents and the data is listed in the Tables 4.1 and 4.2, respectively.

Table 4.1: Molar Absorptivity Data of Cbz in Different Solvents

Solvent	**Concentration**	**Absorbance**	λ_{max}	ε_{max} $(M^{-1}cm^{-1})$
$CHCl_3$	5×10^{-5} M	1.218	303	24360
Methanol	1×10^{-4} M	0.3804	303	7608
DMF	1×10^{-4} M	0.5083	304	10166

Table 4.2: Molar Absorptivity Data of R-Cbz (1×10^{-4}M) in Different Solvents

Solvent	**Asorbance**	$\boldsymbol{\lambda_{max}}$	$\boldsymbol{\varepsilon_{max}}$ $\boldsymbol{(M^{-1}cm^{-1})}$
$CHCl_3$	0.208	308 nm	2080
Acetic acid	0.372	305 nm	3720
THF	0.662	306 nm	6620
TCE	0.413	308 nm	4130
Ethanol	0.565	305 nm	5650
NMP	0.532	306 nm	5320
Methanol	0.202	305 nm	2020
DMF	0.115	309 nm	1150
CH_3CN	0.954	305 nm	9540
DMSO	0.156	307 nm	1560

4.2 Calculations of Full Width Half Maximum (FWHM) of the Selected Absorption ($\Delta\bar{\nu}_{1/2}$)

The full width at half maximum absorptions is called a half-width that can be calculated by the following equation.

$$\Delta\nu_{1/2} = \nu_{I} - \nu_{II}$$

Were,: ν_{I} , ν_{II} : The frequencies from the spectrum (cm^{-1})

$\Delta\nu_{1/2}$: Half-width of the Selected Absorption (cm^{-1})

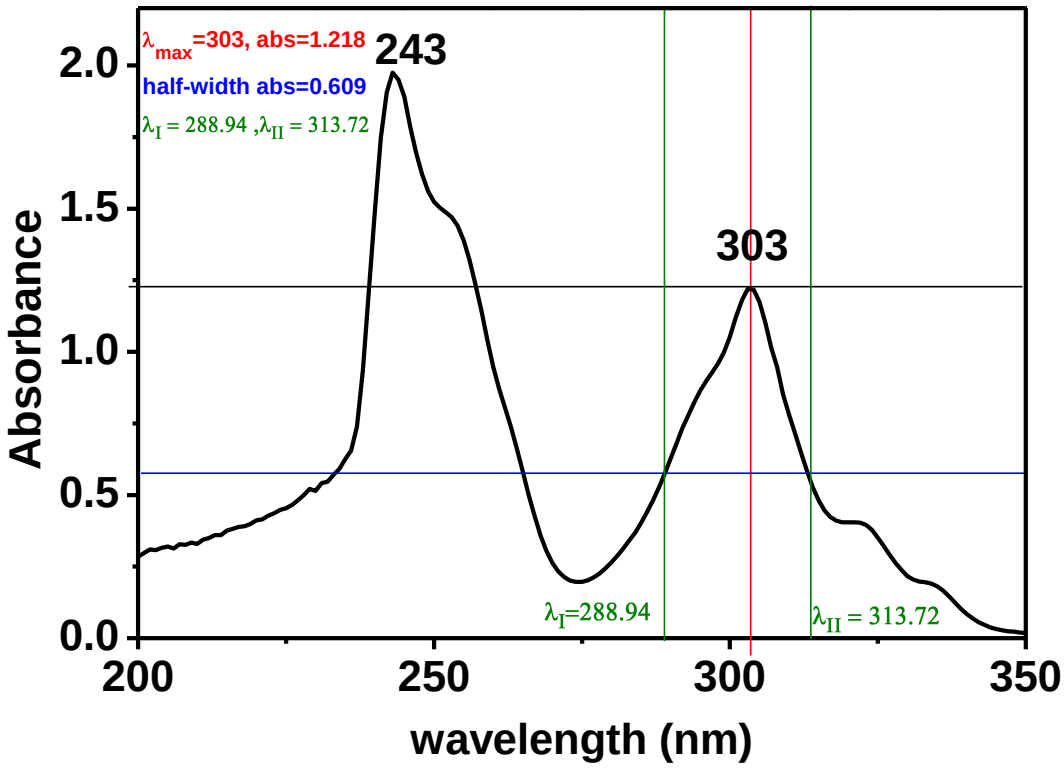

Figure 4.2: FWHM Representation and Absorption Spectrum of Cbz in Chloroform

From the Figure 4.2,

$\lambda_{I} = 288.94$ nm

$\Rightarrow \quad \lambda_{\mathrm{I}} = 288.94\ \mathrm{nm} \times \frac{10^{-9}\mathrm{m}}{1\ \mathrm{nm}} \times \frac{1\mathrm{cm}}{10^{-2}} = 2.8894 \times 10^{-5}\mathrm{cm}$

$\Rightarrow \quad \nu_{\mathrm{I}} = \frac{1}{2.8894 \times 10^{-5}\mathrm{cm}} = 34609.26\ \mathrm{cm}^{-1}$

$\lambda_{\mathrm{II}} = 313.72\ \mathrm{nm}$

$\Rightarrow \quad \lambda_{\mathrm{II}} = 313.72\ \mathrm{nm} \times \frac{10^{-9}\mathrm{m}}{1\ \mathrm{nm}} \times \frac{1\mathrm{cm}}{10^{-2}} = 3.1372 \times 10^{-5}\mathrm{cm}$

$\Rightarrow \quad \nu_{\mathrm{II}} = \frac{1}{3.1372 \times 10^{-5}\mathrm{cm}} = 31875.56\ \mathrm{cm}^{-1}$

$\Delta\nu_{1/2} = \nu_{\mathrm{I}} - \nu_{\mathrm{II}} = 34609.26\ \mathrm{cm}^{-1} - 31875.56\ \mathrm{cm}^{-1} = 2733.7\ \mathrm{cm}^{-1}$

$\Rightarrow \Delta\nu_{1/2} = 2733.7\ \mathrm{cm}^{-1}$

The half-width of the selected absorptions of both of the Cbz and R-Cbz in different solvents were calculated in the same way that shown above and the data are presented in Table 4.3 and Table 4.4, respectively.

Table 4.3: FWHM Data of the Selected Absorptions of Cbz in Different Solvent

Solvent	**Concentration**	$\boldsymbol{\lambda_I}$ **(nm)**	$\boldsymbol{\lambda_{II}}$ **(nm)**	$\boldsymbol{\Delta\nu_{1/2}}$ **(cm^{-1})**
$CHCl_3$	5×10^{-5} M	288	313	2733.7
Methanol	1×10^{-4} M	276	310	3910.7
DMF	1×10^{-4} M	288	312	2593.43

Table 4.4: FWHM of the Selected Absorptions of R-Cbz (1×10^{-4} M) in Different Solvents

Solvent	**$\Delta\nu_{1/2}$(cm^{-1})**
$CHCl_3$	2361.24
Acetic acid	2279.06
THF	2254.96
TCE	2228.62
Ethanol	2215.8
NMP	2370.98
Methanol	2400.64
DMF	3245.85
CH_3CN	2215.8
DMSO	2235.27

4.3 Calculations of Natural Radiative Lifetimes (τ_0)

The natural radiative lifetime of an excited molecule can be calculated from the equation:

$$\tau_0 = \frac{3.5 \times 10^8}{\nu_{max}^2 \times \varepsilon_{max} \times \Delta\nu_{1/2}}$$

Where, τ_0: Natural radiative lifetime (ns)

ν_{max} : Frequency of the maximum absorption band (cm^{-1})

ε_{max}: Maximum molar absorptivity in $L \cdot mol^{-1} \cdot cm^{-1}$ at λ_{max}

$\Delta\nu_{1/2}$: Full width half maximum of the selected absorption (cm^{-1})

Theoretical Radiative Lifetime of Cbz:

With the help of calculated (ν_{max} and $\Delta\nu_{1/2}$) of selected absorptions of Cbz,

From the Figures 4.1 and 4.2, at $\lambda_{max} = 303$

$$\lambda_{max} = 303 \text{ nm} \times \frac{10^{-9}\text{m}}{1\text{ nm}} \times \frac{1\text{cm}}{10^{-2}} = 3.03 \times 10^{-5}\text{cm}$$

$$\Rightarrow \quad \nu_{max} = \frac{1}{3.03\times10^{-5}\text{cm}} = 33003.3 \text{ cm}^{-1}$$

$$\Rightarrow \quad \nu_{max}^2 = (33003.3 \text{ cm}^{-1})^2 = 1.089 \times 10^9 \text{cm}^{-2}$$

Now, can be calculate the theoretical radiative lifetime of compounds from the above mentioned equation,

$$\tau_0 = \frac{3.5 \times 10^8}{\nu_{max}^2 \times \varepsilon_{max} \times \Delta\nu_{1/2}} = \frac{3.5 \times 10^8}{(33003.3)^2 \times 24360 \times 2733.7}$$

$$\Rightarrow = 4.82 \times 10^{-9}\text{s}$$

$$\Rightarrow \ _0 = 4.82 \text{ ns}$$

With the similar manner, the natural radiative lifetimes of both of the Cbz and R−Cbz in different solvents were calculated and the data were presented below in Tables 4.5 and 4.6, respectively.

Table 4.5: τ_0 of Cbz in Different Solvents

Solvent	**Concentration**	$\boldsymbol{\tau_0}$ **(ns)**
$CHCl_3$	5×10^{-5} M	4.82
Methanol	1×10^{-4} M	10.8
DMF	1×10^{-4} M	12.2

Table 4.6: τ_0 of R-Cbz (1×10^{-4} M) Measured in Different Solvents

Solvent	$\boldsymbol{\tau_0}$ **(ns)**
$CHCl_3$	67.69
Acetic acid	38.43
THF	21.9
TCE	36.07
Ethanol	26.03
NMP	26.00
CH_3OH	67.3
DMF	89.7
CH_3CN	15.41
DMSO	94.6

4.4 Calculation of Fluorescence Rate Constants (k_f)

The k_f of the synthesized compounds can be calculated by the equation:

$$k_f = \frac{1}{\tau_0}$$

Where, k_f: Fluorescence rate constant (s^{-1})

$\boldsymbol{\tau_0}$: Theoretical radiative lifetime (s)

Fluorescence Rate Constant of Cbz:

⇨ $k_f = \frac{1}{4.82\times 10^{-9}\text{s}} = 2.07 \times 10^{8}\text{s}^{-1}$

⇨ $k_f = 2.07 \times 10^{8} s^{-1}$

The fluorescence rate constant of Cbz and R-Cbz in different solvents were obtained theoretically in the similar methods that shown above and the data of both of them were presented in Tables 4.7 and 4.8, respectively.

Table 4.7: Fluorescence Rate Constants of Carbazole in Different Solvents

Solvent	**Concentration**	$\boldsymbol{\tau_{0\ (ns)}}$	$\boldsymbol{k_f\ (s^{-1})}$
$CHCl_3$	5×10^{-5}M	4.82	2.07×10^{8}
Methanol	1×10^{-4}M	10.8	9.25×10^{7}
DMF	1×10^{-4}M	12.2	8.19×10^{7}

Table 4.8: Fluorescence Rate Constants of Dodecylcbz (1×10^{-4}) in Different Solvents

Solvent	$\tau_{0\ (ns)}$	$k_f\ (s^{-1})$
$CHCl_3$	67.69	1.47×10^7
Acetic acid	38.43	2.60×10^7
THF	21.9	4.56×10^7
TCE	36.07	2.77×10^7
Ethanol	26.03	3.84×10^7
NMP	26.00	3.84×10^7
Methanol	67.3	1.48×10^7
CH_3CN	15.41	6.48×10^7
DMSO	94.6	1.07×10^7

4.5 Calculation of Oscillator Strengths (f)

The electronic transition strength of an electron that deduced by dimensionless quantity is called oscillator strength. It can be calculated by the following equation:

$$f = 4.32 \times 10^{-9} \times \Delta\nu_{1/2} \; \varepsilon_{max}$$

Where, f: Oscillator Strength

$\Delta\nu_{1/2}$: Half-width of the Selected Absorption (cm^{-1})

ε_{max}: maximum molar absorptivity in $L \cdot mol^{-1} \cdot cm^{-1}$ at maximum wavelength (λ_{max})

Oscillator Strength of Cbz:

$\Rightarrow f = 4.32 \times 10^{-9} \times \Delta\nu_{1/2} \; \varepsilon_{max}$

$\Rightarrow f = 4.32 \times 10^{-9} \times 2733.7 \times 24360$

$\Rightarrow f = 2.87 \times 10^{-1}$

The calculated oscillator strength of radiationless deactivation for Cbz and R-Cbz in different solvents was shown in the following tables.

Table 4.9: Oscillator Strength Data of Cbz Measured in Different Solvents

Solvent	**Concentration**	f
$CHCl_3$	5×10^{-5}M	0.287
Methanol	1×10^{-4}M	0.128
DMF	1×10^{-4}M	0.011

Table 4.10: Oscillator Strength Data of R-Cbz (1×10^{-4}) Measured in Different Solvents

Solvent	$\Delta\nu_{1/2}$ **(cm^{-1})**	ε_{max} **(M^{-1} cm^{-1})**	f
$CHCl_3$	2361.24	2080	0.0212
Acetic acid	2279.06	3720	0.0366
THF	2254.96	6620	0.0644
TCE	2228.62	4130	0.0397
Ethanol	2215.8	5650	0.0540
NMP	2370.98	5320	0.0544
Methanol	2400.64	2020	0.0209
DMF	3245.85	1150	0.0161
CH_3CN	2215.8	9540	0.0913
DMSO	2235.27	1560	0.0150

4.6 Calculations of Singlet Energies (E_s)

The required amount of energy to promote the electron from the ground state of chromophore to an excited state is called singlet energy.

$$E_s = \frac{2.86 \times 10^5}{\lambda_{max}}$$

Where, E_s: the singlet energy in unit of (kcal . mol^{-1})

λ_{max}: The maximum absorption wavelength in unit of $\mathring{A}$

Singlet Energy of Cbz:

$E_s = \frac{2.86 \times 10^5}{\lambda_{max}} = \frac{2.86 \times 10^5}{3030} = 94.39 \text{ kcal} \cdot \text{mol}^{-1}$

$E_s = 94.39 \text{ kcal} \cdot \text{mol}^{-1}$

The singlet energies of Cbz and R-Cbz were calculated in the similar ways that shown above and were tabulated below in the tables Table 4.11 and 4.12, respectively.

Table 4.11: Singlet Energy Data of Carbazole Measured in Different Solvents

Solvent	**Concentration**	**E_s (kcal mol^{-1})**
$CHCl_3$	5×10^{-5}M	94.39
Methanol	1×10^{-4}M	94.39
DMF	1×10^{-4}M	94.08

Table 4.12: Singlet Energy Data of R-Cbz (1×10^{-4}) Measured in Different Solvents

Solvent	**Cut off λ (Å)**	E_s **(kcal mol^{-1})**
$CHCl_3$	3080	92.86
Acetic acid	3050	93.77
THF	3060	93.46
TCE	3080	92.86
Ethanol	3050	93.77
NMP	3060	93.46
Methanol	3050	93.77
DMF	3090	92.56
CH_3CN	3050	93.77
DMSO	3070	93.16

4.7 Calculation of Optical Band Gap Energies (E_g)

The measurement of the optical band gap energies of materials can be calculated from:

$$E_g = \frac{1240 \text{ eV nm}}{\lambda}$$

Where, E_g: energy band gap in units of eV

λ: Cut-off wavelength of the absorption band in units of nm

Band Gap Energy of Cbz:

From the maximum absorption band, can be estimated cut-off wavelength of the absorption band by induction it to zero.

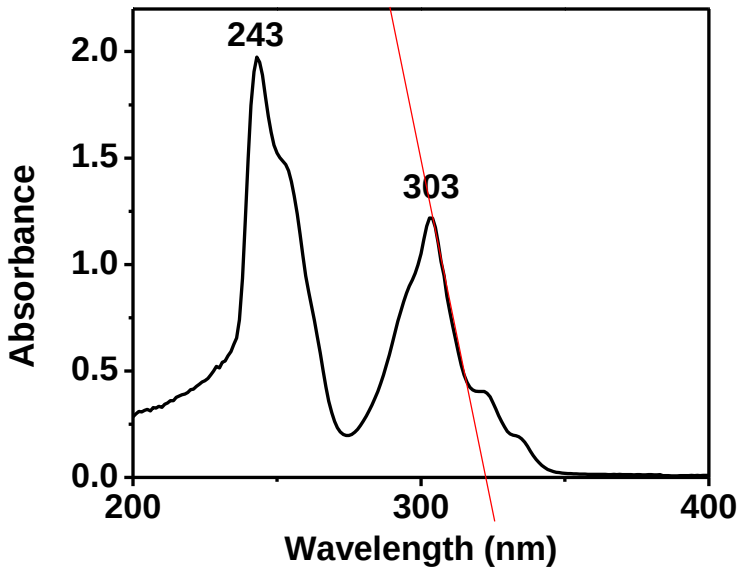

Figure 4.3: Cut-Off Wavelength is Shown on the Absorption Spectrum of Cbz

$$E_g = \frac{1240 \text{ eV nm}}{\lambda}$$

$$\Rightarrow E_g = \frac{1240 \text{ eV nm}}{\lambda} = \frac{1240 \text{ eV nm}}{322.87} = 3.84 \text{ ev}$$

$$E_g = 3.84 \text{ ev}$$

The band gap energies of Cbz and R-Cbz in different solvents were calculated in the similar ways that used above for carbazole itself in $CHCl_3$ and listed in the following tables.

Table 4.13: Band Gap Energies Data of Carbazole Measured in Different Solvents
Band Gap Energies Data of Carbazole Measured in Different Solvents

Solvent	**Concentration**	**Cut-off λ**	E_g **(eV)**
$CHCl_3$	5×10^{-5}M	322.87	3.84
Methanol	1×10^{-4}M	316.03	3.92
DMF	1×10^{-4}M	319.41	3.88

Table 4.14: Band Gap Energies Data of R-Cbz (1×10^{-4}M) Measured in Different Solvents

Solvent	**Cut-off λ**	E_g **(eV)**
$CHCl_3$	318.88	3.88
Acetic acid	315.05	3.93
THF	315.50	3.93
TCE	319.05	3.88
Ethanol	314.52	3.94
NMP	316.21	3.92
Methanol	315.41	3.93
DMF	320.03	3.87
CH_3CN	314.52	3.94
DMSO	316.74	3.91

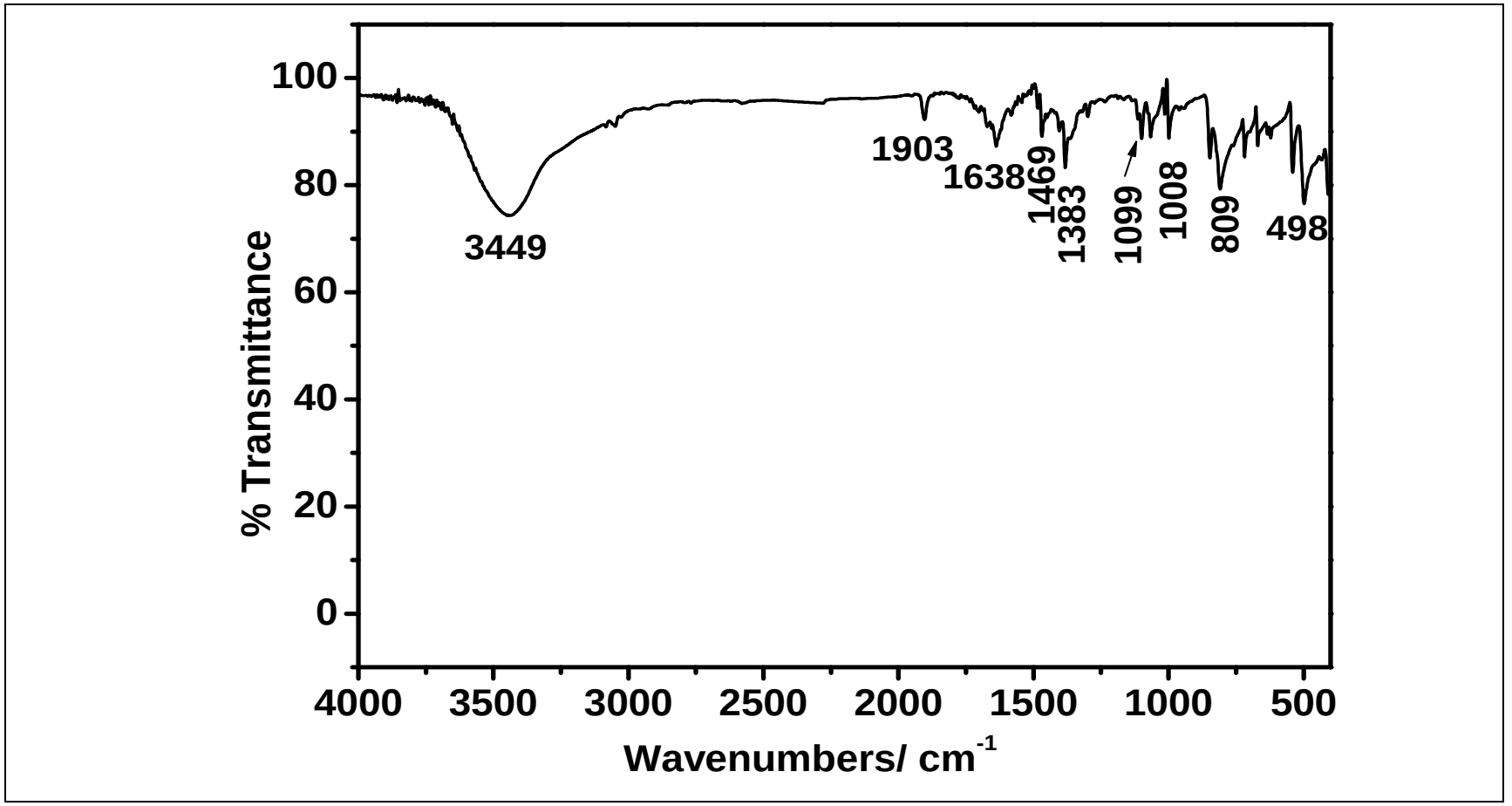

Figure 4.4: FTIR Spectrum of DBBP

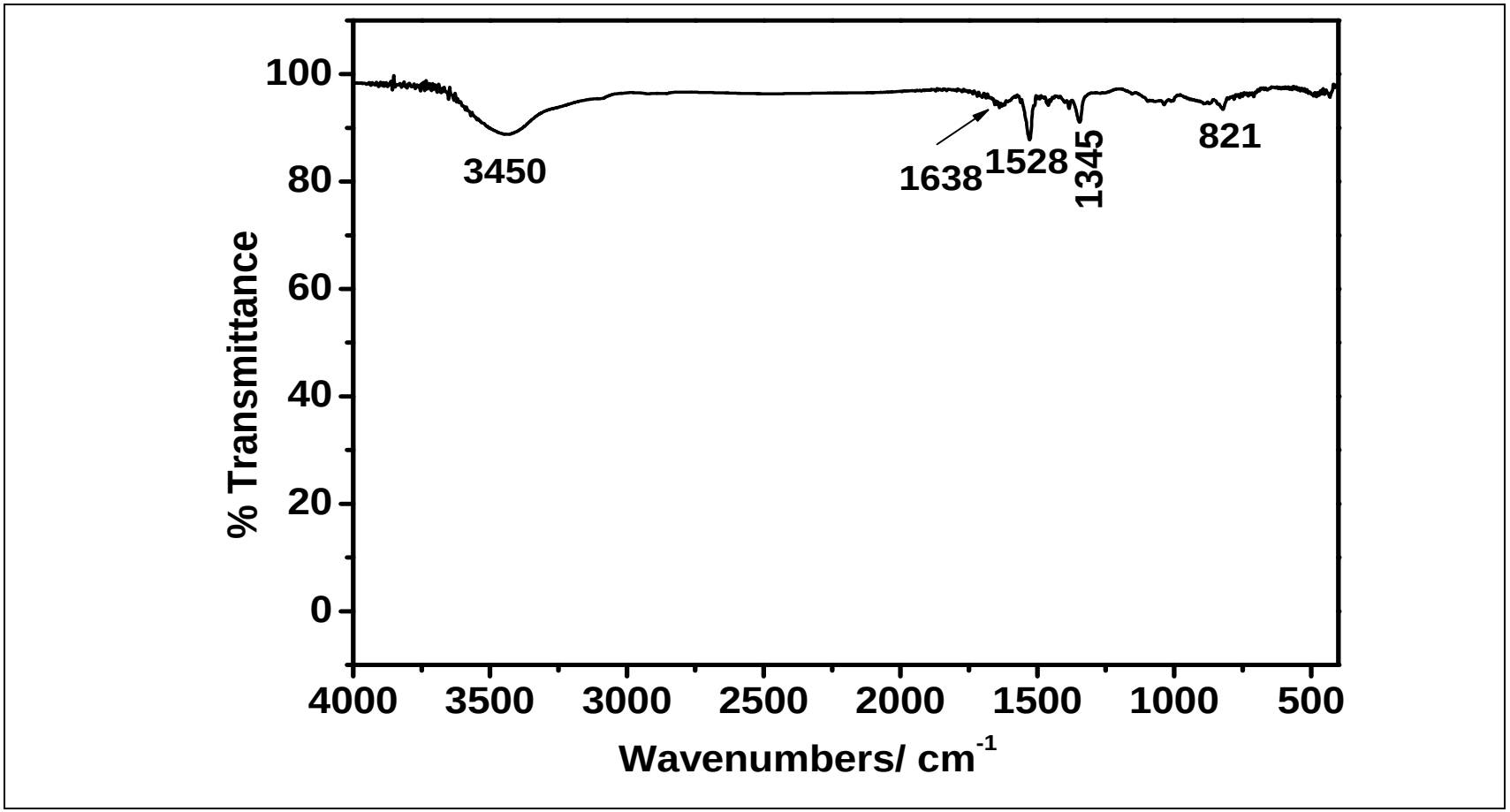

Figure 4.5: FTIR Spectrum of DBNBP

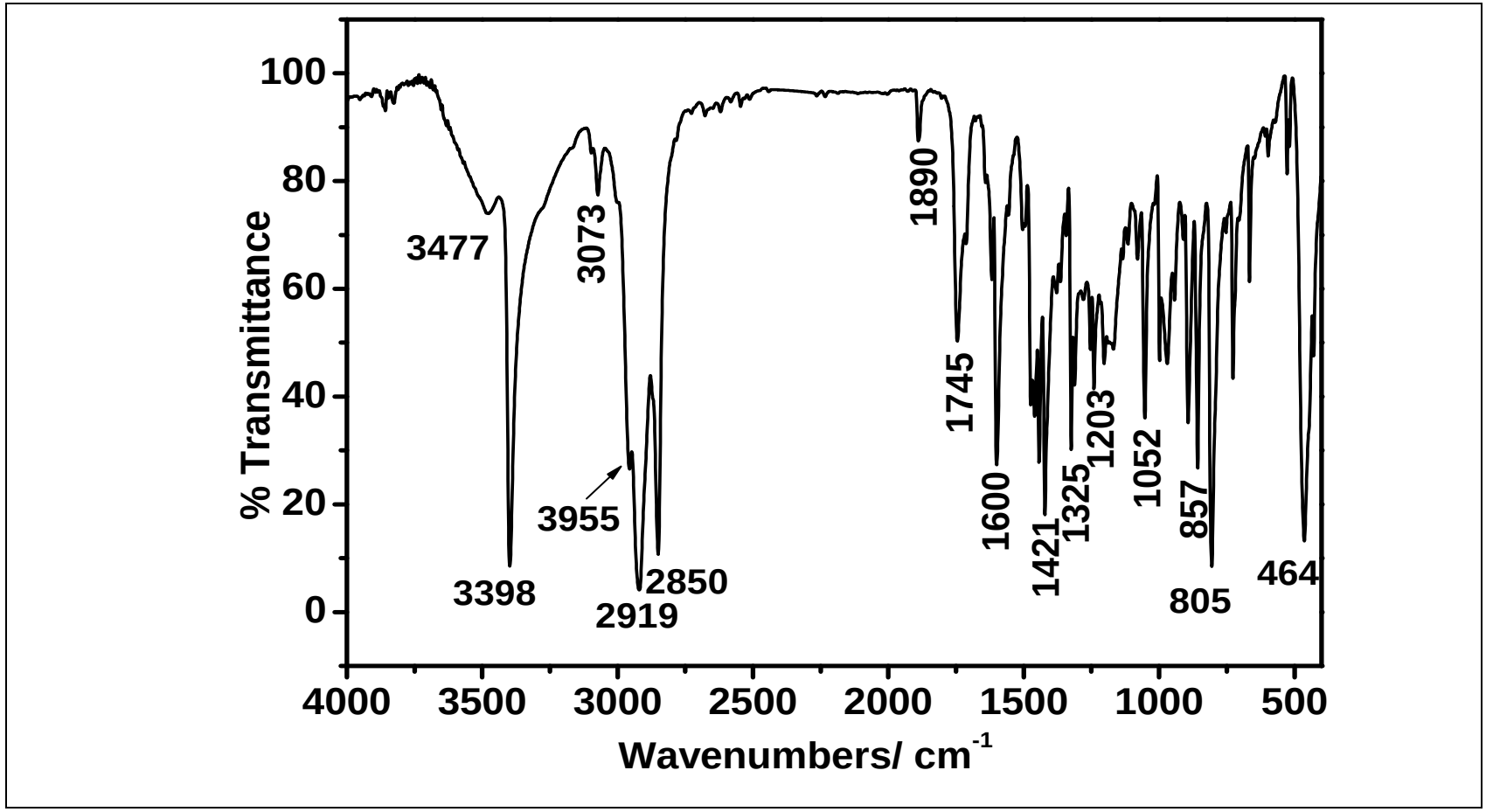

Figure 4.6: FTIR Spectrum of Cbz

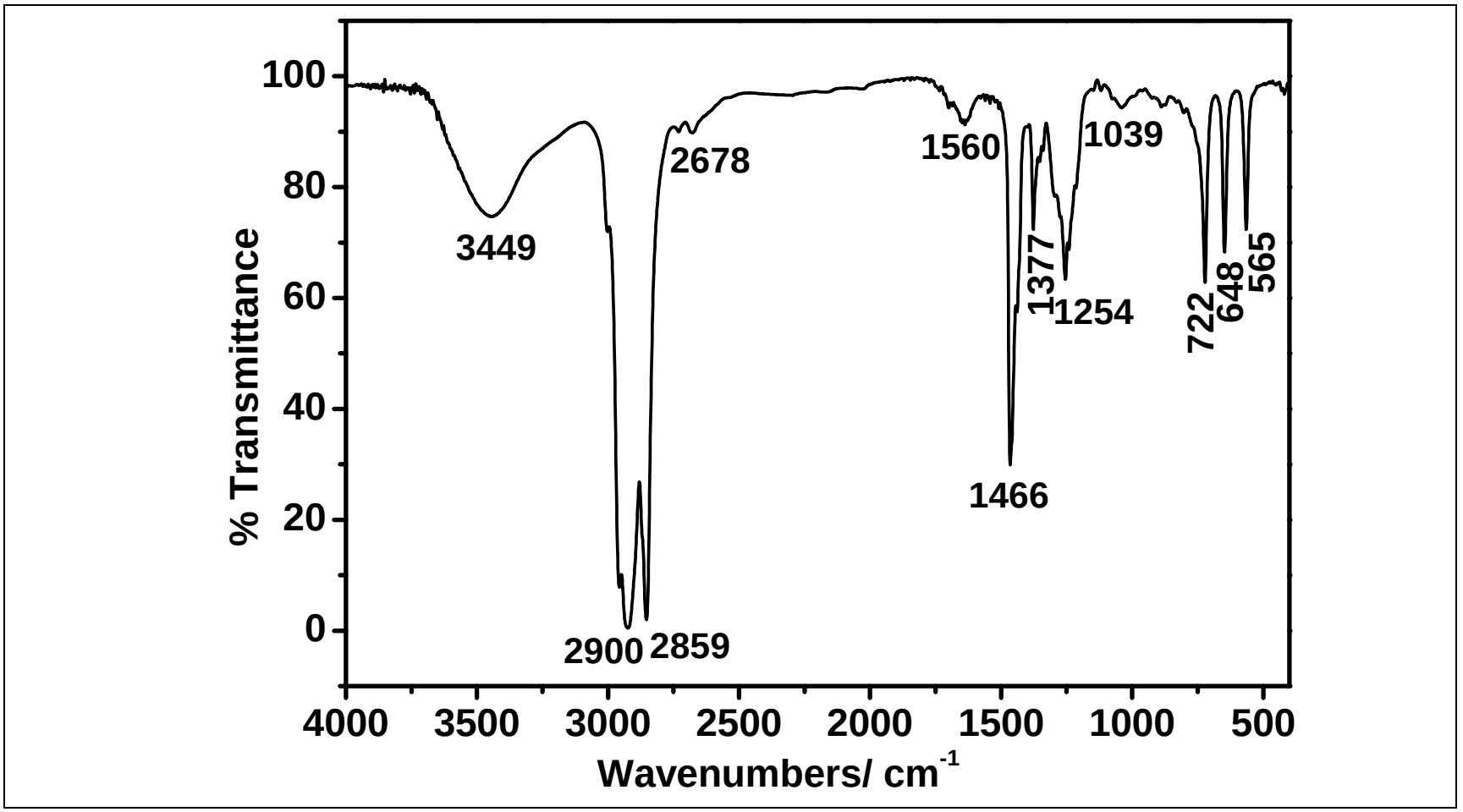

Figure 4.7: FTIR Spectrum of R-Br

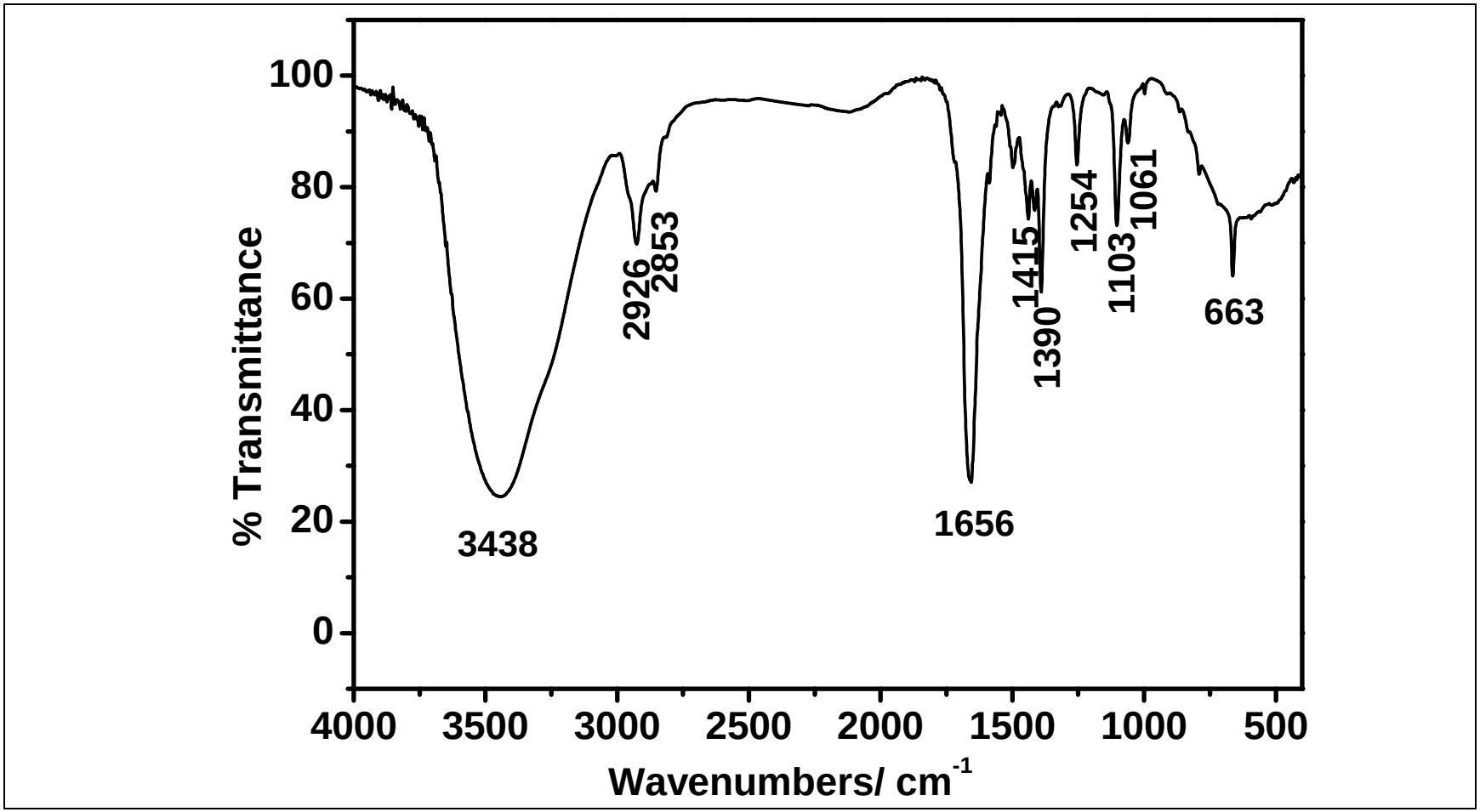

Figure 4.8: FTIR Spectrum of Dodecylcarbazole R-Cbz

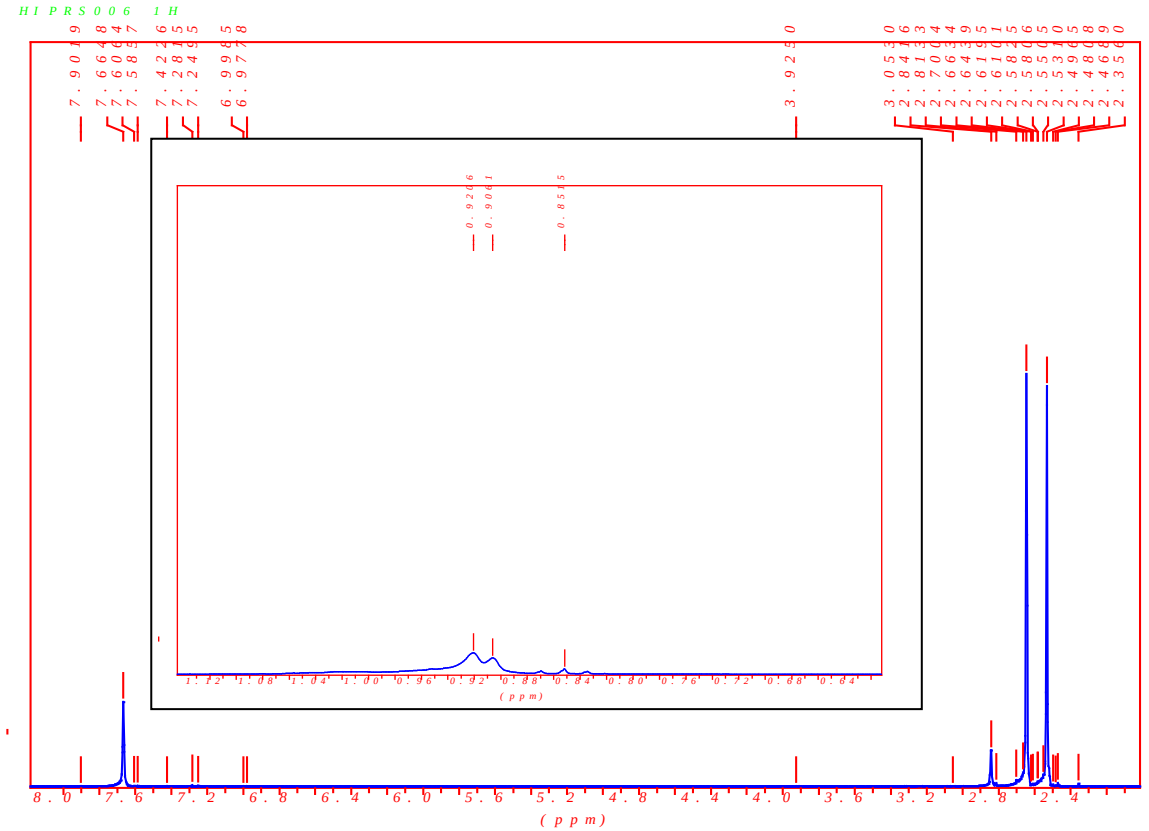

Figure 4.9: ^{1}H NMR Spectrum of R-Cbz in $CDCl_3$

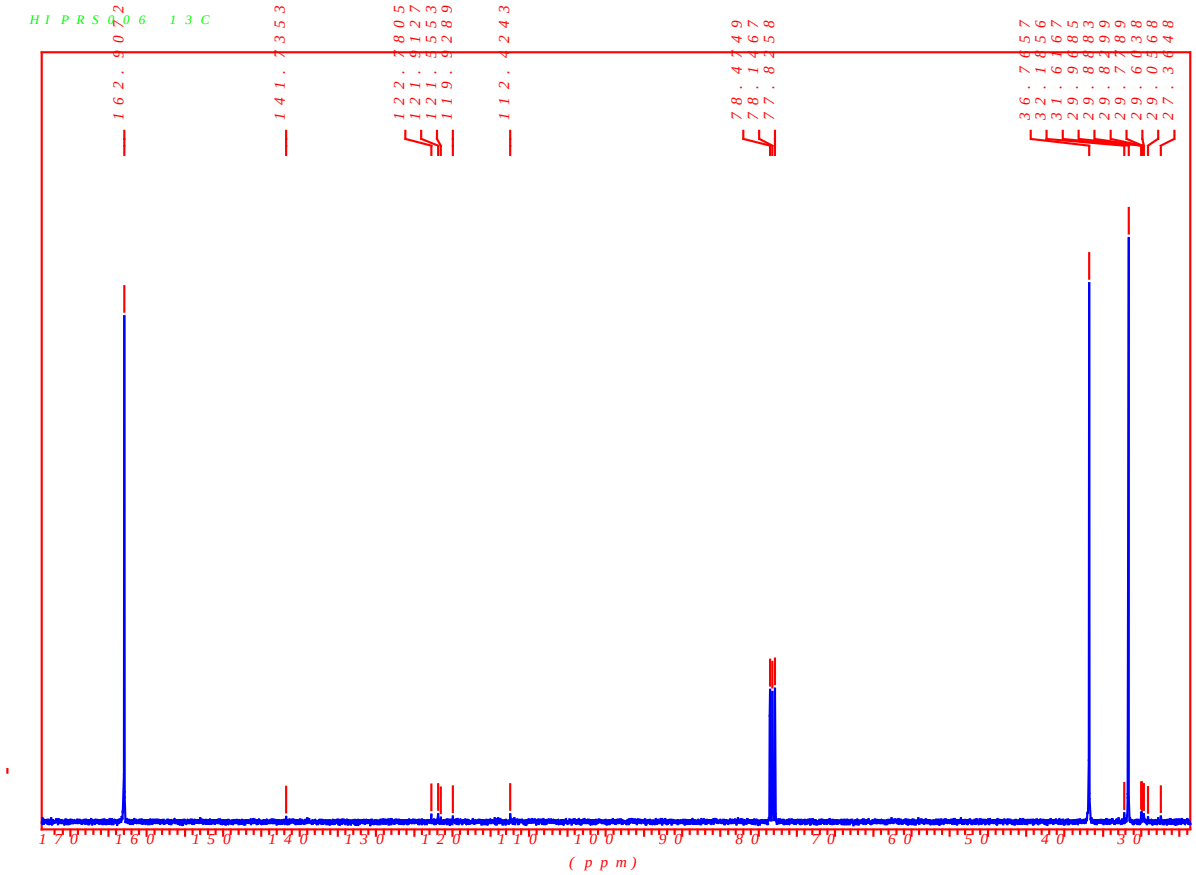

Figure 4.10: ^{13}C NMR Spectrum of R-Cbz in $CDCl_3$

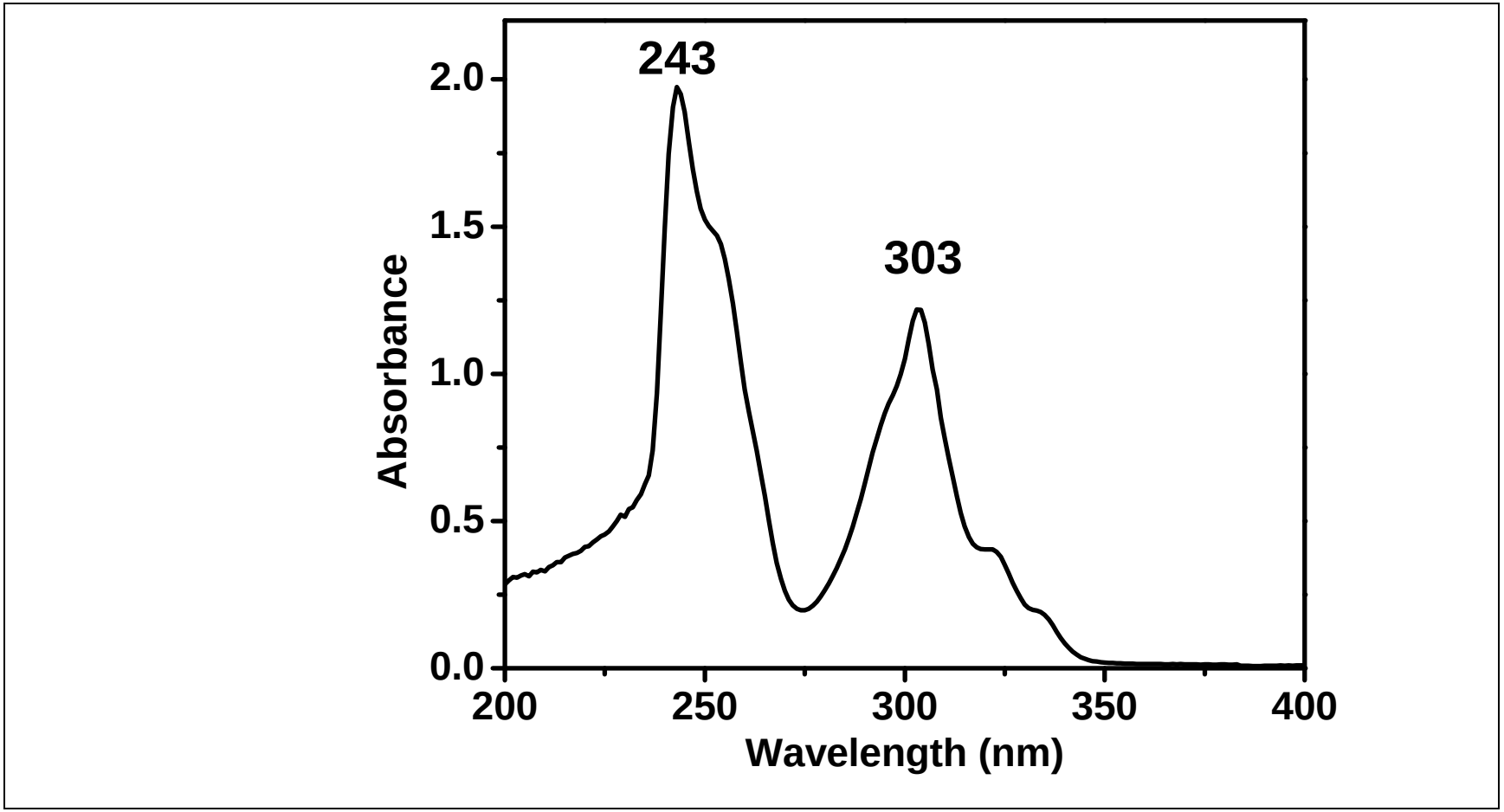

Figure 4.11: UV-vis Absorption of Cbz in $CHCl_3$

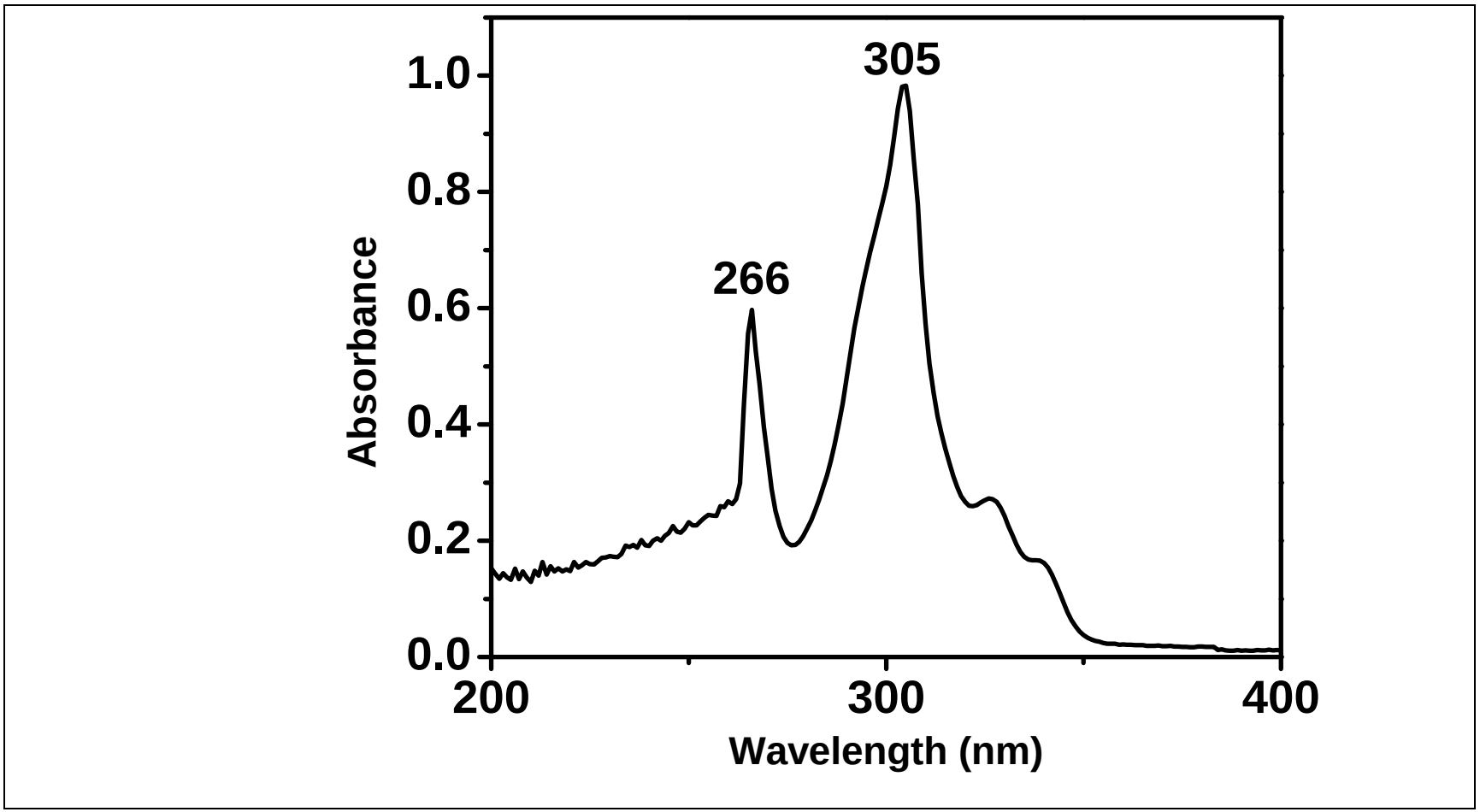

Figure 4.12: UV-vis Absorption of Cbz in DMF

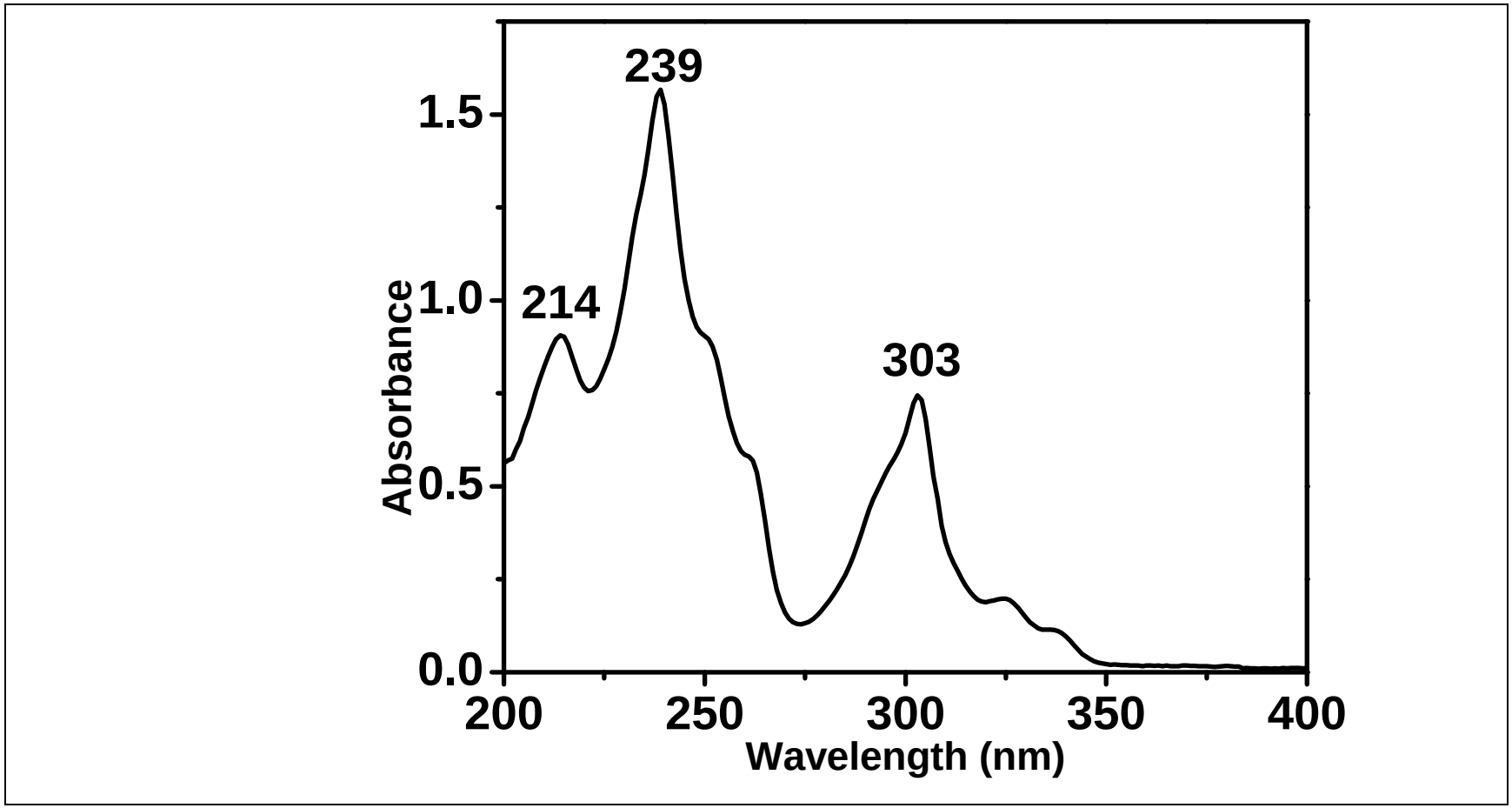

Figure 4.13: UV-vis Absorption of Cbz in Methanol

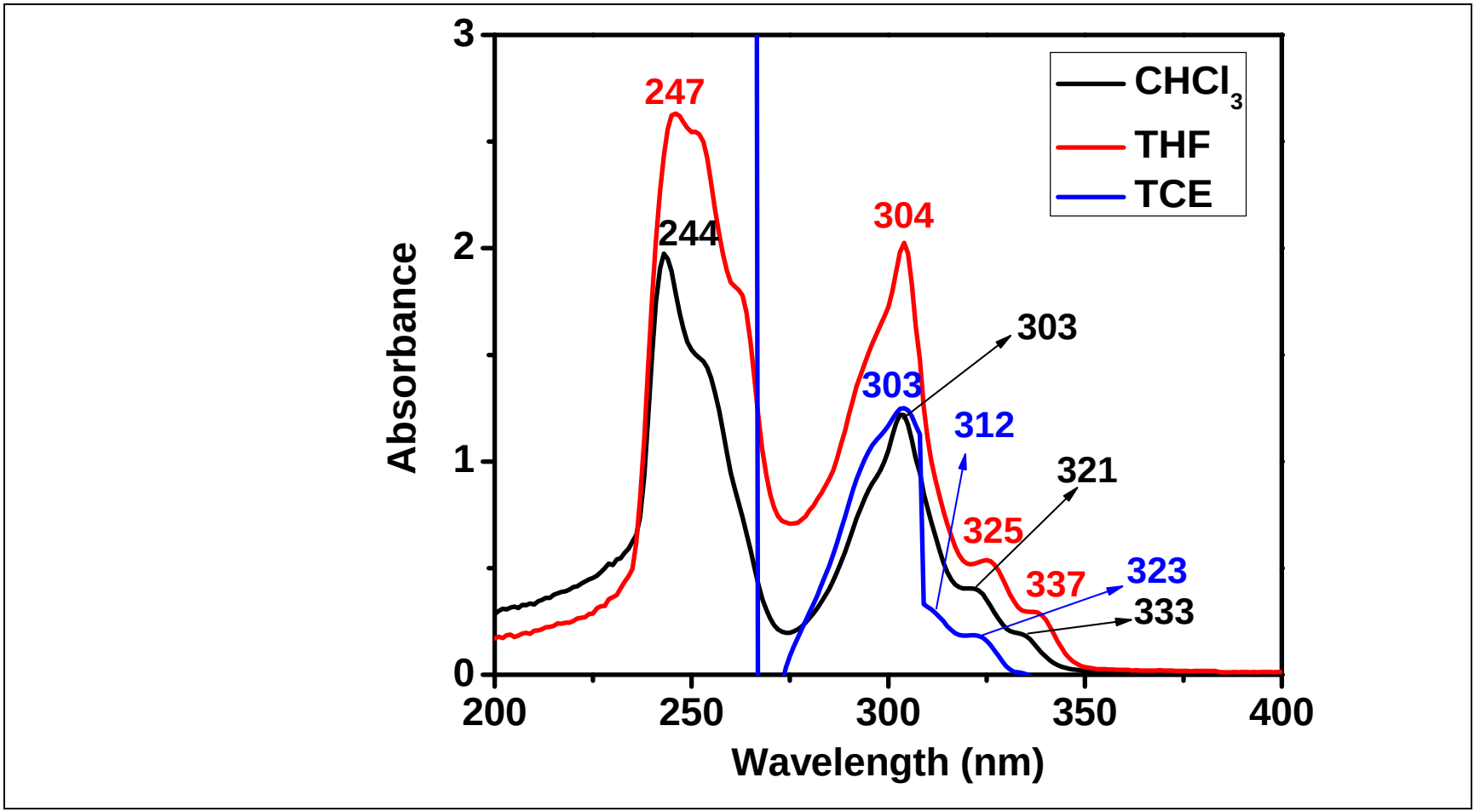

Figure 4.14: UV-vis Absorption Spectra of Cbz in Various Nonpolar Solvents

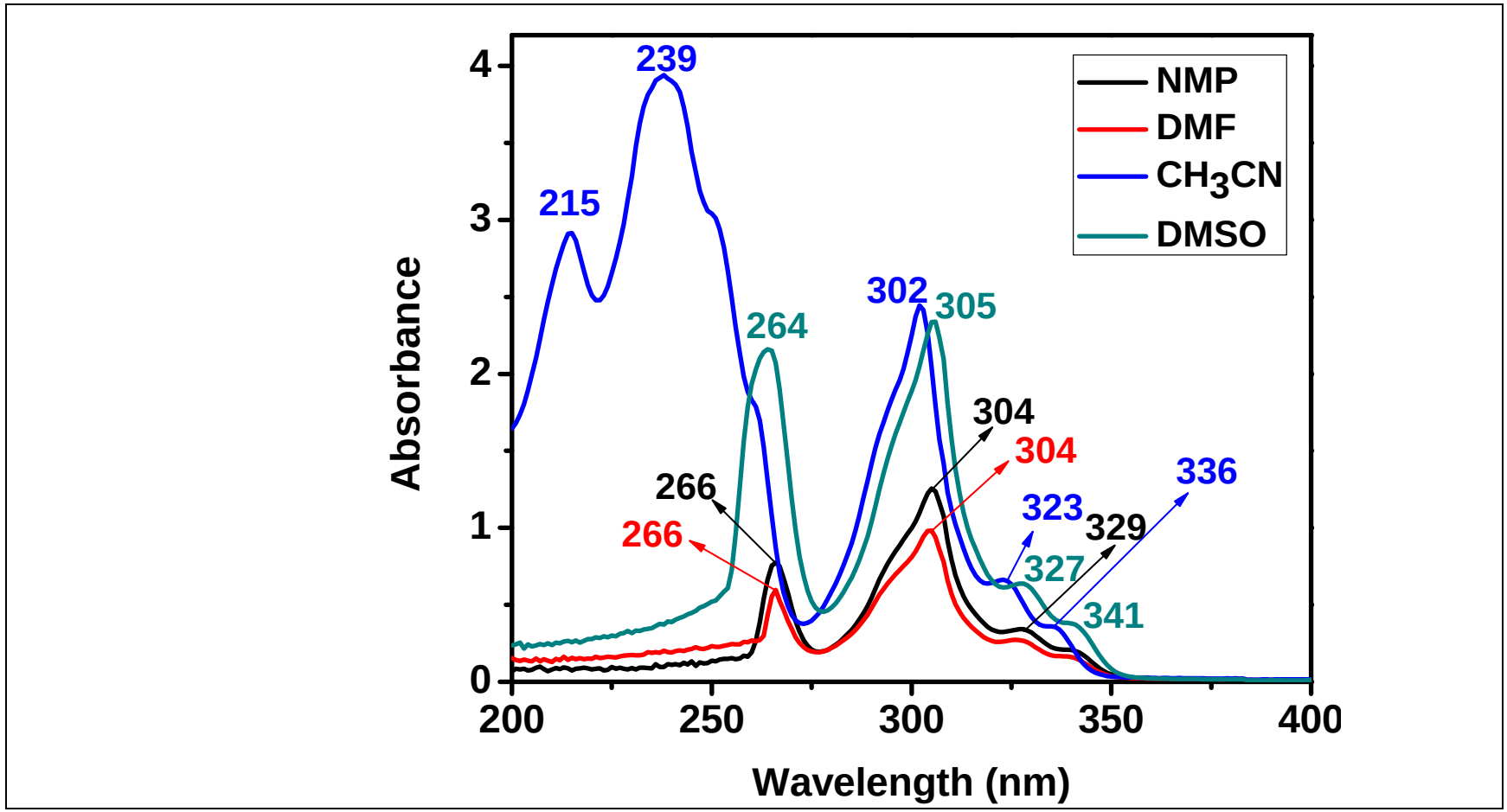

Figure 4.15: UV-vis Absorption Spectra of Cbz in Various Dipolar Aprotic Solvents

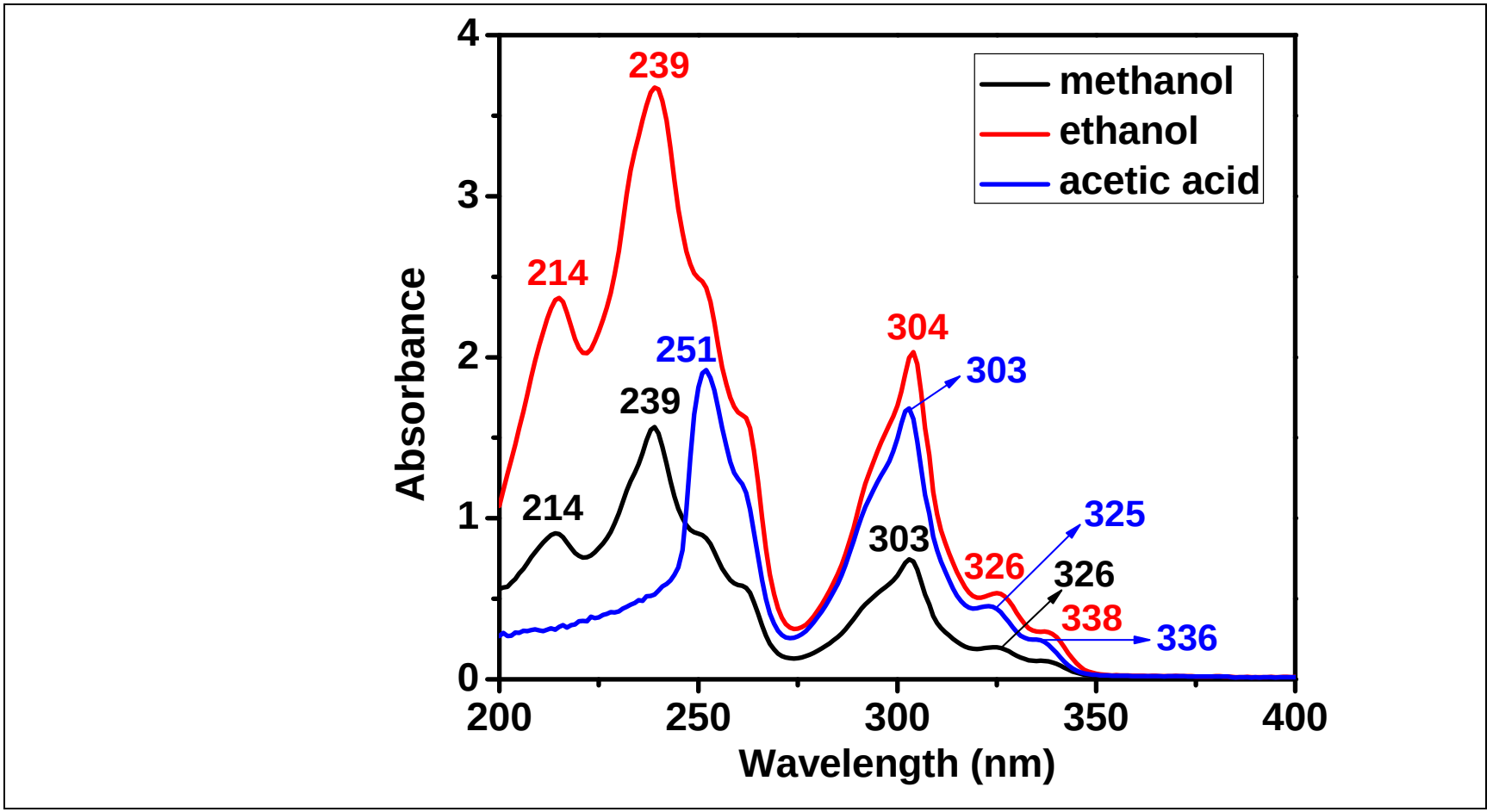

Figure 4.16: UV-vis Absorption Spectra of Cbz in Various Polar Protic Solvents

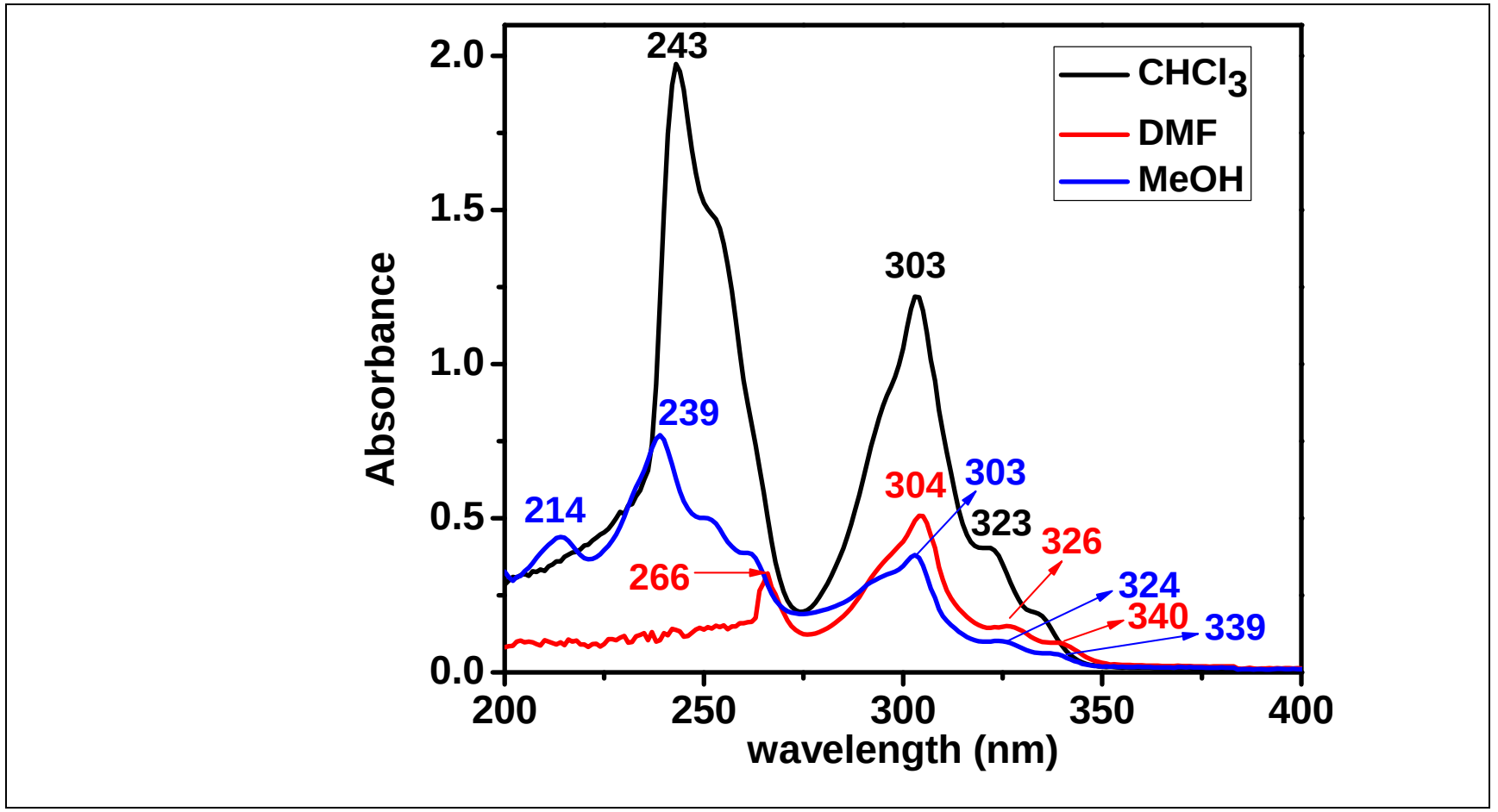

Figure 4.17: Comparison of UV-vis Absorption Spectra of Cbz in Solvents of Different Polarity

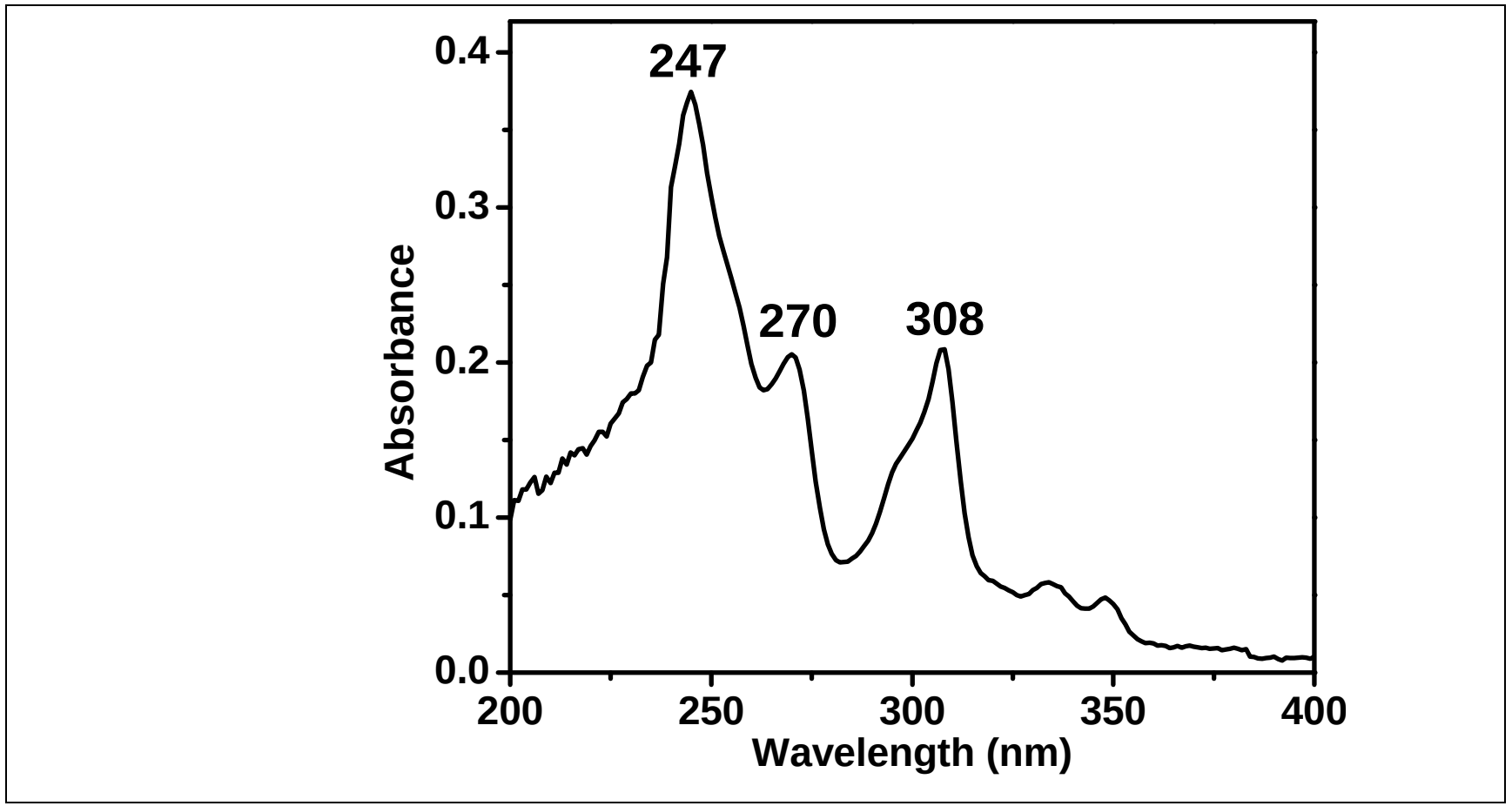

Figure 4.18: UV-vis Absorption Spectrum of R-Cbz in $CHCl_3$

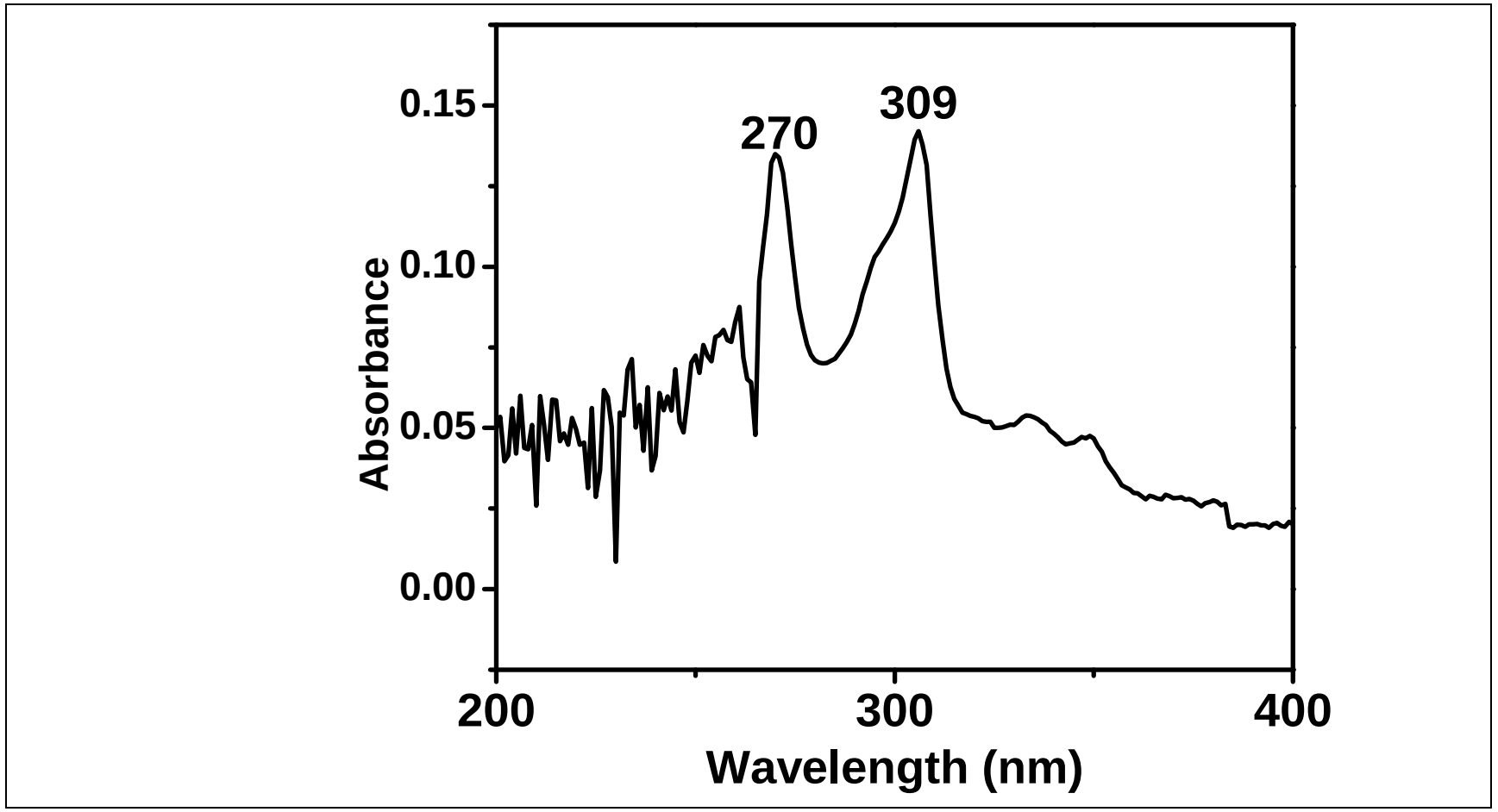

Figure 4.19: UV-vis Absorption Spectrum of R-Cbz in DMF

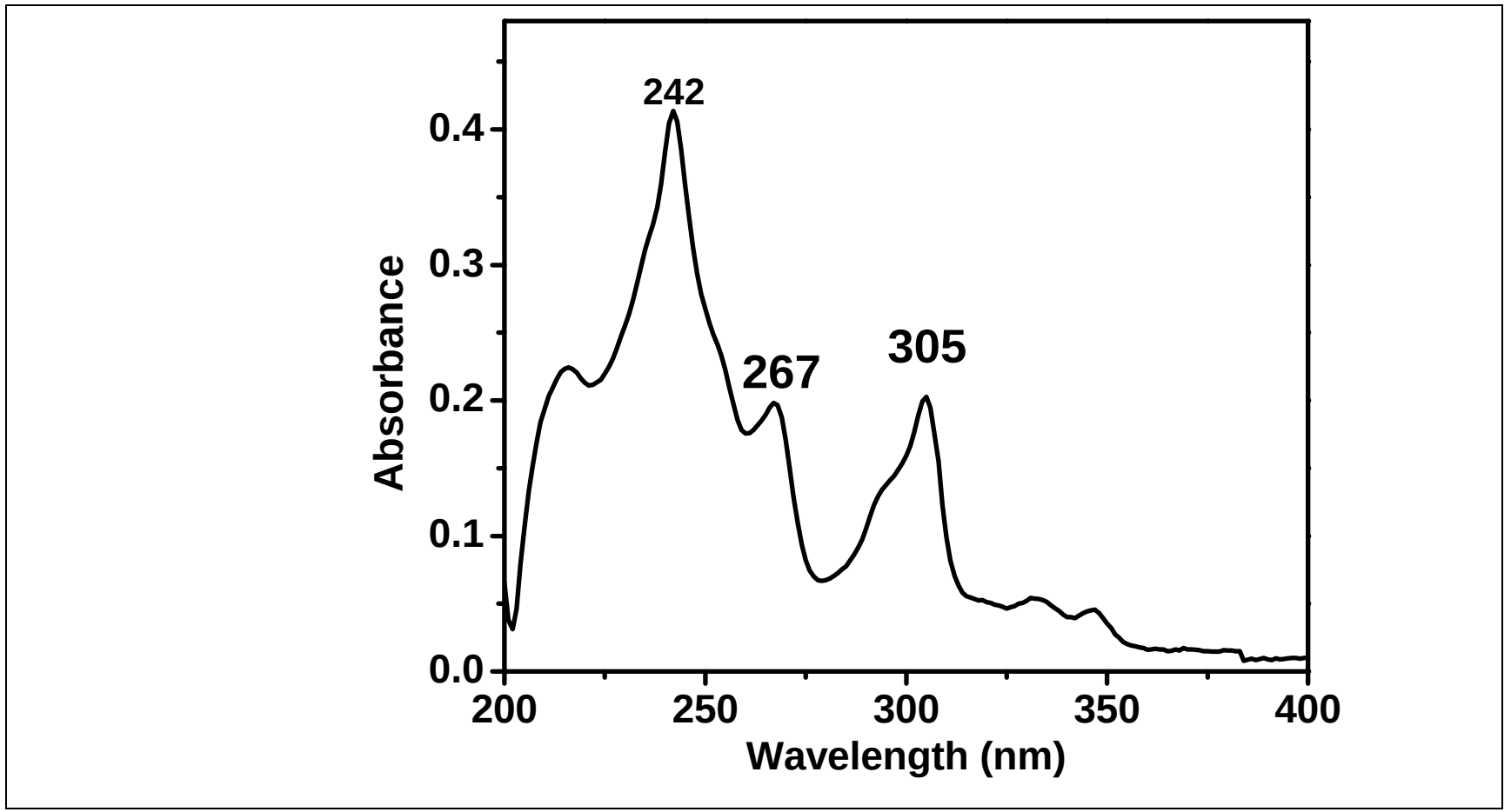

Figure 4.20: UV-vis Absorption Spectrum of R-Cbz in Methanol

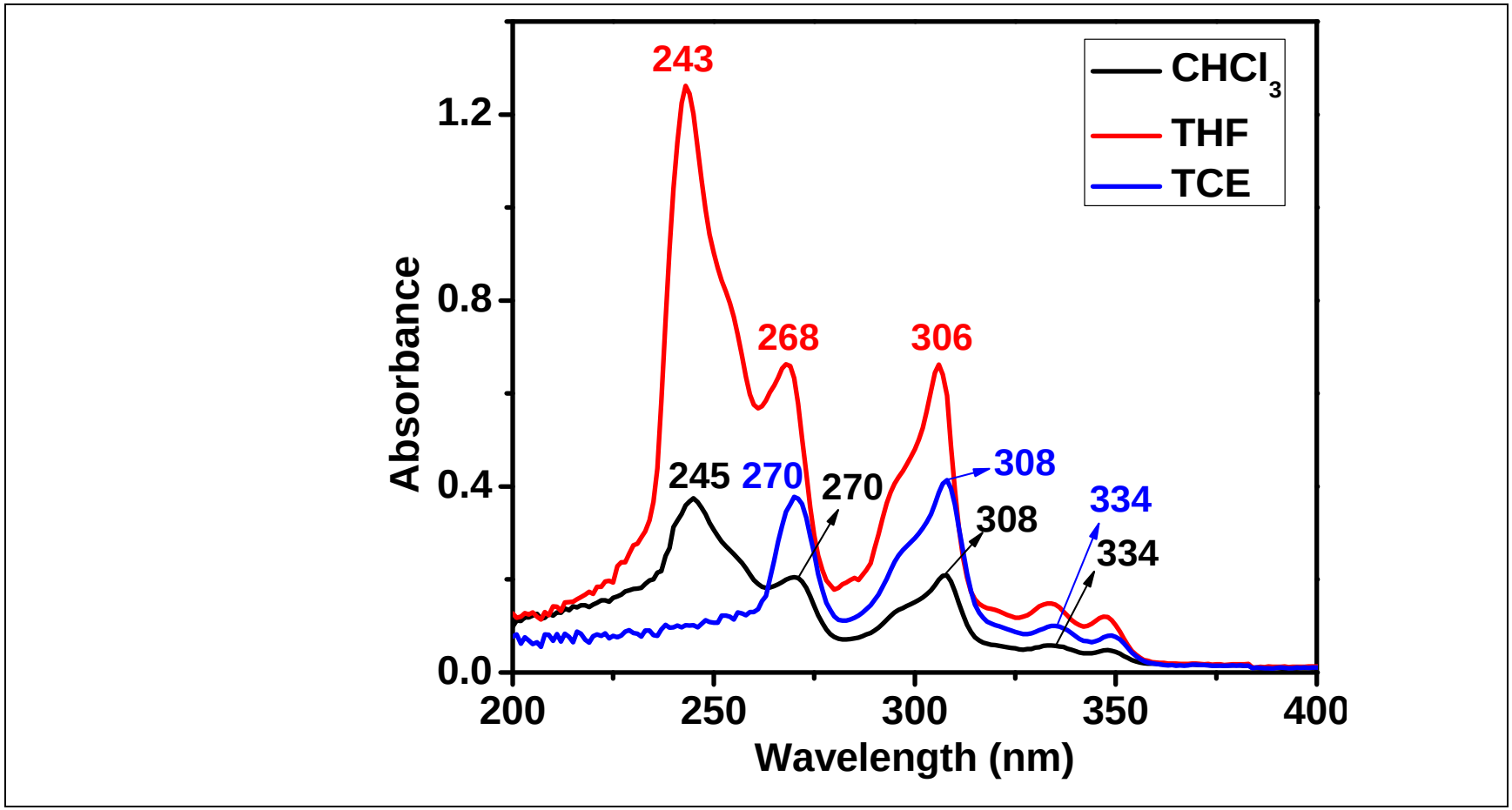

Figure 4.21: UV-vis Absorption Spectra of R-Cbz in Various Nonpolar Solvents

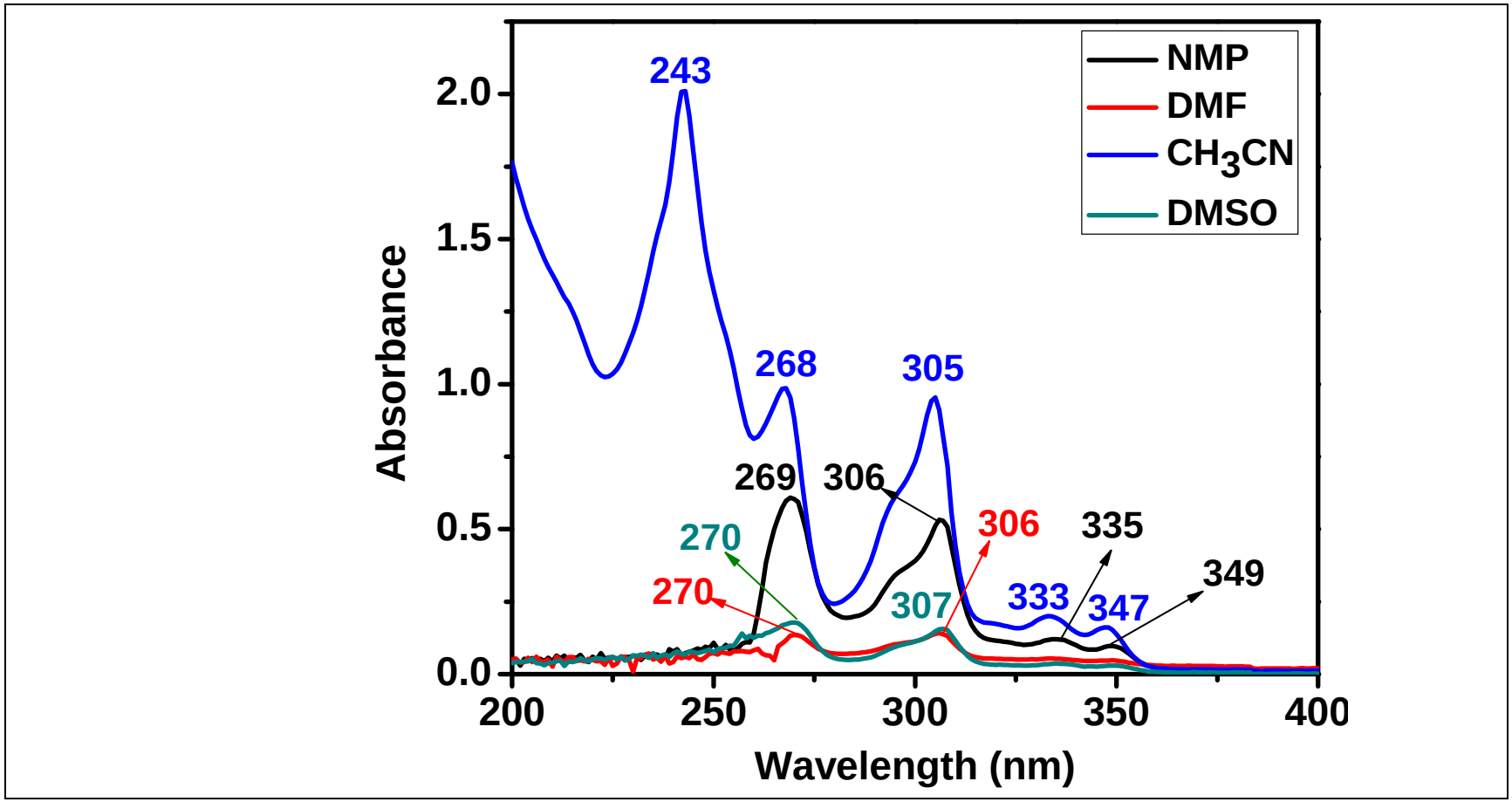

Figure 4.22: UV-vis Absorption Spectra of R-Cbz in Various Dipolar Aprotic Solvents

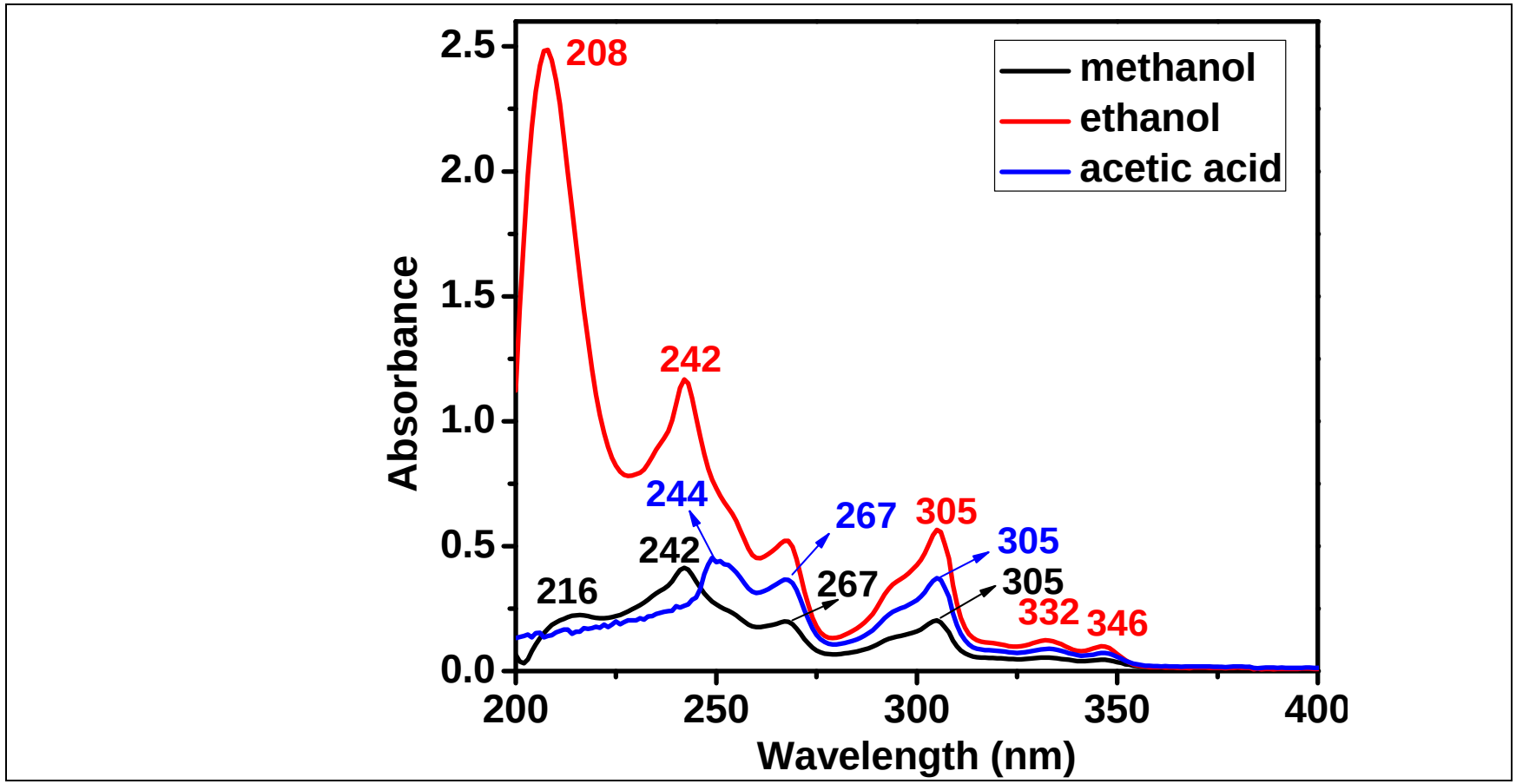

Figure 4.23: UV-vis Absorption Spectra of R-Cbz in Various Polar Protic Solvents

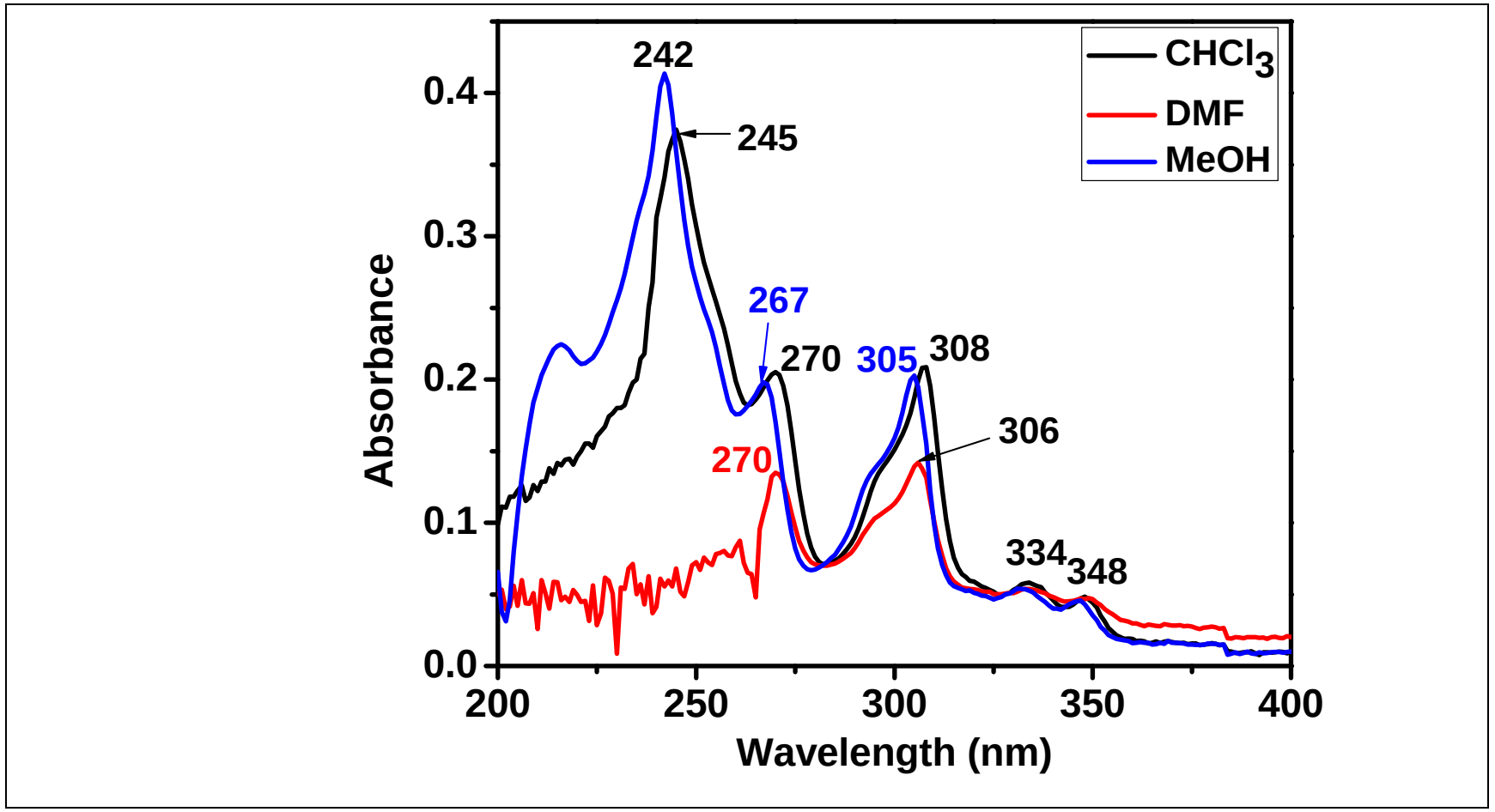

Figure 4.24: Comparison of UV-vis Absorption Spectra of R-Cbz in Solvents of Different Polarity

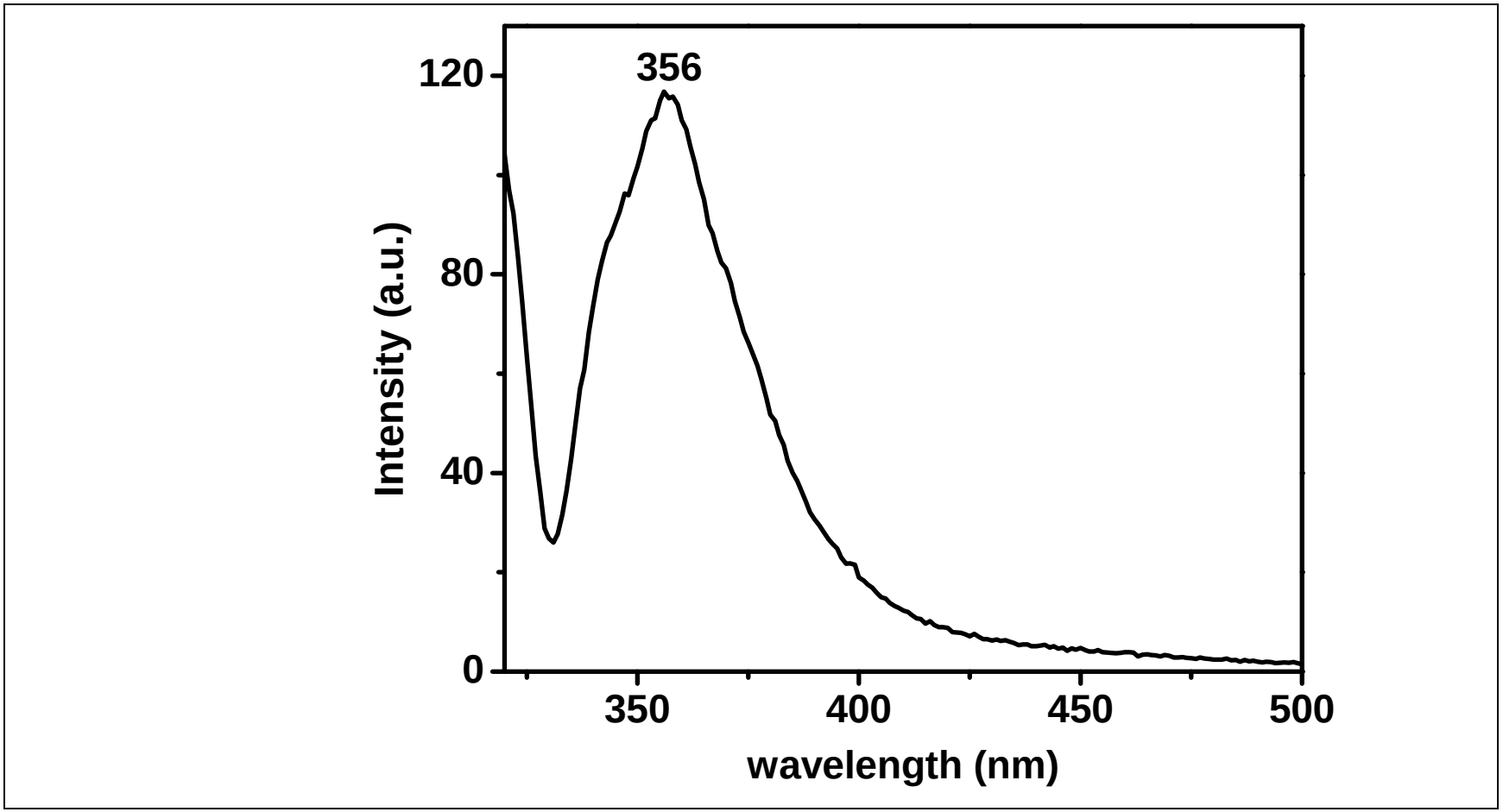

Figure 4.25: Emission ($\lambda_{exc} = 318$ nm) Spectrum of Cbz in $CHCl_3$

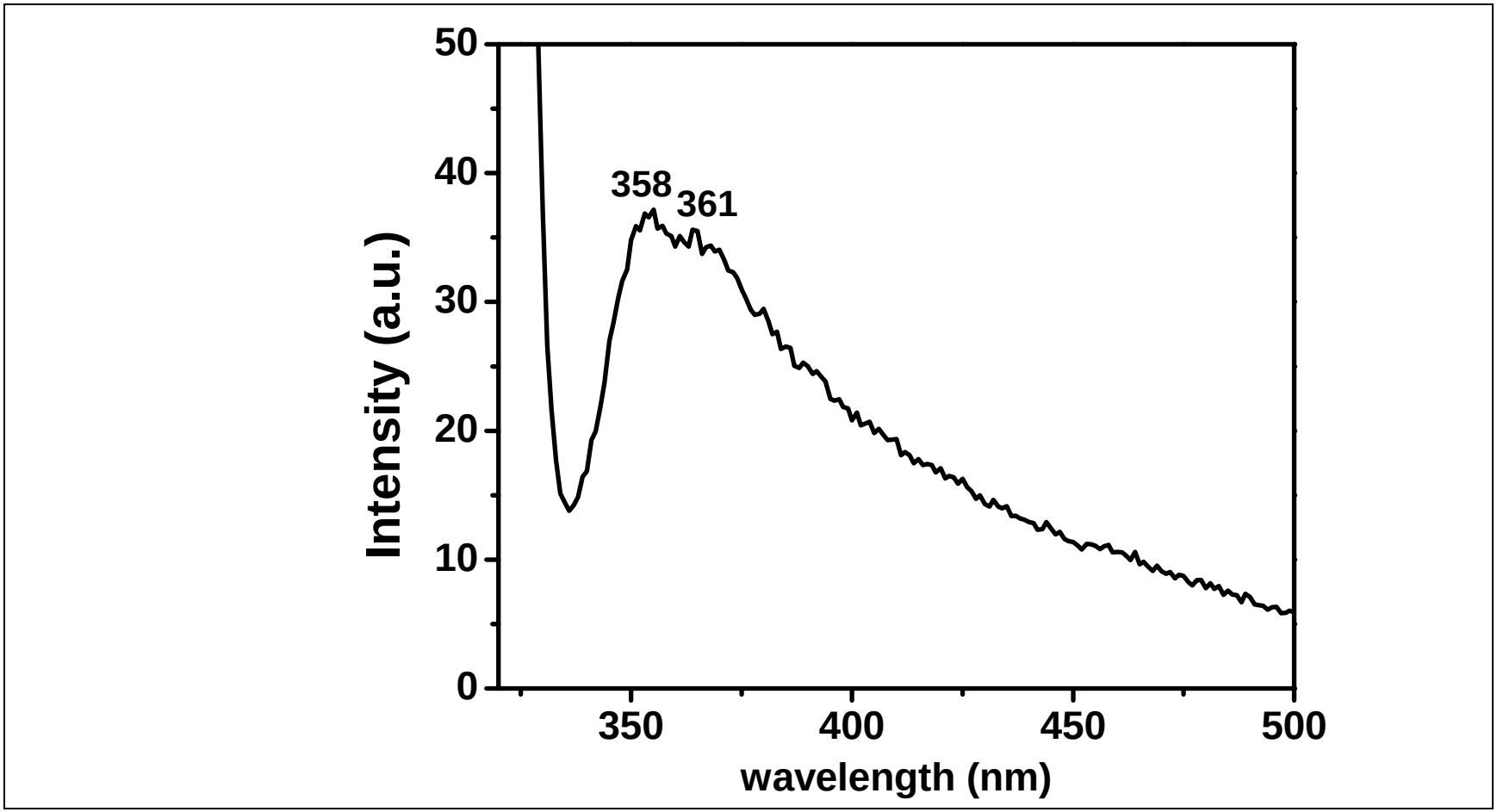

Figure 4.26: Emission ($\lambda_{exc} = 318$ nm) Spectrum of Cbz in DMF

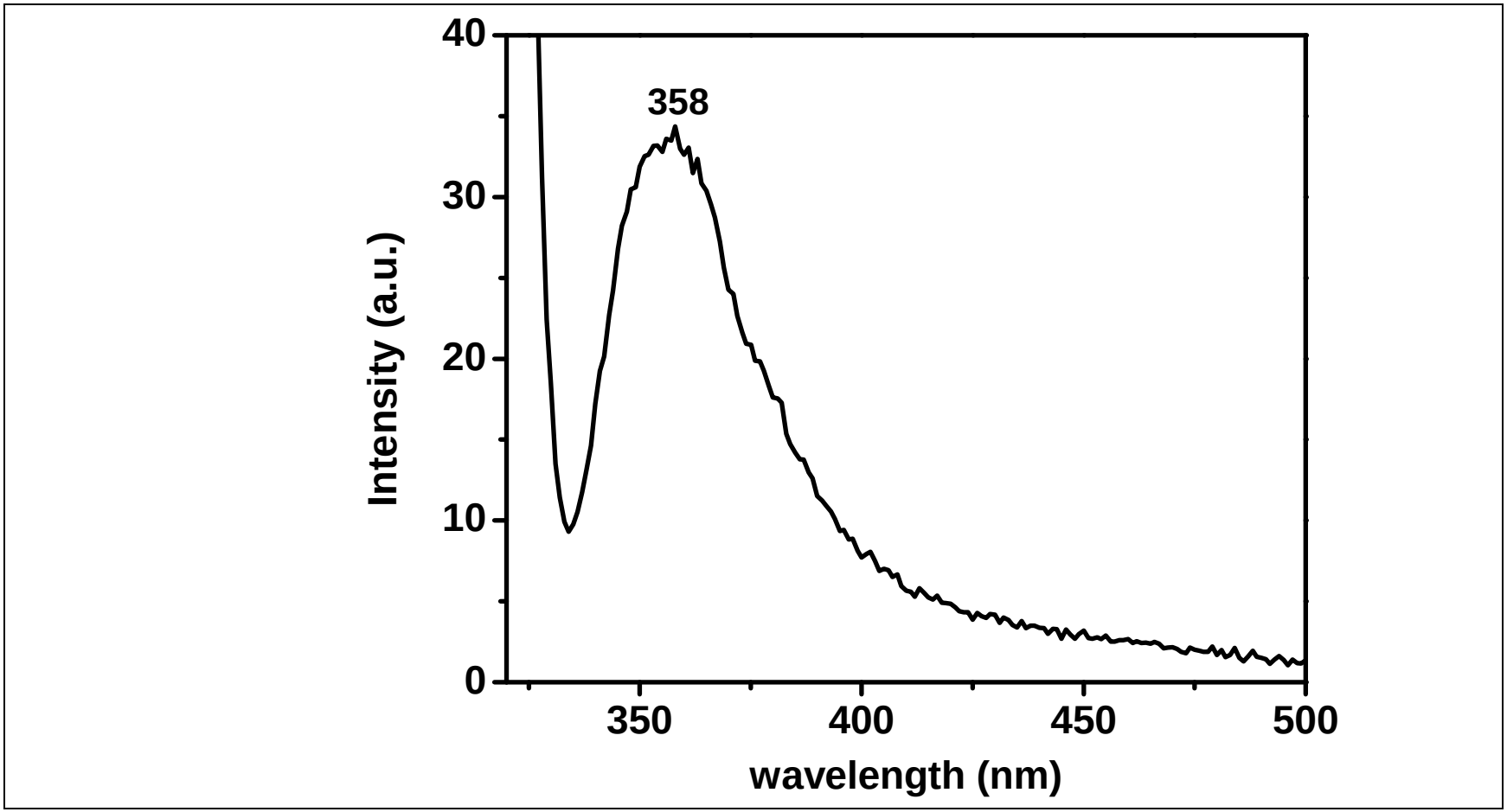

Figure 4.27: Emission (λ_{exc} = 318 nm) Spectrum of Cbz in MeOH

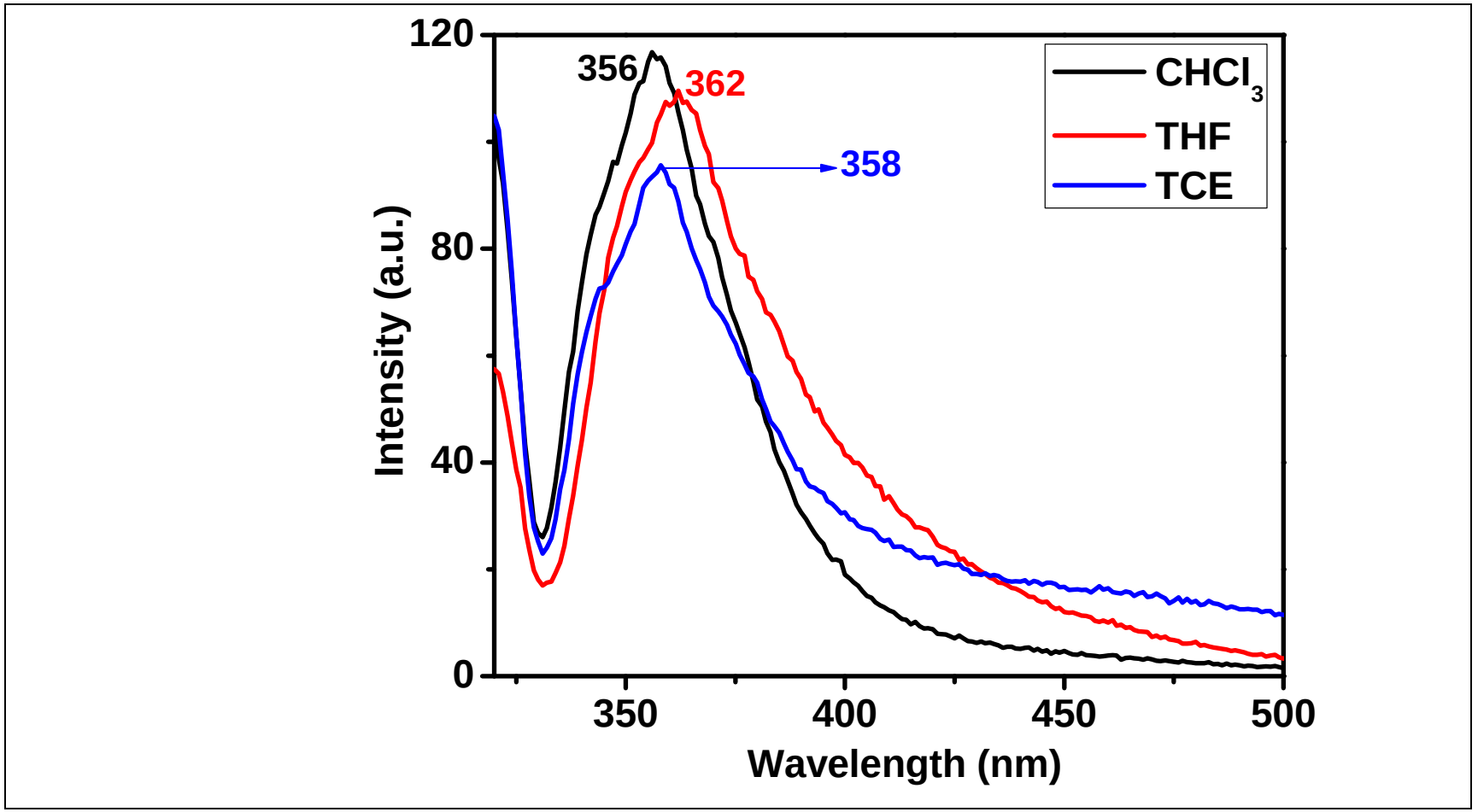

Figure 4.28: Emission (λ_{exc} = 318 nm) Spectrum of Cbz in Various Nonpolar Solvents

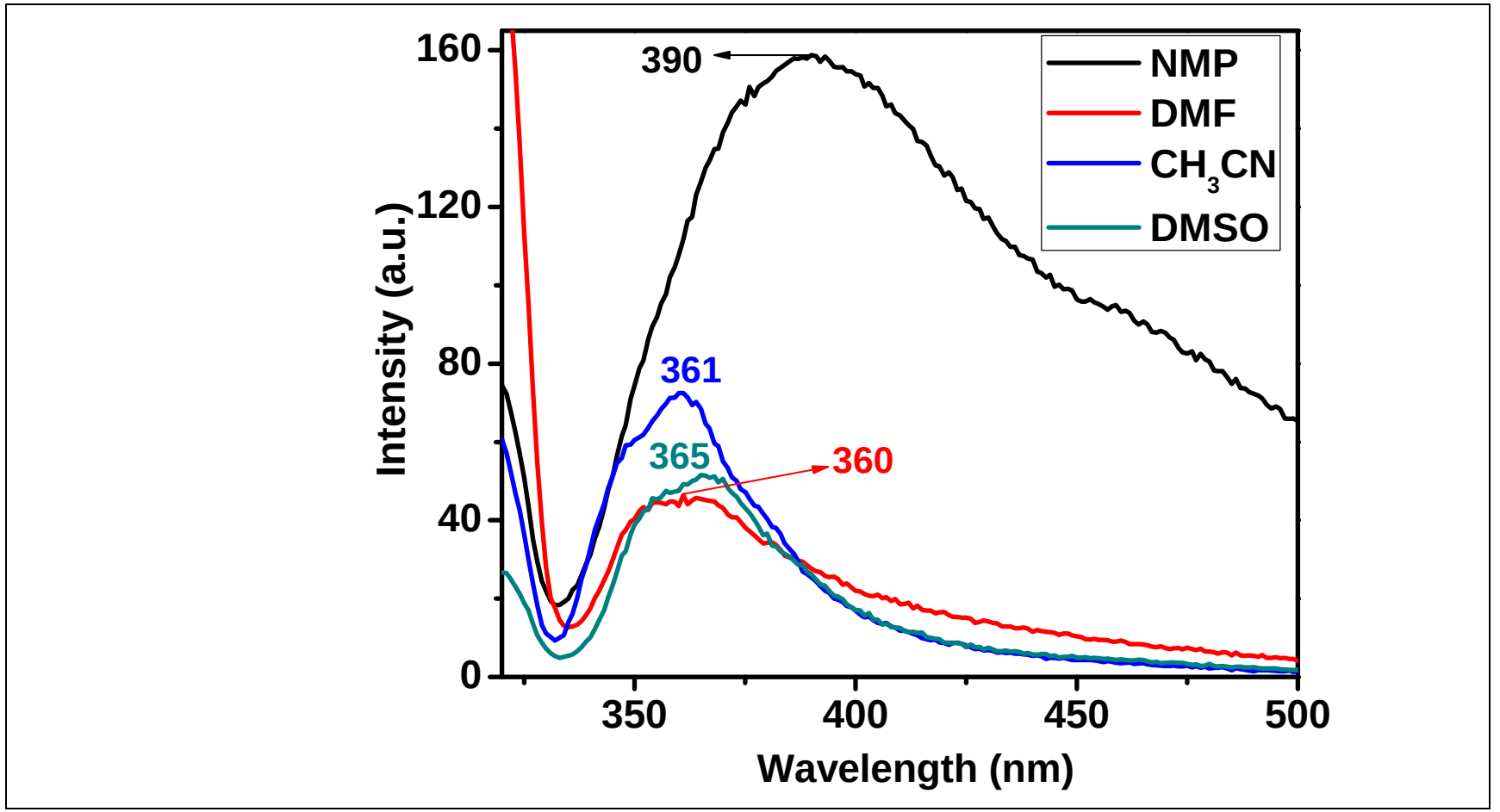

Figure 4.29: Emission (λ_{exc} = 318 nm) Spectrum of Cbz in Various Dipolar Aprotic Solvents

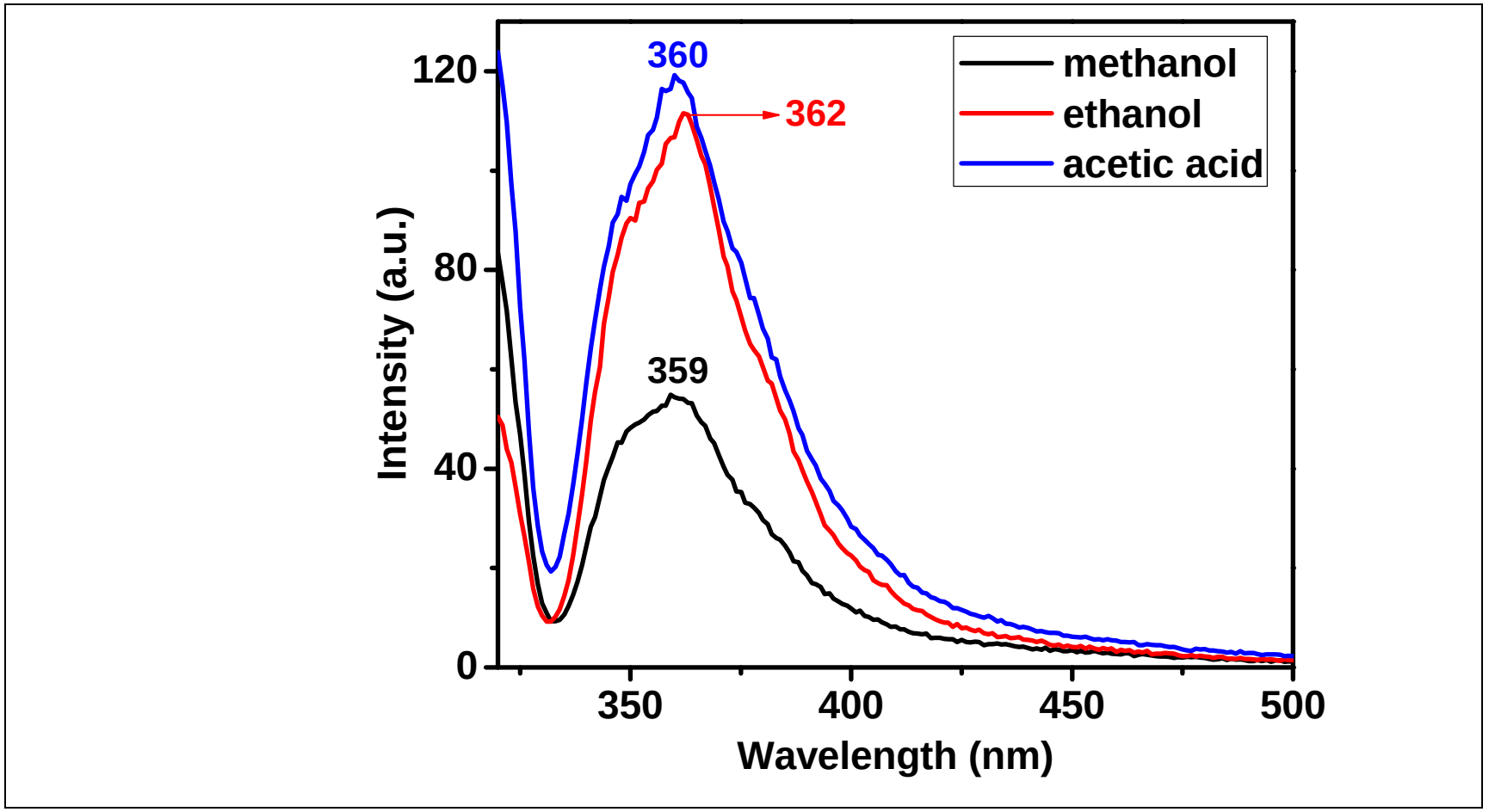

Figure 4.30: Emission ($\lambda_{exc} = 318$ nm) Spectrum of Cbz in Various Polar Protic Solvents

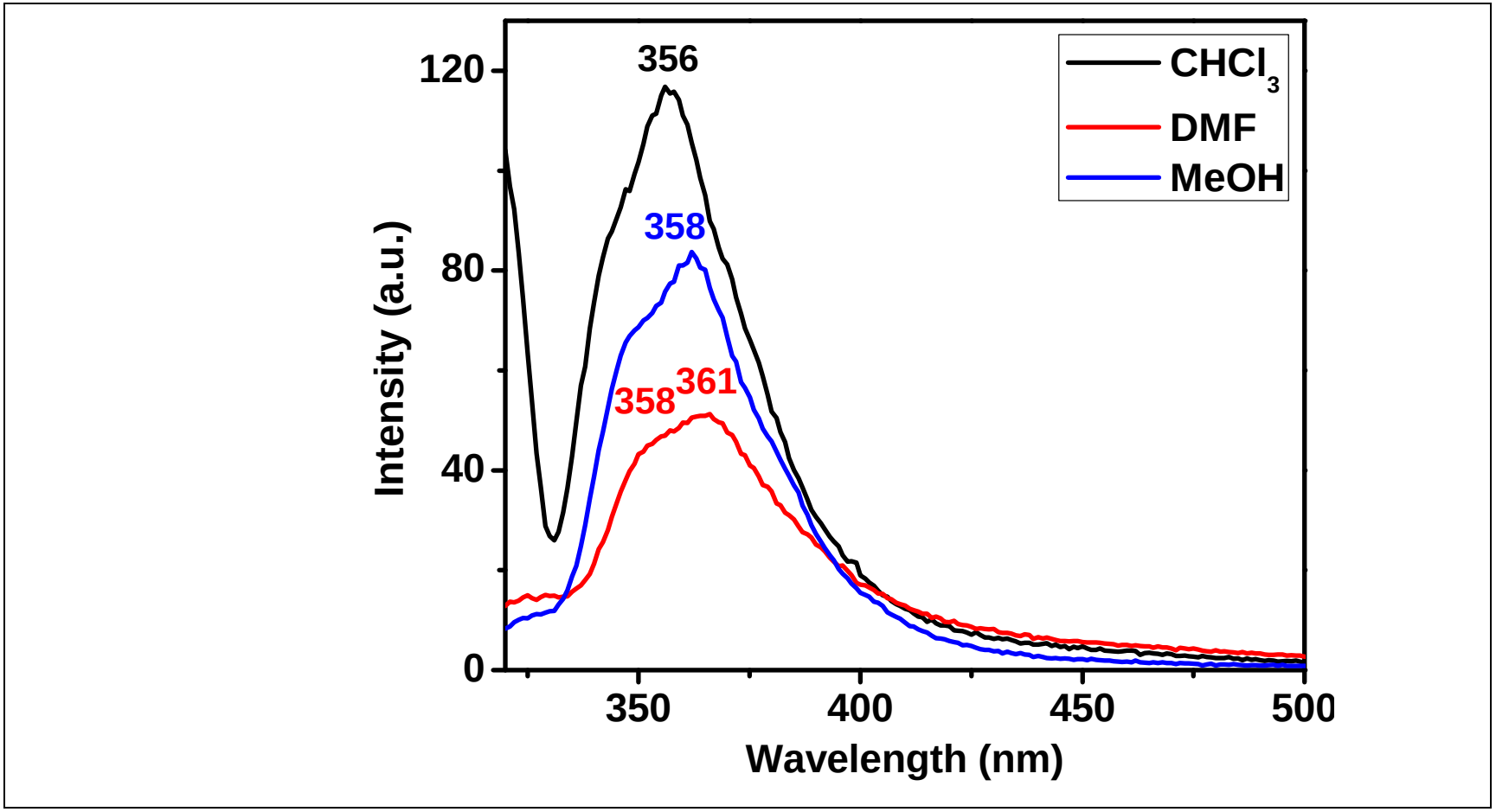

Figure 4.31: Comparison of Emission ($\lambda_{exc} = 318$) Spectra of Cbz in Different Solvents of Varying Polarity

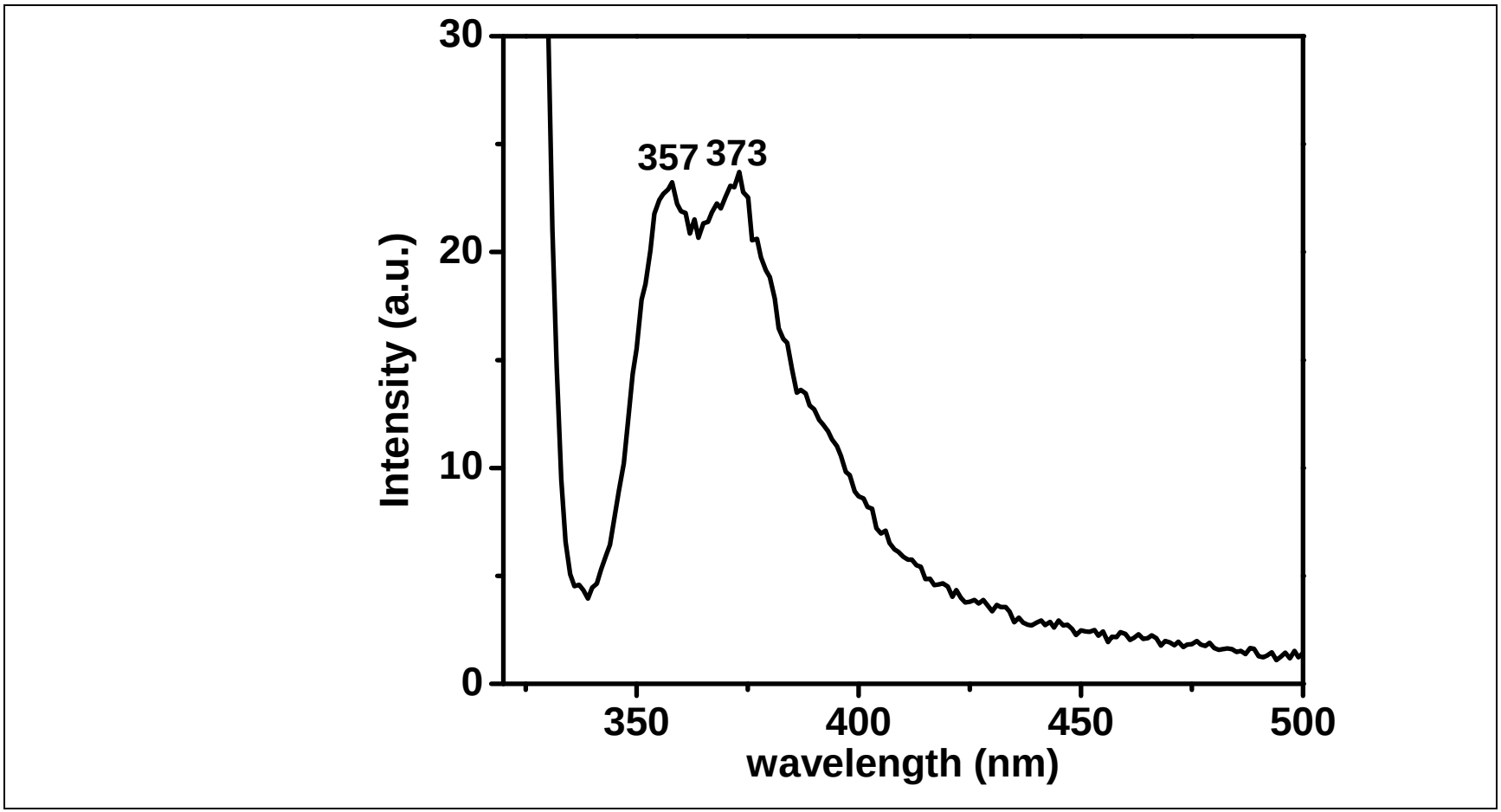

Figure 4.32: Emission ($\lambda_{exc} = 318$ nm) Spectrum of R-Cbz in $CHCl_3$

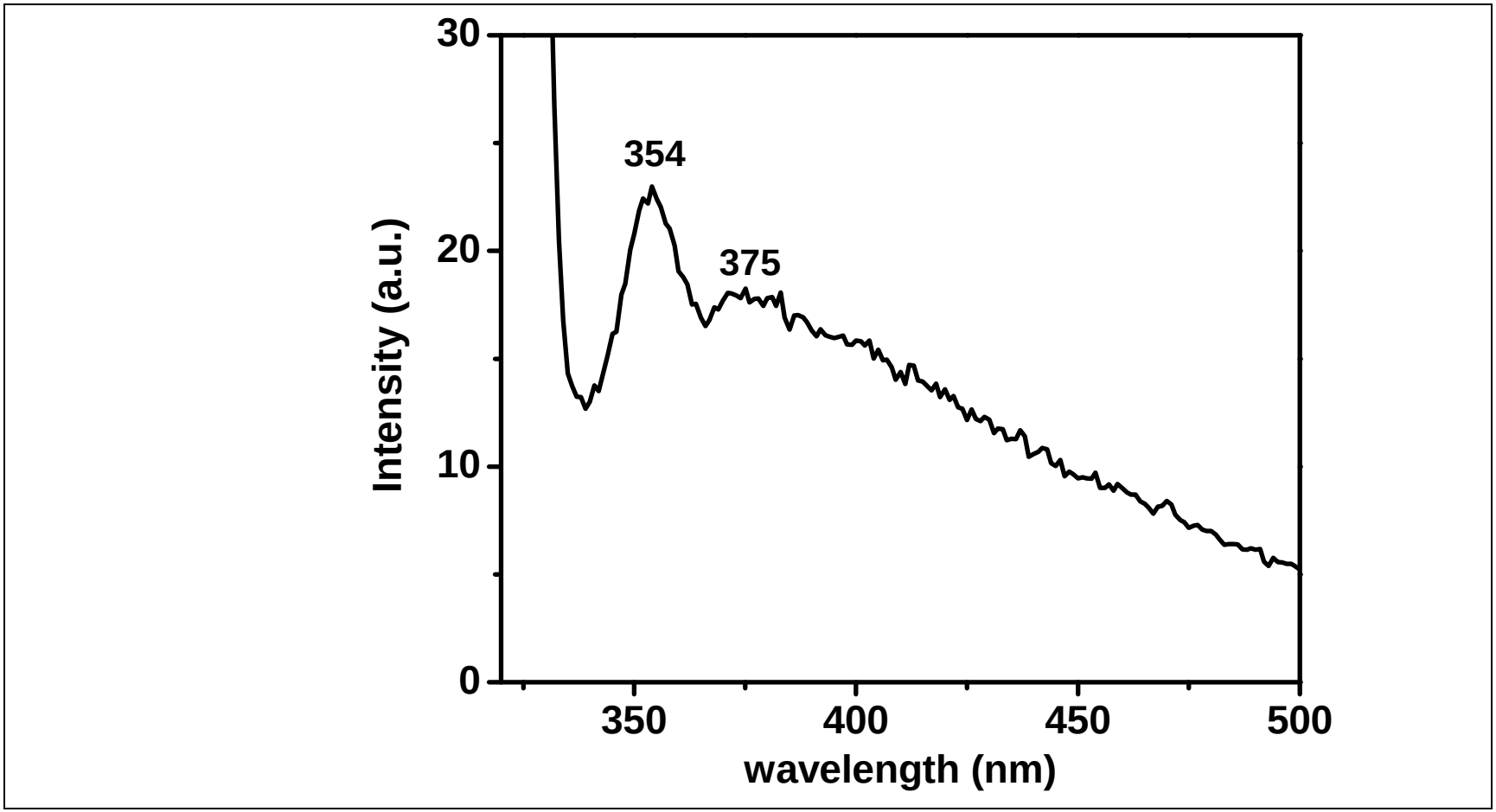

Figure 4.33: Emission (λ_{exc} = 318 nm) Spectrum of R-Cbz in DMF

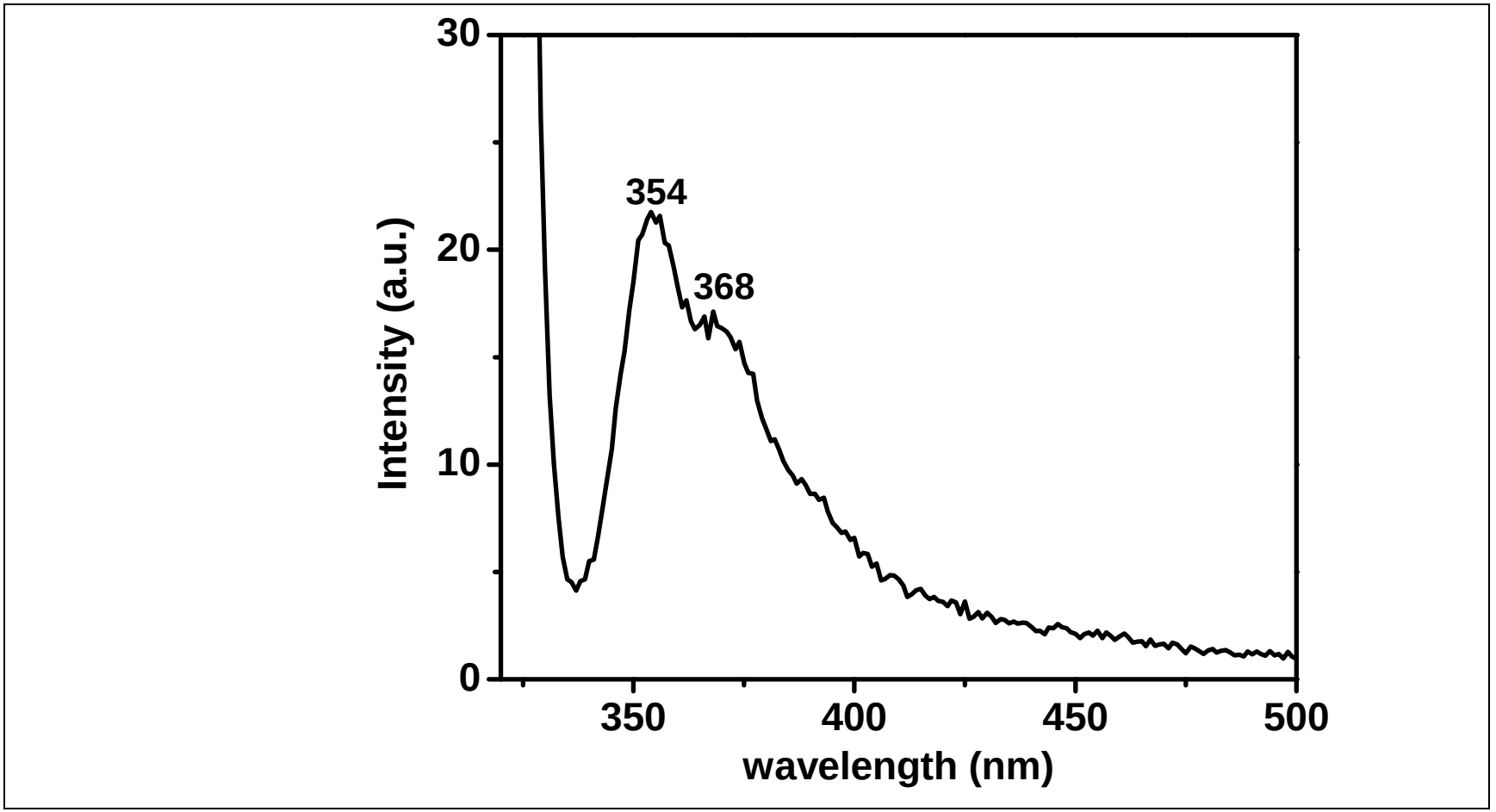

Figure 4.34: Emission ($\lambda_{exc} = 318$ nm) Spectrum of R-Cbz in Methanol

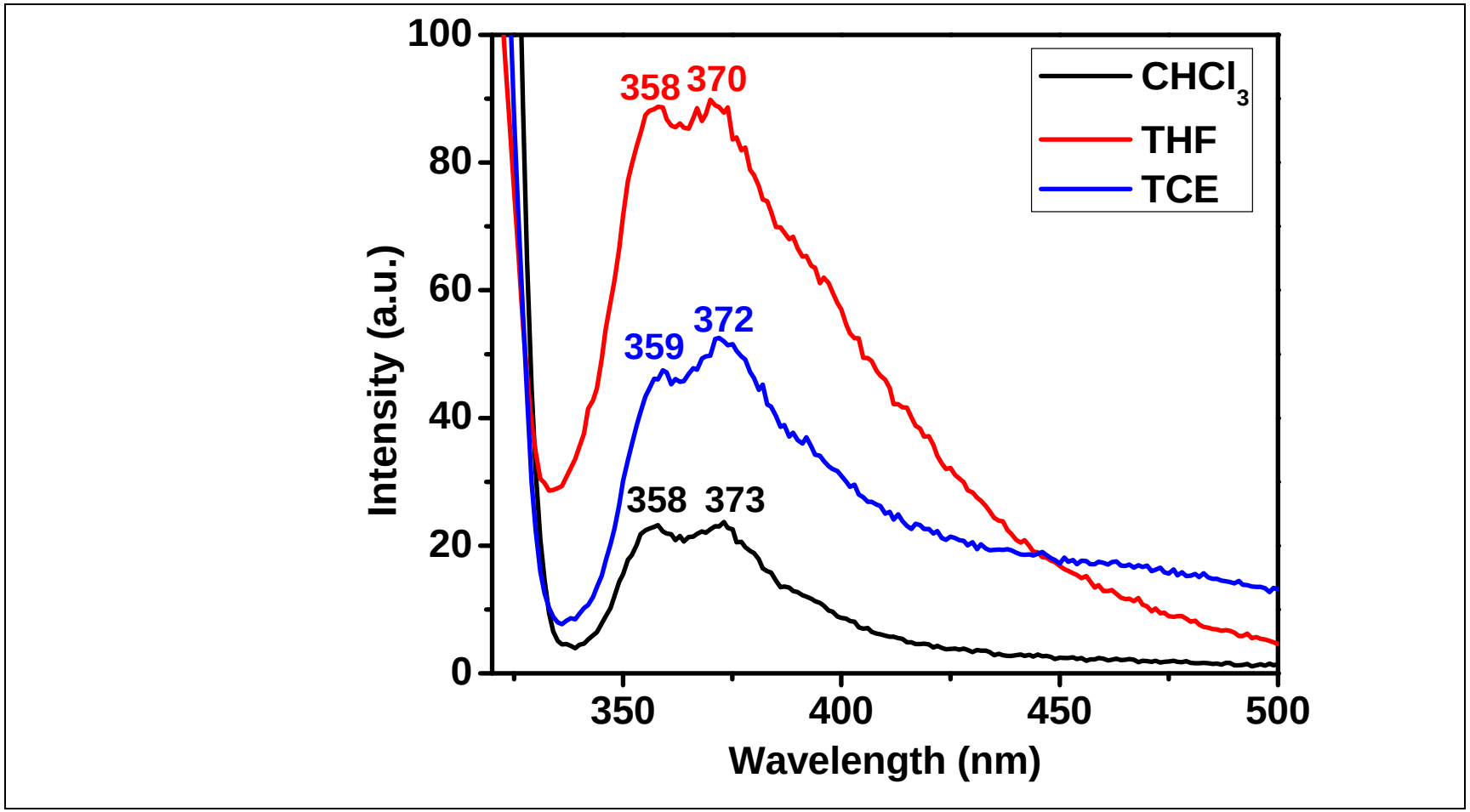

Figure 4.35: Emission ($\lambda_{exc} = 318$ nm) Spectrum of R-Cbz in Various Nonpolar Solvents

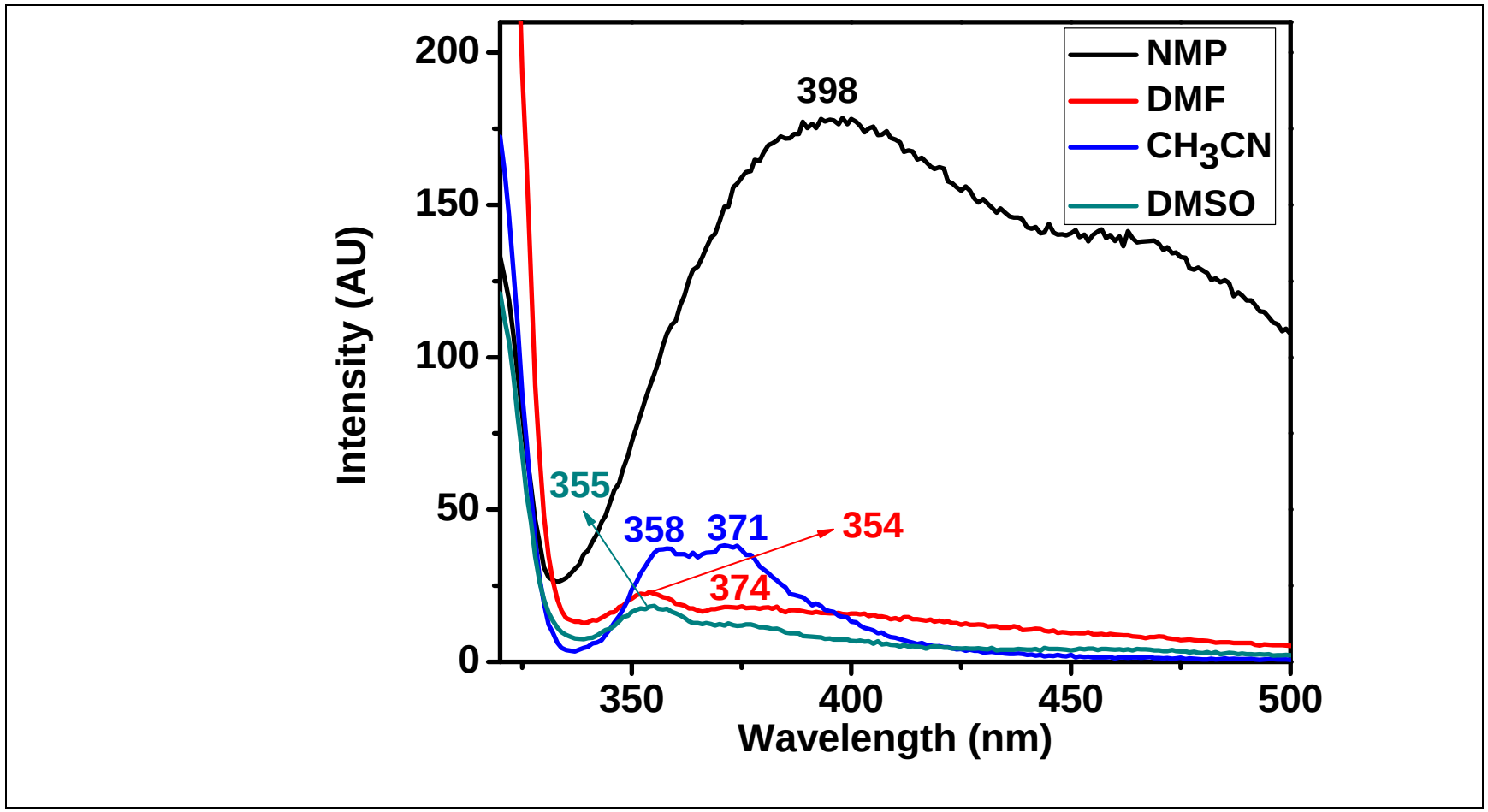

Figure 4.36: Emission ($\lambda_{exc} = 318$ nm) Spectrum of R-Cbz in Various Dipolar Aprotic Solvents

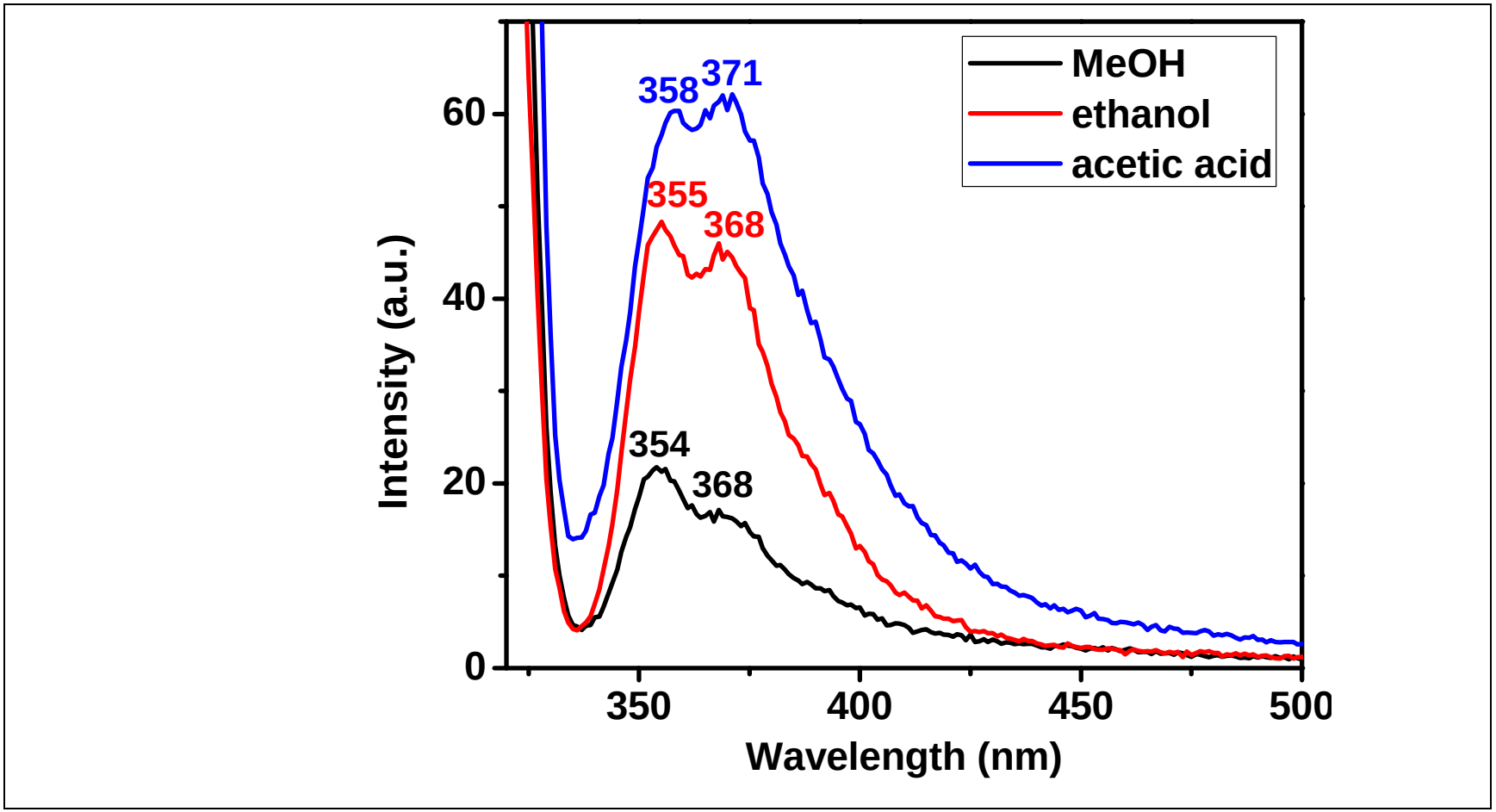

Figure 4.37: Emission (λ_{exc} = 318 nm) Spectrum of R-Cbz in Various Polar Protic Solvents

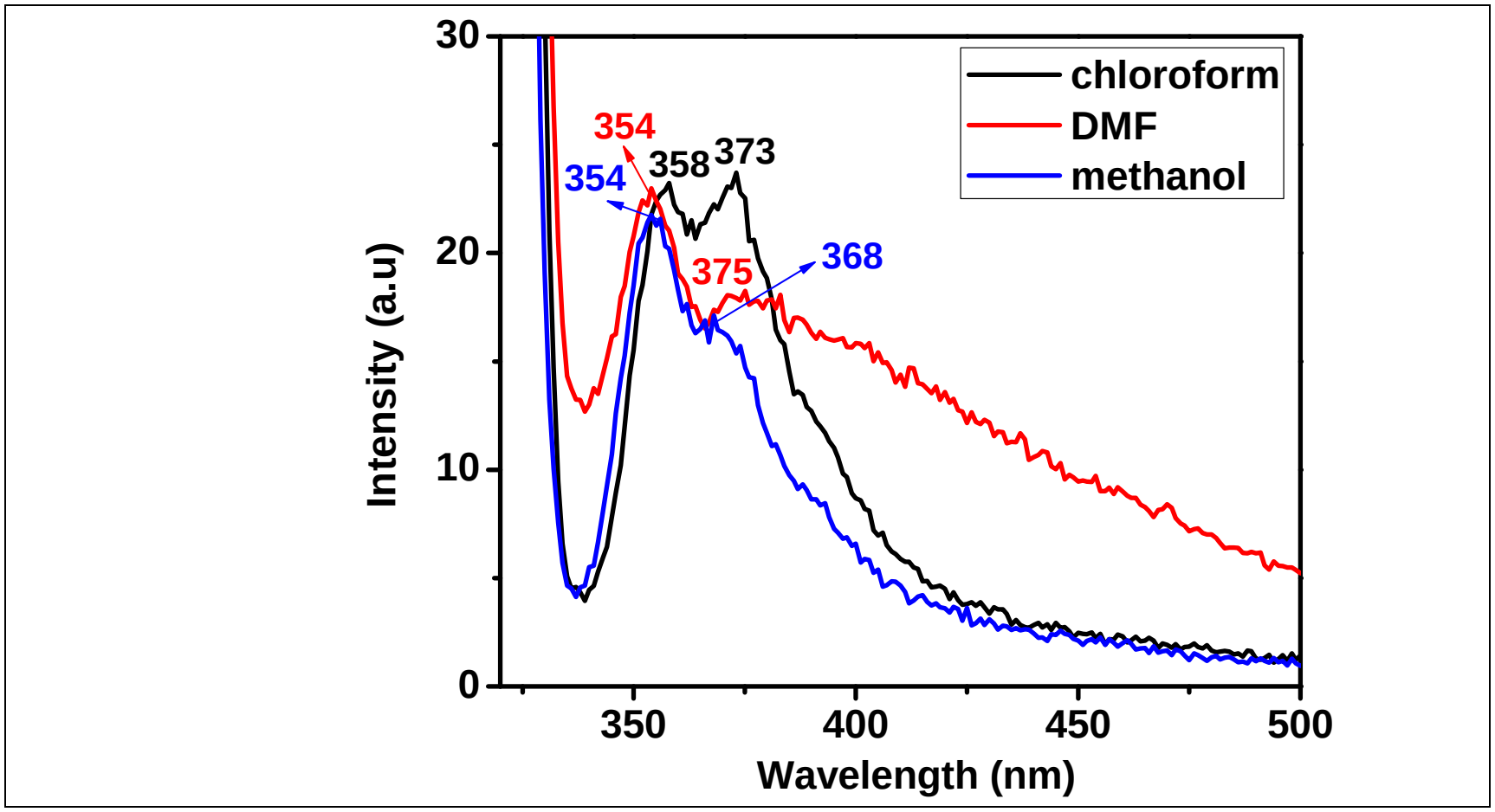

Figure 4.38: Comparison of Emission ($\lambda_{exc} = 318$) Spectra of R-Cbz in Different Solvents of Varying Polarity

Chapter 5

RESULTS AND DISCUSSION

5.1. Syntheses and Characterization

2,7-Dibromo-substituted carbazole was synthesized sucessfully in two steps. Due to the unreactive 2,7-positions, the synthesis was started with commercial dibromobiphenyl starting material and finally synthesized the 2,7-carbazole via the synthesis of dibromonitrobiphenyl.

The targeted dodecylcarbazole was synthesized by nucleophilic substitution reaction of 2,7-dibromo-NH-carbazole and 1-dodecylbromide.

The syntheses were basically confirmed by FTIR spectra (Figures 4.4 – 4.8). The products, dibromobiphenyl and 2,7-dibromocarbazole were also confirmed by melting point tests (dibromobiphenyl: found, 125 ^{o}C (lit, 124 ^{o}C); 2,7-dibromo-9H-carbazole: found, 235 ^{o}C (lit, 234 ^{o}C)).

The FTIR spectra of starting material, dibromobiphenyl and the product, dibromonitrobiphenyl were quite different from the FTIR spectrum of 2,7-dibromocarbazole. The spectra of the former ones show very weak aromatic stretchings (Figures 4.4 and 4.5). On the other hand, the FTIR spectrum of the later one shows

complete evidence of secondary –NH stretch at 3398 cm^{-1}, aromatic C–H stretch at 3073 cm^{-1}, aliphatic C–H stretch at 2955 – 2850 cm^{-1}, aromatic C=C stretch at 1600 cm^{-1}, and aromatic C–H bend at 805 cm^{-1} (Figure 4.6).

Figure 4.8 shows the aliphatic C–H stretch at 2926 and 2853 cm^{-1} and strong aromatic C=C stretch at 1600 cm^{-1} which are completely proving the structure of N-alkyl 2,7-dibromo carbazole. Notably, the clearence in other peaks which were dominant in both 2,7-dibromocarbazole (Figure 4.6) and 1-bromododecane (Figure 4.7) evidences the purity of the N-alkyl 2,7-dibromocarbazole.

The solubility of both carbazole and dodecyl carbazole is very high in all common organic nonpolar, dipolar aprotic and protic solvents.

5.2. NMR Spectra Analysis

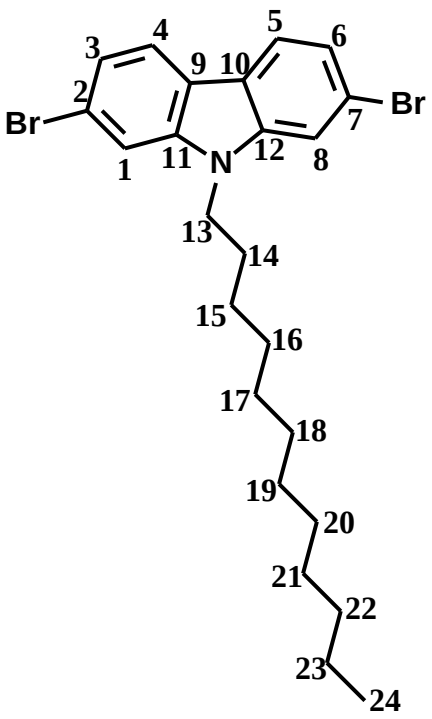

^{1}H NMR (400 MHz, $CDCl_3$, ppm): 7.66 (s, 6Ar-H (C – 1,3-6,8)), 2.84 (s, CH_2, H-C(13), 2.64 – 2.53 (br d, 10CH_2, H-C(14-23), 0.94 (s, CH_3, H-C(24)) (Figure 4.9).

^{13}C NMR (100 MHz, $CDCl_3$, ppm):, 162.9, 141.73, 122.78, 121.93, 121.55, 119.92, 112.42 (C–2,7,(9–12)), 36.77, 32.39, 31.62, 29.96, 29.88 (C–(13–23)), 29.6 (C – 24) (Figure 4.10).

5.3. Photophysical Properties

a) Absorption Spectra

The Figures 4.11 – 4.17 show the absorption spectra of carbazole in various solvents. The solvents are treated as polar/nonpolar with respect to the dielectric constant values. The UV-vis spectrum of cbz in $CHCl_3$ (Figure 4.11) shows two major peaks at 243 and 303 nm. The peak at 303 nm is ascribed to the $\pi \rightarrow \pi^*$ electronic transitions of rich aromatic structure. The high intense and high energy absorption peak at 243 nm is ascribed to the forbidden transitions, $S_0 \rightarrow S_2$ transitions. On the other hand, there are two weak shoulder peaks observed at higher wavelengths around 323 and 333 nm.

The absorption spectrum in DMF shows the similar $\pi \rightarrow \pi^*$ electronic transition absorption peak at 305 nm, whereas, the high energy peak was red shifted by 20–25 nm and is related to the high polarity of solvent DMF (Figure 4.12).

Interestingly, there are two different high energy peaks observed in methanol for carbazole absorption (Figure 4.13) which is different from the other two absorption spectra in chloroform and DMF. Whereas, the main absorption peak responsible for $\pi \rightarrow \pi^*$ electronic transition of cbz is observed at 303 nm. This is similar to the other two absorption spectra. The differences are due to the possible intermolecular hydrogen bonding of carbazole with the solvent molecules.

Figures 4.14 – 4.17 show the comparisons of absorption spectra in various kinds of solvents. Figure 4.14 shows that as the polarity is increased gradually among nonpolar

solvents, the absorption intensity of $S_0 \rightarrow S_2$ transition is increased, whereas, there was no big difference in the absorsption intensity of $\pi \rightarrow \pi^*$ electronic transition.

Figure 4.15 Shows the absorption spectra comparisons in dipolar aprotic solvents. As can be seen, the spectrum in acetonitrile is different from other absorption spectra. This is due to the strong electron withdrawing nature of cyano group and consequent electronic interactions. Notably, in all the dipolar aprotic solvents studied including acetonitrile, the shift in absorption of $\pi \rightarrow \pi^*$ electronic transition is unaffected.

Similar to the above absorption spectra comparisons, Figure 4.16 shows absorption in polar protic solvents. High polar ethanol and methanol have resulted in similar absorption peaks. In acetic acid, the two high intense and high energy absorption peaks were combined and resulted as one peak. In other words, as the polarity increased, the absorption intensity of $S_0 \rightarrow S_2$ transition is increased. This is analogous to the previous trend noticed for nonpolar solvents.

Figure 4.17 represents the absorption details of cbz in nonpolar, polar aprotic and polar protic solvents. As discussed in Figures 4.11 – 4.13, the absorption in polar protic methanol is different from other two absorption spectra with two intense absorption peaks of $S_0 \rightarrow S_2$ transitions.

The Figures 4.18 – 4.20 show the absorption spectra of dodecylcarbazole (R-cbz) in various solvents. The UV-vis spectrum of R-cbz in $CHCl_3$ (Figure 4.11) shows three major peaks at 247, 270 and 308 nm. The peak at 308 nm is ascribed to the $\pi \rightarrow \pi^*$

electronic transitions of rich aromatic structure. The high intense and high energy absorption peaks at 247 nn and 270 nm are ascribed to the forbidden transitions, $S_0 \rightarrow S_2$ transitions. Especially, the peak at 270 nm is like a weak shoulder which was observed for carbazole (in chloroform) but was more in absorption intensity for R-cbz. On the other hand, there are two weak shoulder peaks observed at higher wavelengths around 323 and 333 nm.

The absorption spectrum in DMF shows the similar $\pi \rightarrow \pi^*$ electronic transition absorption peak at around 309 nm, whereas, the first high energy peak that was observed in chloroform at around 247 nm is completely disappreared and only the absorption at 270 nm was evidenced. This is related to the high polarity of solvent DMF (Figure 4.19) and related to the polar ground state.

Interestingly, there are three different high energy peaks (216, 242, and 270 nm) observed in methanol for R-carbazole absorption (Figure 4.20) which is different from the other two absorption spectra in chloroform and DMF but similar in trend with carbazole's absorption spectrum in methanol. Whereas, the main absorption peak responsible for $\pi \rightarrow \pi^*$ electronic transition of R-cbz is observed at 305 nm. This is similar to the other two absorption spectra. The differences are due to the possible intermolecular hydrogen bonding of R-carbazole with the solvent molecules. The appreciable red shifts in absorption wavelengths of R-cbz comparing to the cbz absorption wavelengths are attributed to the N-substituted long alkyl chains attached to the carbazole moiety.

Figures 4.21 – 4.24 show the comparisons of absorption spectra in various kinds of solvents. Figure 4.21 shows that as the polarity is increased gradually among nonpolar solvents, the very high energy peak at 243 nm was disappeared similar to the spectrum in DMF, whereas, there was no big difference in the absorsption intensity of $\pi \rightarrow \pi^*$ electronic transition.

Figure 4.22 Shows the absorption spectra comparisons in dipolar aprotic solvents. As can be seen, the spectrum in acetonitrile is different from other absorption spectra. This is due to the strong electron withdrawing nature of cyano group and consequent electronic interactions. Notably, in all the dipolar aprotic solvents studied including acetonitrile, the shift in absorption of $\pi \rightarrow \pi^*$ electronic transition is unaffected. Except in acetonitrile, the first high energy peak at around 242 nm was disapperead for other dipolar aprotic solvents.

Similar to the above absorption spectra comparisons, Figure 4.23 shows absorption in polar protic solvents. High polar ethanol and methanol have resulted in similar absorption peaks, but noticeably, the high energy peak at 216 nm was more in intensity in ethanol. In acetic acid, similar to the trend observed for cbz absorptions, only two high intensity absorption peaks were observed for R-cbz.

Figure 4.24 represents the absorption details of R-cbz in nonpolar, polar aprotic and polar protic solvents. As discussed in Figures 4.18 – 4.20, the absorption in polar protic methanol is different from other two absorption spectra with three intense absorption peaks of $S_0 \rightarrow S_2$ transitions in combination with unchanged $\pi \rightarrow \pi^*$ absorption.

Table 4.1 lists the molar absorptivity data of 2,7-dibromocarbazole in three different kinds of solvents of varying polarity. Comparatively, in nonpolar chloroform, the Cbz has highest molar absorptivity. This is due to intermolecular interactions which are feasible for intense absorption. In methanol and DMF, due to high polarity, the solution of carbazole is having lower absorptivity.

On the other hand, Table 4.2 lists the molar absorption coefficients of dodecyl carbazole (R-Cbz) in various solvents (the solvents are arranged in the increasing order of polarity). There was no proper order in the molar absorptivity values of dodecylcarbazole in these solvents. This is attributed to respective intermolecular interactions of dodecylcbz with the solvent molecules.

Similar to the values, the consequent results of FWHM (Tables 4.3 and 4.4), natural radiative lifetimes (Tables 4.5 and 4.6), natural/theoretical fluorescence rate constants (Tables 4.7 and 4.8), oscillator strengths (Tables 4.9 and 4.10), singlet energies (Tables 4.11 and 4.12), and band gap energies (Tables 4.13 and 4.14) are calculated.

b) Emission Spectra

The trends in absorption spectra for carbazole and R-cbz are similar in all solvents studied and therefore a parallel comparison and discussion was made on the emission spectra of carbazole and dodecylcarbazole.

Figures 4.25 and 4.32 show emission spectra of cbz and R-cbz in chloroform at the same concentrations. As can be inferred from the figures, the emission spectrum of cbz represents an excimer emission with λ_{max} at 356 nm (Figure 4.25). The spectrum of R-

cbz was also similar and represent excimer-like emission but a small separation was occurred with two peak maxima at around 357 and 373 nm, respectively (Figure 4.32). This is related to the lower emission intensity of R-cbz comparing to the excimer emission of cbz.

Figures 4.26 and 4.33 depicts the emission spectra of cbz and dodecylcbz in dipolar aprotic DMF solvent. Similar to the above trend observed in chloroform, excimer emission was noticed for cbz at λ_{max} of 358 nm followed by a very weak separated emission peak at 361 nm. On the other hand, a clear separation in peaks was evidenced for the emission spectrum of R-cbz in DMF at 354 and 375 nm (with higher intenisty for 354 nm peak). It can be noticed that excimer-like emission was still observed at 375 nm regardless of separation in two emission peaks.

Similar behavior was noticed for cbz and R-cbz in methanol. The excimer peak of cbz is noticed at 358 nm, whereas, excimer –like emission for dodecylcbz was observed at 354 nm with a shoulder at 368 nm (Figures 4.27 and 4.34).

The excimer like emissions of cbz and R-cbz is very attractive property for optoelectronic applications.

Figures 4.28 and 4.35 show the comparisons of cbz and dodecylcbz emission spectra in nonpolar solvents. There was no considrable change noticed for the excimer emissions of cbz in these solvents of low polarity. On the other hand, the excimer-like emissions of R-cbz were also similar in excimer-peak shapes and intensity except a very small

gradual increase in intenisty at 370 nm as the polarity of the solvent increased from chloroform to TCE.

Figures 4.29 and 4.36 show the comparisons of cbz and dodecylcbz emission spectra in dipolar aprotic solvents. There was no considrable change noticed for the excimer emissions of cbz in these solvents of high polarity except in NMP. Interestingly, in NMP, there was a very broad excimer emission observed and is ascribed to the solute solvent effects. Similarly, the excimer-like emissions of R-cbz were also similar in excimer-peaks shapes and intensities. Interestingly, the same trend observed for cbz was once again evidenced in the emission spectrum of R-cbz with much broader excimer emission at 398 nm.

Emission spectra recorded for 2,7-dibromo-9H-carbazole and dodecylcarbazole from Figures 4.30 and 4.37 in polar protic solvents also represent the similar trends noticed for the emission spectra in nonpolar solvents. No changes in both excimer emission at 360 nm for cbz and small separated excimer-like emissions at around 357 nm and 370 nm for R-cbz supports the strong excimer-light emission ability of both the compounds.

To summarize the emission spectra for both cbz and R-cbz in different kinds of polar solvents, cbz exhibits excimer emissions at around 357 nm, whereas, R-cbz emits a little weak excimer-like emissions at around 357 nm (Figures 4.31 and 4.38).

Chapter 6

CONCLUSION

A 2,7-dibromo-substituted-N-alkyl carbazole was successfully synthesized in 3 steps. In the first step, using a commercial dibromobiphenyl compound, nitrobiphenyl was synthesized by nitration and 2,7-dibromo-9H-carbazole was synthesized in the second step by Cadogan ring closing mechanism. The second step product, dibromocarbazole was used to synthesize the targeted dibromo-N-alkyl substituted carbazole in the final third step. The syntheses were confirmed by thin layer chromatography, NMR and FTIR spectra.

The compounds synthesized were soluble at room temperature in all of the common organic solvents.

The absorption spectra of carbazole show high energy forbidden $S_0 \rightarrow S_2$ transition absorptions at around 240 nm and $\pi \rightarrow \pi^*$ electronic transition absorptions at around 303 nm, respectively in all of the common organic solvents studied.

Similarly, the absorption spectra of dodecyl carbazole were shown similar trends with that of carbazole absorptions at around 240, 270, and 305 nm, respectively.

The high energy absorptions were increased in number in polar protic solvent methanol and dipolar aprotic acetonitrile solvents and is attributed to the solvent effects causing hydrogen bonding (in methanol) and electron withdrawing effects (in acetonitrile), respectively.

Most importantly, $\pi \rightarrow \pi^*$ electronic transition absorptions of both carbazole and dodecylcarbazole were unchanged in all of the solvents studied.

Carbazole has shown excellent excimer emissions in all of the solvents studied at around 356 nm.

Dodecylcarbazole has also exhibited an excimer-like emissions in all of the solvents studied at around 357 nm. The excimer peak shapes were a little bit different from that of carbazole excimer emissions.

The solvent-independent $\pi \rightarrow \pi^*$ electronic transition absorptions and excimer light emissions of electron donating carbazole derivatives were potential properties for present organic-based optoelectronic device technology.

REFERENCES

Al- Sultani, K. T. (2010). Synthesis and evaluation of the biological activity for some of carbazole derivatives. Journal of Al-Nahrain University , 13 (4), 31-38.

Bian L. and etal (2012). Recent progress in the design of narrow bandgap conjugated polymers for high-efficiency organic solar cells. Progress in Polymer Science. 37. 1292–1331.

Bouchard J. and etal (2004). Synthesis of N-Octyl-2,7-dimethoxy-1,8-bistrimethylsilyl-3,6-dibromocarbazole. Synthetic Communications. Vol. 34, No. 15, pp. 2737–2742.

Cabaj J. and etal (2006). Development in synthesis and electrochemical properties of thienyl derivatives of carbazole. Tetrahedron. 62. 758–764.

Chen Y. and etal (2012). Efficient non-doped blue light emitting diodes based on novel carbazole-substituted anthracene derivatives. Organic Electronics.13. 43–52.

Fujita H. and etal.(2012). Synthesis and Photovoltaic Properties of 1,8-Carbazole-Based Donor–Acceptor Type Conjugated Polymers.Macromolecular Chemistry and Physics. *213*. 447−457.

Gupta V. D. and etal (2011). The synthesis and photo-physical properties of extended styryl fluorescent derivatives of N-ethyl carbazole. Dyes and Pigments. 88. 378-384.

Hu B. and etal (2010). Synthesis and photophysical properties of tetrafluorophenyl-modified carbazole oligomers. Tetrahedron. 66. 7583-7589.

Hussain M. and etal (2011). Synthesis of carbazoles and 1,2-dihydrocarbazoles by domino ‘twofold Heck/6p-electrocyclization’ reactions of di-, tri- and tetrabromoindoles. Tetrahedron. 67. 5304-5318.

Kanaparthi R. and etal (2012). Metal-free organic dyes for dye-sensitized solar cells: recent advances. Tetrahedron. 68. 8383-8393.

Kawabata K. etal (2010). Electrosynthesis of 2,7-linked polycarbazole derivatives to realize low-bandgap electroactive polymers. Synthetic Metals. 160. 2290–2298.

Kim D. and etal (1999). Synthesis of photoconducting nonlinear optical side-chain polymers containing carbazole derivatives. Reactive & Functional Polymers. 42. 73–86.

Kim K. and etal (2001). Synthesis and luminescence properties of poly(p phenylenevinylene) derivatives carrying directly attached carbazole pendants. J. Mater. Chem. 11. 3023–3030.

Koyuncu S. and etal (2009). A New Donor–Acceptor Double-Cable Carbazole Polymer with Perylene Bisimide Pendant Group: Synthesis, Electrochemical, and Photovoltaic Properties. Journal of Polymer Science: Part A: Polymer Chemistry. Vol. 47. 6280–6291.

Lao W. and etal (2000). Electronic and vibrational spectra of a series of substituted carbazole derivatives. Spectrochimica Acta Part A. 56. 2049–2060.

Lao W. and etal (2012). Fluorescence and b-cyclodextrin inclusion properties of three carbazole-based dyes. Dyes and Pigments. 95. 619-626.

Liawa D. and etal (2012). Advanced polyimide materials: Syntheses, physical properties and applications. Progress in Polymer Science. 37. 907– 974.

Liu B.S. and etal (2009). Controlled Deposition of Crystalline Organic Semiconductors for Field-Effect-Transistor Applications. Advanced. Materials. 21. 1217–1232.

Liu L. and etal (2006). Synthesis, spectroscopy, structures and photophysics of metal alkynyl complexes and polymers containing functionalized carbazole spacers. Journal of Organometallic Chemistry. 691. 4028–4041.

Liu R. and etal (2008). Novel red light-emitting polymers based on 2,7-carbazole and thiophene derivatives. Chinese Journal of Polymer Science. Vol. 26. No. 2. 231−240.

Liu R. and etal (2010). Synthesis, optical properties and crystal structures of carbazole end-capped phenylene ethynylene blue light-emitting materials. Journal of Luminescence. 130. 1183–1188.

Michinobu T. and etal (2008). Alkyne-Linked Poly(1,8-carbazole)s: A Novel Class of Conjugated Carbazole Polymers. Macromol. Rapid Commun. 29. 111–116.

Perez-Gutierrez E. and etal (2011). Synthesis, Characterization and Photophysical Properties of Pyridine-Carbazole Acrylonitrile Derivatives. Material. 4. 562-574.

Promarak V. and etal. (2007). Synthesis and characterization of novel N-carbazole end-capped oligothiophene-fluorenes. Tetrahedron Letters. 48. 1151–1154.

Ruiren T. and etal (2009). Synthesis, fluorescence properties of Eu(III) complexes with novel carbazole functionalized β-diketone ligand. Journal of Rare Earths. Vol. 27. No. 3. p. 362-367.

Tomkeviciene A. and etal (2011). Glass-Forming Organic Semiconductors for Optoelectronics. Materials Science (Medziagotyra). Vol. 17. No. 4. 1392–1320.

Vehoff T. and etal (2008). Atomistic force field and electronic properties of carbazole: from monomer to macrocycle. p hys. stat. sol. (b). 1–5.

Velasco D. and etal (2007).Red Organic Light-Emitting Radical Adducts of Carbazole and Tris(2,4,6-trichlorotriphenyl)methyl Radical That Exhibit High Thermal Stability and Electrochemical Amphotericity. J. Org. Chem.72. 7523-7532.

Vyprachticky D.and etal (2012). Efficient synthesis of N-alkyl-2,7-dihalocarbazoles by simultaneous carbazole ring closure and N-alkylation.Tetrahedron.68. 5075-5080.

Wang L. and etal (2011). Synthesis and photovoltaic properties of low-bandgap polymers based on N-arylcarbazole. Polymer. 52. 1748-1754.

Xie H. etal (2012). New acceptor-pended conjugated polymers based on 3,6- and 2,7-carbazole for polymer solar cells. Polymer.53. 5675-5683.

Zhao W. and etal (2010). Novel conjugated alternating copolymer based on 2,7 carbazole and 2,1,3-benzoselenadiazole. Polymer. 51. 3196-3202.